Spark Ignition of Monodisperse Fuel Sprays

by

Allen M. Danis

Submitted in partial fulfillment of the requirements for

the degree of

Doctor of Philosophy

Approved by Nicholas P. Cernansky

Dr. Nicholas P. Cernansky and Dr. Izak Namer
Co-Principal Investigators

Research Sponsored by the NASA Lewis Research Center
Grant No. NAG 3-382 and by Drexel University

Department of Mechanical Engineering and Mechanics
Drexel University, Philadelphia, PA 19104

September 1987

ABSTRACT

A study of spark ignition energy requirements was conducted with a monodisperse spray system allowing independent control of droplet size, equivalence ratio and fuel type. Minimum ignition energies were measured for n-heptane and methanol sprays characterized at the spark gap in terms of droplet diameter, equivalence ratio (number density) and extent of prevaporization. The droplet diameter was varied between 30 and 57 μm, and the equivalence ratios ranged from 0.45 to 1.8. The extent of prevaporization of the sprays was held approximately constant for each fuel, 0.45 for n-heptane and 0.34 for methanol. Droplet Reynolds numbers of the sprays ranged from 0.1 to 1.0, and interdroplet spacings varied between 15 and 30 droplet diameters. In addition to sprays, minimum ignition energies were measured for completely prevaporized mixtures of the same fuels over a range of equivalence ratios to provide data at the lower limit of droplet size.

Results showed that spray ignition was enhanced with decreasing droplet size and increasing equivalence ratio over the ranges of these parameters studied. No optimum equivalence ratio for ignition was observed for sprays, but an optimum did occur at $\phi \approx 1.8$ for prevaporized n-heptane ignition. A corresponding optimum for prevaporized methanol could not be obtained due to excessive fuel condensation.

By comparing spray and prevaporized ignition results, the existence of an optimum droplet size for ignition (below 30 μm) was indicated for both fuels. This optimum was attributed to the maximum flame propagation rates

observed by previous researchers for sprays in this droplet size range (10 - 40 μm), where both premixed and diffusive types of combustion occur simultaneously. Extension of the lean ignition limits was also observed for sprays compared to prevaporized mixtures. This extension occured for both fuels over the range of droplet sizes studied, and was attributed to fuel distribution effects (i.e. fuel rich regions surrounding evaporating droplets). Both the optimum droplet size and the extension of the lean ignition limit indicate the importance of the gas-phase stoichiometry in the interdroplet spacing to spray ignition.

Fuel volatility was seen to be a critical factor in spray ignition. The more volatile n-heptane sprays required roughly one-fifth the ignition energy required by methanol sprays of corresponding size and equivalence ratio. For prevaporized ignition, however, activation energy was the important fuel property. Prevaporized methanol, with its lower activation energy, required roughly 50% less ignition energy than prevaporized n-heptane.

The spray ignition results were analyzed using two different empirical ignition models for quiescent mixtures. Both models employed a characteristic time approach, relating the time required for fuel evaporation in the spark kernel to the quenching time of the kernel by thermal conduction to its surroundings. The major difference between the models was that while the general ignition model developed by Ballal and Lefebvre equated the two times, the Characteristic Time Model of Peters and Mellor stated that they were only proportional and determined the correlation between them. Both models accurately predicted the experimental ignition energies for the majority of the spray conditions. Their performance deteriorated for lean equivalence ratios (< 0.7) and smaller droplet sizes (< 40 μm) however. This was probably because the models did not account for the time required

for chemical reaction in the spark kernel, which becomes important for leaner and smaller droplet size sprays.

Spray ignition was observed to be probabilistic in nature, and ignition was quantified in terms of an ignition frequency for a given spark energy. The criterion for the minimum ignition energy was the spark energy which produced an ignition frequency of 50%. A model was developed to predict ignition frequencies based on the variation in spark energy and equivalence ratio (number density) in the spark gap. Random normal distributions of these two parameters were generated with a Monte-Carlo routine and used in conjunction with the Characteristic Time Model for ignition. The resulting ignition frequency simulations were nearly identical to the experimentally observed values, indicating that the probabilistic nature of spray ignition is the result of variations in the energy levels of individual sparks and the random distribution of droplets in a fuel spray.

SPARK IGNITION OF MONODISPERSE FUEL SPRAYS

A Thesis

Submitted to the Faculty

of

Drexel University

by

Allen M. Danis

in partial fulfillment of the

requirements for the degree

of

Doctor of Philosophy

September 1987

ACKNOWLEDGEMENTS

I wish to thank my co-advisors, Professors Nicholas P. Cernansky and Izak Namer, for their guidance, support and friendship throughout this project. Their positive attitude and continued interest influenced me tremendously. Special thanks are also extended to the members of my thesis advisory committee, Professors David L. Miller, Aurthur M. Mellor, Bakhtier Farouk and Charles B. Weinberger, whose suggestions and recomendations were very much appreciated.

Financial support for the initial portion of this research by NASA Lewis Research Center (Grant No. NAG 3-382) is gratefully acknowledged. Sincere thanks are also extended to Mrs. Frederic O. Hess for financial support through the Hess Fellowship Program in 1984.

My colleagues and friends in the Combustion and Fuels Group at the Frederic O. Hess Engineering Research Laboratory, Dr. Hamid Sarv, Dr. Richard Wilk, Robert Tidona (Lab Supervisor) and Kevin Tallio, have been extremely helpful and important to me. Special acknowledgement goes to Daniel Dietrich, whose discussions and assistance during the modeling aspects of the program were invaluable.

I also wish to thank my family, especially my father and my future in-laws, for their continued support and encouragement throughout this work.

Finally, and probably most importantly, I thank my future wife Paula for giving me the motivation to see this project through to its fruition.

TABLE OF CONTENTS

Page

LIST OF FIGURES

LIST OF TABLES

NOMENCLATURE

A = Surface Area

A_p = LDV Probe Area

B = Combustion Mass Transfer Number

c_p = Specific Heat at Constant Pressure

C = Capacitance

d = Distance

D = Droplet Diameter

E_{act} = Activation Energy

E_{min} = Minimum Ignition Energy

E_{sp} = Spark Energy

f = Focal Length

f_d = Disturbance Frequency (Droplet Generation Rate)

f/a_m = Fuel to Air Ratio (by mass)

I = Current, Intensity of Diffracted Light

J = Bessel Function

k = Thermal Conductivity

L = Latent Heat of Vaporization

n = Droplet Number Density

n_{inst} = Instantaneous Droplet Number Density

N = Droplet Rate

Q = Volumetric Flow Rate

r = Radial Distance

R = Universal Gas Constant

Re_d = Droplet Reynold s Number

S_L = Laminar Flame Speed

SMD = Sauter Mean Diameter

t = Time

ℓ = Spark Duration

T = Adiabatic Flame Temperature

V = Velocity, Voltage

z = Axial Distance

Subscripts

a = Air

c, hc = Chemical Reaction

d = Droplet

e, eb = Evaporation

f = Fuel

g = Spark Gap

i = Counting Index

o = Initial, Overall

q = Quenching

sl = Mixing

sp = Spark

st = Stoichiometric

Greek Symbols

α = Particle Size Number, Thermal Diffusivity

β = Evaporation Coefficient

λ = Wavelength

Ω = Extent of Prevaporization, Ohms

ϕ = Equivalence Ratio

ρ = Density

θ = Scattering Angle

ABSTRACT

SPARK IGNITION OF MONODISPERSE FUEL SPRAYS

Allen M. Danis

Nicholas P. Cernansky

Izak Namer

A study of spark ignition energy requirements was conducted with a monodisperse spray system allowing independent control of droplet size, equivalence ratio and fuel type. Minimum ignition energies were measured for n-heptane and methanol sprays characterized at the spark gap in terms of droplet diameter, equivalence ratio (number density) and extent of prevaporization. The droplet diameter was varied between 30 and 57 μm, and the equivalence ratios ranged from 0.45 to 1.8. The extent of prevaporization of the sprays was held approximately constant for each fuel, 0.45 for n-heptane and 0.34 for methanol. Droplet Reynolds numbers of the sprays ranged from 0.1 to 1.0, and interdroplet spacings varied between 15 and 30 droplet diameters. In addition to sprays, minimum ignition energies were measured for completely prevaporized mixtures of the same fuels over a range of equivalence ratios to provide data at the lower limit of droplet size.

Results showed that spray ignition was enhanced with decreasing droplet size and increasing equivalence ratio over the ranges of these parameters studied. No optimum equivalence ratio for ignition was observed for sprays,

but an optimum did occur at $\phi \approx 1.8$ for prevaporized n-heptane ignition. A corresponding optimum for prevaporized methanol could not be obtained due to excessive fuel condensation.

By comparing spray and prevaporized ignition results, the existence of an optimum droplet size for ignition (below 30 μm) was indicated for both fuels. This optimum was attributed to the maximum flame propagation rates observed by previous researchers for sprays in this droplet size range (10 - 40 μm), where both premixed and diffusive types of combustion occur simultaneously. Extension of the lean ignition limits was also observed for sprays compared to prevaporized mixtures. This extension occured for both fuels over the range of droplet sizes studied, and was attributed to fuel distribution effects (i.e. fuel rich regions surrounding evaporating droplets). Both the optimum droplet size and the extension of the lean ignition limit indicate the importance of the gas-phase stoichiometry in the interdroplet spacing to spray ignition.

Fuel volatility was seen to be a critical factor in spray ignition. The more volatile n-heptane sprays required roughly one-fifth the ignition energy required by methanol sprays of corresponding size and equivalence ratio. For prevaporized ignition, however, activation energy was the important fuel property. Prevaporized methanol, with its lower activation energy, required roughly 50% less ignition energy than prevaporized n-heptane.

The spray ignition results were analyzed using two different empirical ignition models for quiescent mixtures. Both models employed a characteristic time approach, relating the time required for fuel evaporation in the spark kernel to the quenching time of the kernel by thermal conduction to its surroundings. The major difference between the models was that while the general ignition model developed by Ballal and Lefebvre equated the two

times, the Characteristic Time Model of Peters and Mellor stated that they were only proportional and determined the correlation between them. Both models accurately predicted the experimental ignition energies for the majority of the spray conditions. Their performance deteriorated for lean equivalence ratios (< 0.7) and smaller droplet sizes (< 40 μm) however. This was probably because the models did not account for the time required for chemical reaction in the spark kernel, which becomes important for leaner and smaller droplet size sprays.

Spray ignition was observed to be probabilistic in nature, and ignition was quantified in terms of an ignition frequency for a given spark energy. The criterion for the minimum ignition energy was the spark energy which produced an ignition frequency of 50%. A model was developed to predict ignition frequencies based on the variation in spark energy and equivalence ratio (number density) in the spark gap. Random normal distributions of these two parameters were generated with a Monte-Carlo routine and used in conjunction with the Characteristic Time Model for ignition. The resulting ignition frequency simulations were nearly identical to the experimentally observed values, indicating that the probabilistic nature of spray ignition is the result of variations in the energy levels of individual sparks and the random distribution of droplets in a fuel spray.

CHAPTER 1

INTRODUCTION

The combustion of liquid hydrocarbon fuels is the principal source of energy production in today's society. Although their percentage of total worldwide energy consumption dropped from 48% in 1975 to 40% in 1985, liquid petroleum products still account for the major portion of energy consumed in the U.S. and worldwide (DOE/EIA, 1985). Roughly 50% of these liquid hydrocarbon fuels are burned in spray form, by combustion devices such as furnaces and gas turbine and diesel engines.

Studying the ignition characteristics of liquid hydrocarbon sprays is important for several reasons. Since many of the combustion devices mentioned above use spark ignition systems, the amount of spark energy required for successful ignition over a range of operating conditions must be known. Information about the ignition characteristics of fuel sprays and vapor is also useful for the development of fundamental models of ignition, combustion and flame propagation. Finally, knowledge of ignition mechanisms is necessary for the prevention of unwanted explosions and fires.

A local source of ignition, such as an electric spark, initiates chemical reaction by energizing a small volume (or kernel) of combustible mixture around the spark. Energy is lost from this spark kernel by heat transfer and transport processes, and the chemical energy of the mixture in the kernel must be converted into thermal energy at a sufficient rate to overcome these

losses. If this occurs, the kernel will grow into a steadily propagating flame and ignition is successful.

The many interacting factors which influence spark ignition of fuel sprays can be grouped into the three basic categories consisting of spray parameters, physical parameters and spark parameters. Spray parameters include the size or size distribution of droplets in the spray, the interdroplet spacing, the amount of evaporated fuel and oxidizer present in the interdroplet spacing, and the fuel properties. Physical parameters which can affect ignition are flow characteristics such as the spray velocity and level of turbulence, as well as the local temperature, density and pressure at the point of ignition. Spark parameters such as the energy and duration of the spark and the electrode spacing and configuration relative to the spray must also be considered.

Extensive studies have been undertaken previously to measure the minimum spark ignition energy required for a variety of homogeneous fuel-air mixtures. However, measuring the ignition energy of heterogeneous fuel-air mixtures is a much more complex task due to the experimental difficulties in controlling and quantifying the spray parameters mentioned above. The ignition of polydisperse, or multiple droplet size sprays has been studied for a number of fuels, but only over limited ranges of equivalence ratio. Ignition data for monodisperse, or single droplet size sprays is even more sparse, with studies covering only one fuel and a limited size range. This study was undertaken to provide ignition energy data for monodisperse sprays over a range of drop sizes and equivalence ratios more typical of those found in practical combustors.

A well characterized spray facility was used to simulate the spark ignition process which occurs in practical combustors, such as gas turbine

engines. The major experimental variables included fuel type, droplet size and stoichiometry. The main experimental measurements made in this study were ignition frequency and spark energy (from which ignition energy was determined), droplet number density (from which the stoichiometry was determined) and droplet size. Ignition energy measurements were also performed for prevaporized, premixed cases to provide the lower bound of zero droplet size. The analytical portion of the study involved predicting the minimum ignition energy of the fuel sprays as a function of fuel type, droplet size, equivalence ratio and amount of prevaporized fuel. These predictions were made with two existing spark ignition models which used a characteristic time approach. An ignition frequency model was developed which extended the characteristic time models to account for the probabalistic nature of the ignition process.

Chapter 2 includes background information concerning the ignition of combustible mixtures, as well as a review of some previous work in the area. The spray characterization and ignition facilities and experimental results are described in Chapters 3 and 4, respectively. Analytical calculations and predictions are presented in Chapter 5. The conclusions of the study and recommendations for future work comprise Chapter 6.

CHAPTER 2

BACKGROUND AND LITERATURE REVIEW

An electric spark ignites a combustible mixture by means of heat addition followed by flame propagation. Therefore, insight into the spark ignition process can be gained by studying the related processes of thermal ignition and flame propagation. Experimental and theoretical studies done in these areas will be reviewed in the first two sections of this chapter.

Experimental spark ignition studies have been performed with both homogeneous and heterogeneous mixtures. Those studies will be reviewed in the third section of this chapter. The discussion will begin with a brief overview of the homogeneous studies coupled with a review of spark characteristics and their effects on ignition. This will be followed by a more detailed review of the heterogeneous ignition studies.

Theoretical work on the spark ignition of sprays will be covered in the final section of this chapter. Global ignition models will be reviewed, as well as attempts to model the local formation and growth of the spark kernel and its effect on spray droplets within and surrounding it.

2.1 Thermal Ignition Studies

The ignition characteristics of single isolated fuel droplets in a hot environment was studied experimentally by Saitoh et al. (1982). They measured the ignition delay time as a function of droplet size and air temperature for n-heptane and n-hexadecane droplets ranging from 0.5-2.5

mm. A minimum droplet size for ignition was observed, and below this minimum the droplet could completely vaporize without igniting. This limiting drop size, as well as the ignition characteristics of fuel droplets in general, depended strongly on the fuel type and ambient conditions.

Law and Chung (1978, 1980) theoretically studied the thermal ignition of single droplets in a hot ambient environment. They found that the ignition delay time could be represented in terms of an ignition Damkohler number.

The thermal ignition of monosized droplet streams in a hot environment was investigated by Sangiovanni and Kesten (1977). They studied the effect of droplet interactions, as controlled by the droplet size (200-300 μm) and interdroplet spacing (2-200 droplet diameters), on the ignition delay time of furfuryl alcohol droplets. Theoretically, they determined ignition delay times for the limiting cases of an isolated droplet and a cylindrical filament of fuel. Results showed that the ignition delay time increased substantially as the interdroplet spacing was decreased. This droplet interaction effect increased with decreasing droplet size, decreasing ambient temperature and increasing fuel volatility.

Aggarwal and Sirignano (1985) developed a numerical model for the ignition of idealized, quiescent monosized droplet arrays by a heated wall. They predicted optimum values of droplet size and overall equivalence ratio for ignition. The optimum droplet size depended on the overall equivalence ratio and was attributed to the distribution of fuel vapor in the ignition zone, which was affected by the total droplet surface area. Similarly, the optimum equivalence ratio was a function of the initial droplet size and fuel volatility. The authors also showed that ignition of droplet arrays (and fuel sprays) was a probabalistic phenomenon, since it depended on the location of the droplets relative to the heat source, which was random. They subsequently extended

this work to polydisperse sprays (Aggarwal and Sirignano, 1986) and concluded that the area mean diameter better characterized polydisperse sprays than the Sauter mean diameter. Aggarwal and Nguyen (1987) performed a numerical simulation of the ignition of monosized droplet arrays flowing in a tube. Their ignition source was a localized heat source (flame kernel), and they determined minimum ignition energies and ignition delay times for n-hexane and n-decane droplets ranging from 30-150 μm. Results showed that the minimum ignition energy increased with increasing droplet size, increasing mixture velocity and decreasing fuel volatility. They also indicated an optimum droplet size (minimum ignition delay time) for n-hexane, and that this optimum size increased with increasing mixture velocity.

2.2 Flame Propagation and Transition Region Effects

Burgoyne and Cohen (1954) studied the effect of droplet size on flame propagation through monodisperse tetralin aerosols. They observed that premixed, prevaporized combustion dominated for sprays with droplet sizes below 10 μm. Above 30 μm the droplets burned individually in their own diffusion flame envelope, with burning droplets igniting adjacent droplets. For the combustion of sprays with intermediate droplet sizes (10-30 μm), individual droplets encased in flame envelopes were observed superimposed on the gaseous laminar flame structure. Sprays which exhibited this transitional combustion behavior, both heterogeneous and homogeneous, were said to be in the 'transition region'. They also observed that the presence of droplets extended the lean prevaporized flammability limits to leaner equivalence ratios. They explained this with the observation that even at lean overall equivalence ratios, fuel droplets supported a diffusion flame

burning in stoichiometric proportions. Conversely, a lean prevaporized premixed mixture would never have regions of stoichiometric mixture strength.

Polymeropoulos and Das (1975) observed a maximum flame speed for kerosine sprays at about 30 μm SMD . This was further evidence that flame propagation was enhanced by transition region effects. Hayashi et al. (1976, 1981) studied flame speeds in a closed combustion bomb, which was subject to large pressure increases as the reaction progressed. However, they found that the flame speed increased as drop size increased from 16-40 μm, provided that the mass of liquid fuel droplets was greater than the mass of fuel vapor present. They also showed that the presence of fuel droplets could increase the flame speed compared to that for the fully vaporized case.

Mizutani and Nakajima (1973) observed that the addition of kerosine droplets to a gaseous propane-air mixture increased the flame speed at lean overall equivalence ratios. The optimum drop size for enhancement was found to be 40 μm. They explained this behavior by proposing that the droplets wrinkled and lacerated the flame surface, thereby increasing the flame speed. They also suggested that the drops served as high temperature ignition sources, extending the flammability limits and accelerating the burning velocity of adjacent flame elements. The burning velocity was increased because the flame propagated through regions of optimum fuel to air ratio formed around the evaporating drops. In addition, the burning droplets caused local gas expansions, generating turbulence which further intensified the transport processes. By repeating their experiments with vaporized kerosine, they confirmed that it was the two-phase nature of the flow that was responsible for the observed behavior.

In addition to enhanced flame speeds and broadened flammability limits, several other combustion phenomena have been observed for sprays in the transition region. Nizami et al. (1982) and Sarv (1985) measured minima in NO_x emissions for sprays in the 40-60 μm size range. Chan (1982) and Singh (1986) both observed optimum drop sizes for spark ignition. These ignition studies will be reviewed in detail below.

2.3 Experimental Spark Ignition Studies

2.3.1 Spark Characteristics and Homogeneous Spark Ignition

Some of the earliest experimental ignition work was performed by Lewis and Von Elbe (1961) and Litchfield (1960), who independently determined the minimum spark energy required for ignition of mixtures of 8.5% methane in air to be 0.28 mJ. In both studies, purely capacitive sparks with durations of less than 1 μs were used as the ignition source. The spark energy (E_{sp}) was assumed to be equal to the stored electrical energy of the capacitor, given by:

$$E_{sp} = 0.5CV^2 \qquad (2\text{-}1)$$

where C is capacitance and V is voltage.

Rose and Priede (1958) investigated the minimum ignition energy of hydrogen-air mixtures using a capacitive discharge ignition circuit with series resistance (RLC circuit) to produce their ignition sparks. They found that by increasing the resistance in their circuit while holding the spark energy constant, the energy required for ignition decreased. Increasing the circuit resistance increased the duration of the spark. This decreased the strength of the shock wave produced by the spark, thereby increasing the proportion of the spark energy available for heat addition to the mixtures.

Since some of the stored capacitor energy was dissipated in the circuit resistance, spark energies had to be calculated by integrating the product of the voltage (V) and current (I) across the spark gap over the duration of the spark:

$$E_{sp} = {}_0\int^t VIdt \qquad (2\text{-}2)$$

They also noted that changing the electrode spacing (spark gap width) affected their ignition energy results and that this parameter should be optimized for each condition tested.

In a detailed investigation of spark discharge characteristics Maly and Vogel (1978) studied the three modes of capacitive discharge: breakdown, arc and glow. Breakdown discharge occurs when there is very little or no resistance in series with the capacitor, resulting in spark durations that are very short, typically less than 1 μs. Arc and glow discharges have longer durations (10-300 μs and greater than 300 μs, respectively) due to increased series resistance. Maly and Vogel concluded that breakdown was the most efficient discharge mode because very little energy loss due to conduction of heat from the spark to the electrodes occurred, while substantial conduction losses occurred during both arc and glow discharges. The energy losses due to radiation were also found to be negligible for all three modes. These findings confirmed earlier studies on spark discharges by Roth et al. (1951).

In a study similar to that of Maly and Vogel, Kono et al., (1977) concluded that arc discharge was the most efficient mode of energy transfer for the spark ignition of quiescent propane-air mixtures. They observed that under the condition of optimum spark duration and gap width, arc discharges

resulted in the lowest ignition energy of the three modes.

While investigating the spark ignition of flowing propane-air mixtures, Swett (1956) found the optimum spark duration to be about 100 μs. Ballal and Lefebvre (1975) also observed optimum spark durations of 60-100 μs for flowing propane-air mixtures, as did Ziegler (1984) for methane-air mixtures. In addition, Ballal and Lefebvre (1975) found that the minimum ignition energy decreased with decreasing electrode diameter due to decreasing electrode surface area available for conduction losses.

In summary, arc discharge has been found to be the most efficient form of energy transfer for the spark ignition of combustible mixtures, provided the discharge occurs under optimum conditions of spark duration and spark gap width to minimize energy losses. In reality, all arc discharges are initiated by a breakdown discharge, needed to ionize the medium in the spark gap and provide a conducting path for the arc. However this breakdown phase accounts for a negligible amount of the spark duration and total spark energy relative to the arc discharge.

2.3.2 Heterogeneous Spark Ignition

Spark ignition of polydisperse fuel sprays has been studied extensively by Lefebvre and co-workers. Rao and Lefebvre (1976) measured the minimum ignition energy (E_{min}) of polydisperse kerosine sprays with Sauter mean diameters (SMD) ranging from 30-100 μm and equivalence ratios (Ø) ranging from 0.4-1.0. They observed that droplet size had the strongest effect on ignition, with E_{min} increasing steadily with increasing SMD. They also found that, for a fixed droplet diameter, E_{min} decreased steadily with increasing Ø.

Continuing this work, Ballal and Lefebvre (1978) measured E_{min} over

similar ranges of SMD and Ø for polydisperse sprays of six different fuels ranging in volatility from iso-octane to heavy fuel oil. The observed effects of SMD and Ø on E_{min} were similar to those noted above for kerosine. Moreover, the authors quantified these effects, showing that E_{min} was proportional to SMD^3 and $Ø^{-1.5}$. In addition, E_{min} was seen to decrease with increasing fuel volatility. They concluded that the most critical factor in determining ignition was the mass concentration of fuel vapor generated by the spark in the ignition zone. In the same study, Ballal and Lefebvre investigated the effect of pressure, mean velocity and turbulence intensity on ignition and found that E_{min} increased with decreasing pressure, increasing flow velocity and increasing turbulence intensity.

The first spark ignition study performed with monosized sprays was by Chan (1982), who studied the ignition of monodisperse tetralin sprays with drop sizes ranging from 8-32 µm and equivalence ratios of 0.4-1.0. He observed an optimum droplet size for ignition of about 15 µm and reasoned that as the drop size decreased from 30 to 15 µm the enhanced evaporation made ignition easier. As the drop size decreased below 15 µm, however,the spray approached a homogeneous quality and lost the benefit of individual droplet combustion, thus increasing the energy needed for ignition of lean mixtures.

Singh (1986) performed ignition studies of monodisperse tetralin sprays and observed an optimum drop size for ignition of 22-26 µm, depending on stoichiometric conditions. He concluded that the amount of fuel vapor generated by the spark depended on the drop size. Sprays with drop sizes smaller than the optimum produced fuel vapor concentrations during the spark discharge that were richer than optimum for ignition, while drop sizes larger than optimum produced fuel vapor concentrations leaner than optimum

for ignition. He also reported ignition results in terms of ignition frequency rather than minimum ignition energy, since there was no sharp delineation between spark energies which produced ignition and those which did not.

2.4 Theoretical Spark Ignition Studies

The analysis and modeling of spray formation, evaporation and combustion has been quite extensive. Two review papers which cover this area quite thoroughly have been published by Sirignano (1983) and Faeth (1979).

Modeling of the spark ignition process itself was first performed by Lewis and von Elbe (1961) who related ignition energy to the laminar flame speed of the mixture. They assumed that the entire spark energy was instantaneously converted to thermal energy within a spark kernel. For successful ignition, this spark kernel should achieve some critical volume, or quenching distance, resulting in flame propagation. This critical volume was achieved when the heat release rate within the kernel equalled the rate of heat loss from it.

More recently, Peters and Mellor (1980) used a characteristic time approach to the model ignition energy of quiescent sprays. They subsequently extended the model for use in gas turbine engines (Peters, 1981; Peters and Mellor, 1982), predicting ignition energies as a function of equivalence ratio, SMD and pressure for quiescent and turbulent sprays. Their criterion for ignition was that the residence time of the fuel-air mixture at the spark gap must be longer than the time required for evaporation and chemical reaction. The residence time was the ratio of the quenching diameter to the mean velocity, and the evaporation and ignition delay times were given by the D^2 law and an Arrhenius expression, respectively. These

models predicted ignition energies which correlated well with the experimental data of Ballal and Lefebvre (1977). Ballal and Lefebvre (1981) developed a similar model to predict ignition energies for homogeneous and heterogeneous mixtures under flow conditions ranging from quiescent to turbulent. They related the time required for evaporation and chemical reaction to the time required for the hot kernel to be quenched by heat loss to the surrounding spray. Their ignition delay time was related to the flame speed of the mixture, rather than the activation energy used by Peters and Mellor.

While the spray ignition models noted above have taken a global approach to spark ignition, other investigators have used a more localized approach by taking into account the time dependent nature of the spark discharge. Maly (1981) developed a temporally resolved thermal ignition model which took into account the unsteady nature of the ignition process in a detailed analysis of the different phases of spark discharge and ignition. He proposed that the energy available for ignition was concentrated in a narrow shell around the spark plasma. His criterion for ignition was that the expansion velocity of this outer shell must be equal to that of a self supporting flame front of the same size.

Adelman (1981) developed a theory which related the time dependent energy input from a spark to the kernel expansion. He took into account the strong shock wave spherically expanding from the spark, followed by the hot expanding spark kernel. His criterion for ignition was that the spark kernel must grow to a critical size before its expansion velocity falls below a critical velocity. Using a similar approach, Singh (1986) applied a model of spark kernel growth, including shock wave effects, to his experimental ignition data for qualitative correlation. For sprays of very small droplets

(less than 10 μm), the model predicted that the local flow field generated by the spark discharge resulted in a droplet free annular region around the spark kernel. This fuel free zone acted as a barrier to flame propagation, explaining his experimental observation that sprays with very small droplets (6.7 μm) were very difficult to ignite.

Bradley and Lung (1987) developed a hydrodynamic model to predict the temporal development of the radial profiles of density, pressure, velocity and temperature from a spark discharge channel. They showed that the slow spread of thermal energy from the relatively narrow discharge channel was a limiting factor in spark ignition This spread could be accelerated by higher energy input in the early stages of the spark discharge, resulting in stronger shock waves, thermal waves and outward convection of energy.

CHAPTER 3

EXPERIMENTAL FACILITIES AND METHODS

The basic spray generation and characterization facilities are described in this chapter, along with the spray ignition system and experimental procedures. Representative spray characterization results are presented and discussed in this chapter, while comprehensive spray characterization results appear in Appendix A. Actual spray operating conditions and ignition results will be reported and discussed in Chapter 4.

3.1 Spray Generation

3.1.1 Monodisperse Spray Generation System

A Berglund-Liu Vibrating Orifice Monodisperse Aerosol Generator, Model 3050 (Berglund and Liu, 1973), was used to produce sprays of monosized droplets for this study. Figure 3.1 shows a photograph of a typical spray enlarged 20 times. The picture was taken as the spray exited the test section 10 cm downstream of the point of generation. The curved white line is the bottom rim of the test section. (For reference, the thickness of the white line is about 0.5 mm.) As seen, the droplets are monosized, well dispersed and randomly positioned. This generator has been successfully used previously for a number of monodisperse spray combustion studies (Nizami et al., 1978-1982; Sarv, 1985). The generator was mounted on a traversing mechanism which allowed manual translation of the unit in the x-y-z coordinates.

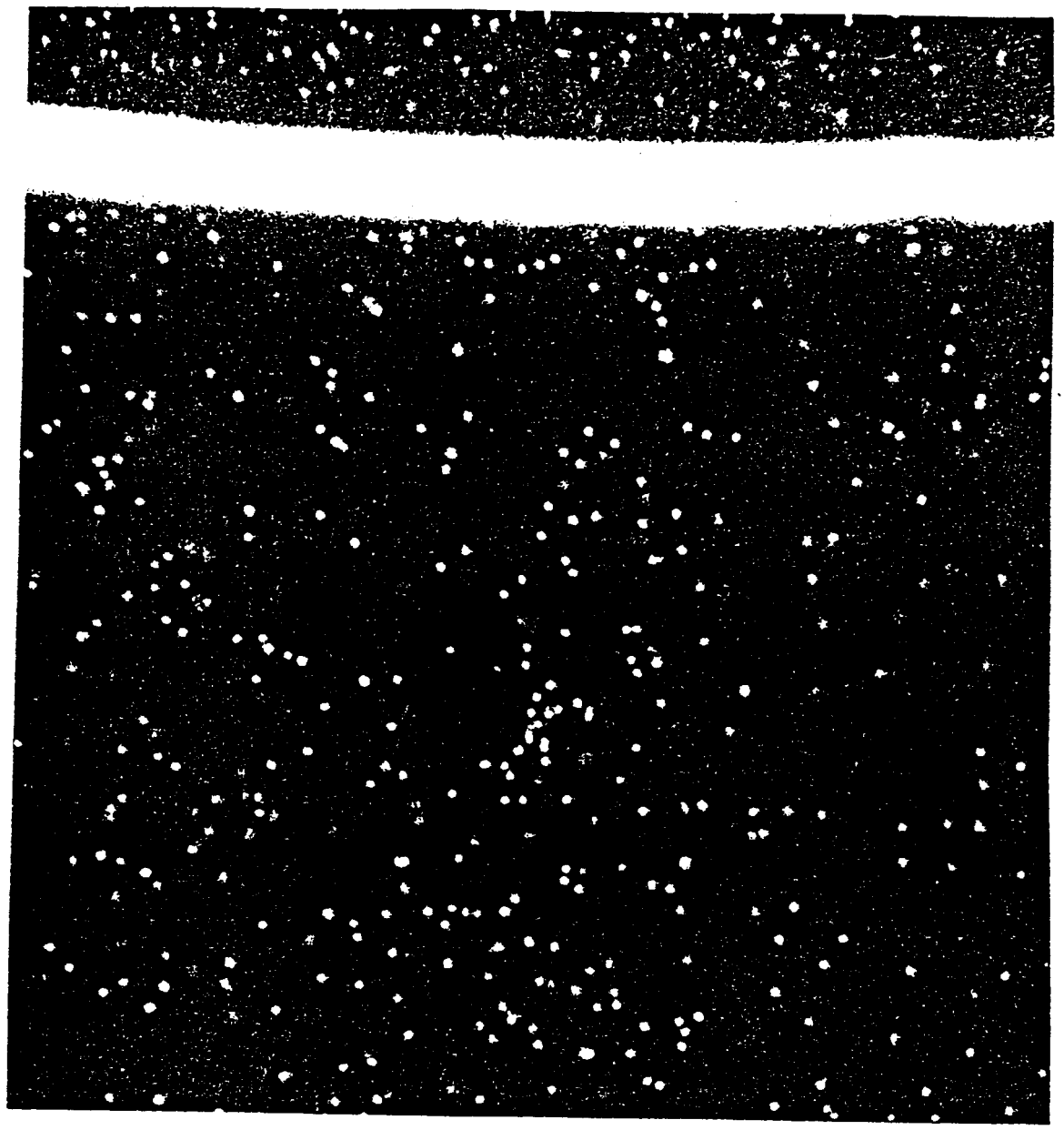

Figure 3.1 Photograph of a Monodisperse N-Heptane Spray Enlarged 20X (D_0 = 50 m; $\emptyset_0$ = 0.55; z = 10 cm)

A cross-section view of the aerosol generator is shown in Figure 3.2. Monosized droplets were generated by applying periodic disturbances from a function generator to a piezoelectric ceramic, which in turn exerted mechanical vibrations on a liquid fuel jet emerging from an orifice plate seated in the ceramic. The perturbed jet then broke into discrete droplets with a standard deviation in size of approximately 1% of the mean diameter. One droplet was created per cycle of disturbance, so the initial droplet diameter (D_o) could be calculated from the volumetric fuel flow rate (Q_f) and the frequency of disturbance (f_d) and is given by:

$$D_o = (6Q_f/\pi f_d)^{1/3} \qquad (3\text{-}1)$$

The droplet diameter was controlled by varying the fuel flow rate and the frequency of disturbance. While the droplet diameter was not a direct function of the orifice diameter, a given sized orifice was only capable of producing monosized droplets within a relatively narrow 'monodisperse' range. Therefore, different diameter orifices were used to produce a broad range of monosized droplet diameters. Table 3.1 shows the monodisperse ranges obtainable for the different orifices and fuel flow rates used in this study.

3.1.2 Fuel and Air Flow Systems

Figure 3.3 shows a simplified schematic diagram of the interior of the spray generator. Also included are the radial and axial coordinate axes (r and z) used in this study. An infusion syringe pump (Harvard Apparatus Model 901) supplied liquid fuel to the spray generator. As the stream of uniform fuel droplets exited the orifice, it entered a turbulent jet of

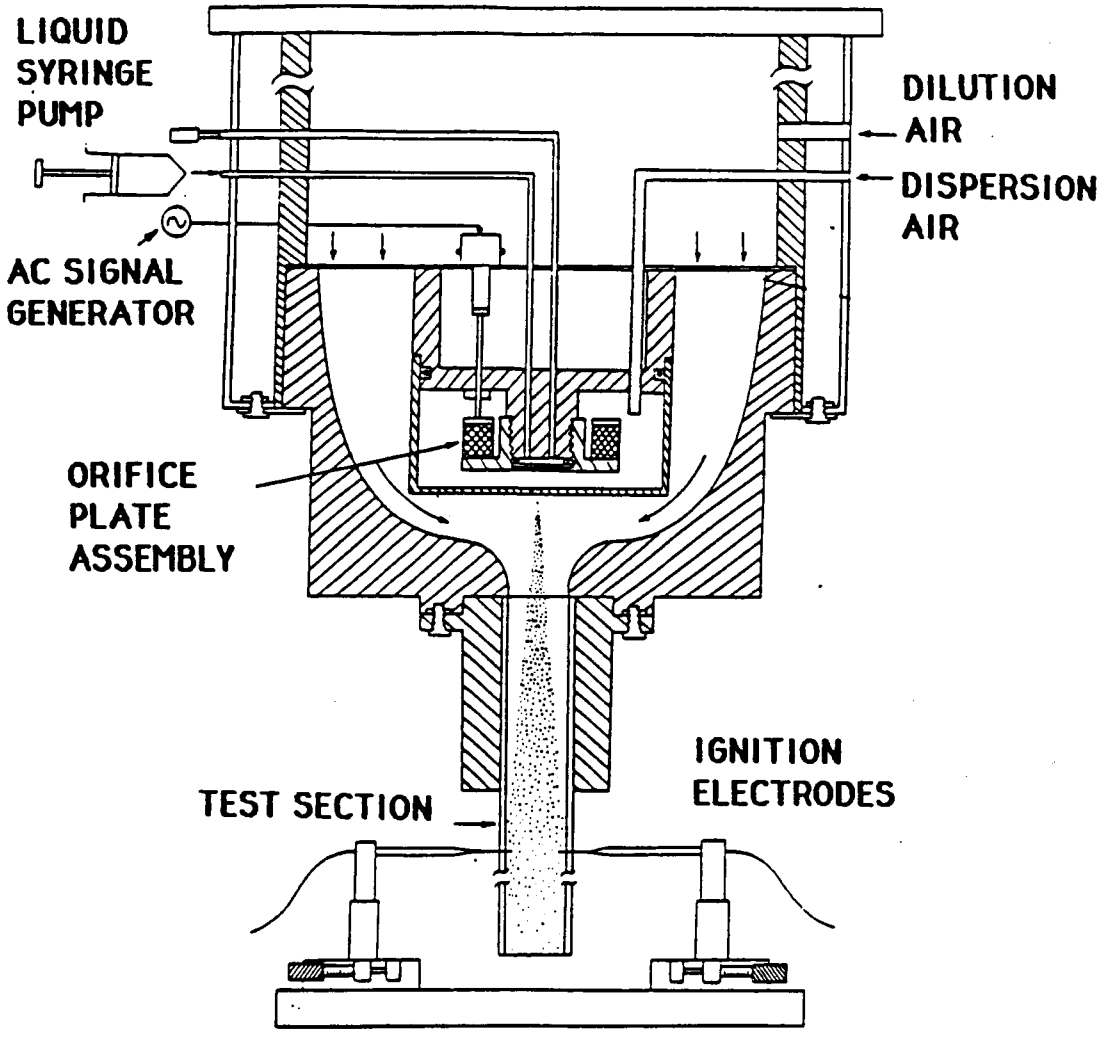

Figure 3.2 Cross Section View of the Monodisperse Spray Generator

ORIFICE DIAMETER (μm)	FUEL	FUEL FLOW RATE (cc/m)	MONODISPERSE RANGE (μm)
7.5	METHANOL	0.075	16-20
12.5	METHANOL	0.075	20-30
17	N-HEPTANE	0.18	30-43
22	N-HEPTANE	0.19	45-57
27	N-HEPTANE	0.19	54-70
17	METHANOL	0.35	30-45
22	METHANOL	0.37	45-58
27	METHANOL	0.375	50-67

Table 3.1 Monodisperse Operating Ranges for Various Orifices and Fuel Flow Rates

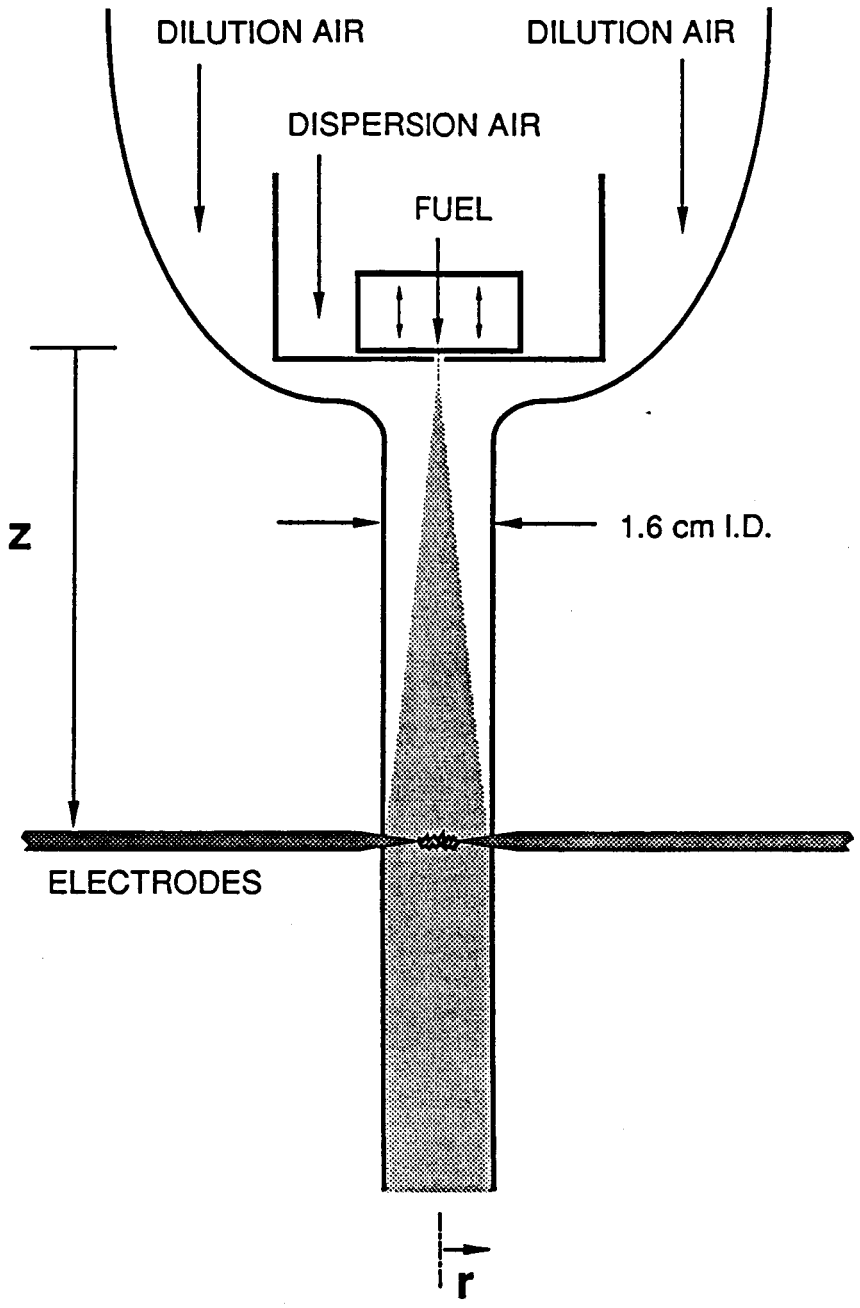

Figure 3.3 Schematic View of the Spray Generator Interior

dispersion air which kept the droplets from coagulating. This air jet was formed by the dispersion air flow exiting the dispersion cup through a 1 mm diameter orifice. The dispersion cup was mounted so the dispersion orifice was 1 mm directly below the fuel orifice.

The dispersion jet with droplets in suspension continued downward through the reducing section, where a co-flow of dilution air was entrained into the spray. This reducing section had smooth rounded edges to minimize flow recirculation. The spray then entered the test section, which was a 1.6 cm I.D. Pyrex tube 18 cm in length, and exited to the atmosphere.

Both the dispersion and dilution air flow rates were set by electronic flow controllers (Tylan Model FC-260), and monitored with mass flow meters (Hastings Model ALL-5K). The overall stoichiometry ($\emptyset_o$) of the sprays was set by the relative flow rates of fuel, dispersion air and dilution air. For a given drop size spray, the fuel and dispersion air flow rates were fixed, and the equivalence ratio was varied by changing the dilution air flow rate.

3.1.3 Fuel Prevaporization System

In order to perform ignition energy measurements on prevaporized, premixed fuel/air mixtures, a fuel prevaporizing apparatus was added to the experimental facility. A schematic of this system is given in Figure 3.4.

Liquid fuel and air entered a spherical 500 cc pyrex vessel, heated to approximately 150 °C, where the liquid fuel evaporated and mixed with the air. The mixture then flowed through a heated secondary mixing section constructed of 1.2 cm I.D. stainless steel tubing 40 cm in length. This section had 4 stainless steel screens spaced evenly along its length to induce turbulence, thus ensuring uniform mixing of the vaporized fuel and air. The mixture then flowed into the dispersion air inlet of the aerosol generator.

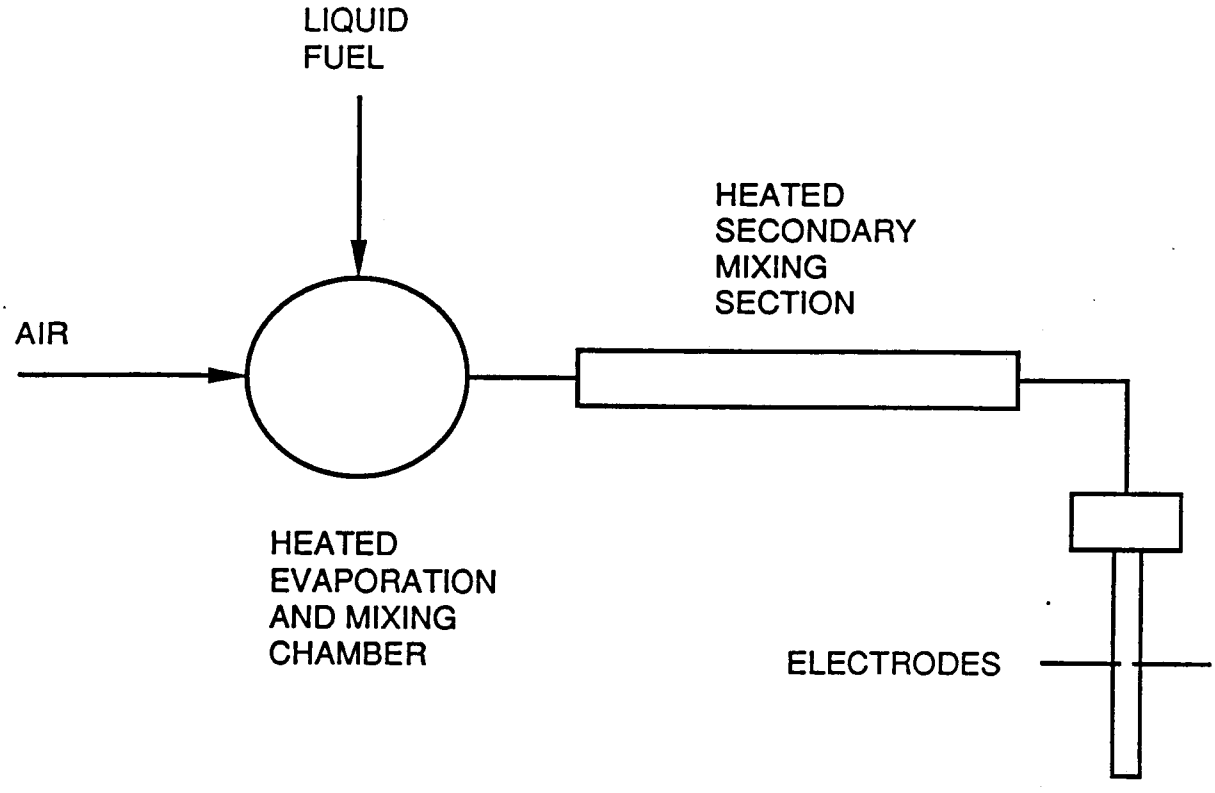

Figure 3.4 Schematic Diagram of the Fuel Prevaporizing and Premixing Apparatus

Since no dilution air flow was needed, the test section was attached directly to the outlet of the dispersion cup for the prevaporized ignition experiments. The test section used was identical to the one used for the spray experiments, as described in the previous section.

3.2 Number Density Measurement

A major portion of the spray characterization procedure involved specifying the local droplet number density at the spark gap, which was directly related to the stoichiometry. Spray number densities were determined from measurements made with a laser Doppler velocimetry (LDV) system. These measurements included droplet velocity and rate, air velocity and LDV probe area, and are detailed in the following sections. Representative results from these measurements are also included below, while comprehensive results appear in Appendix A.

3.2.1 LDV System

Mean droplet and air velocities, turbulence intensities and droplet rates were measured using a dual beam LDV system in the backscatter mode. A schematic of the system is shown in Figure 3.5. The basic system components were the laser (Spectra-Physics Model 124B Laser, Model 255 Power Supply), optics (TSI Model 900 Series), photomultiplier (TSI Model 962) and signal processor (TSI Model 1984 input conditioner and TSI Model 1985 timer). The signal from the processor was sent through an analog to digital converter and analyzed with a DEC LSI-11 microcomputor. The FORTRAN and MACRO data analysis programs are listed in Appendix B. A complete description of the physical principles involved in LDV measurements can be found in a paper by Stevenson (1976).

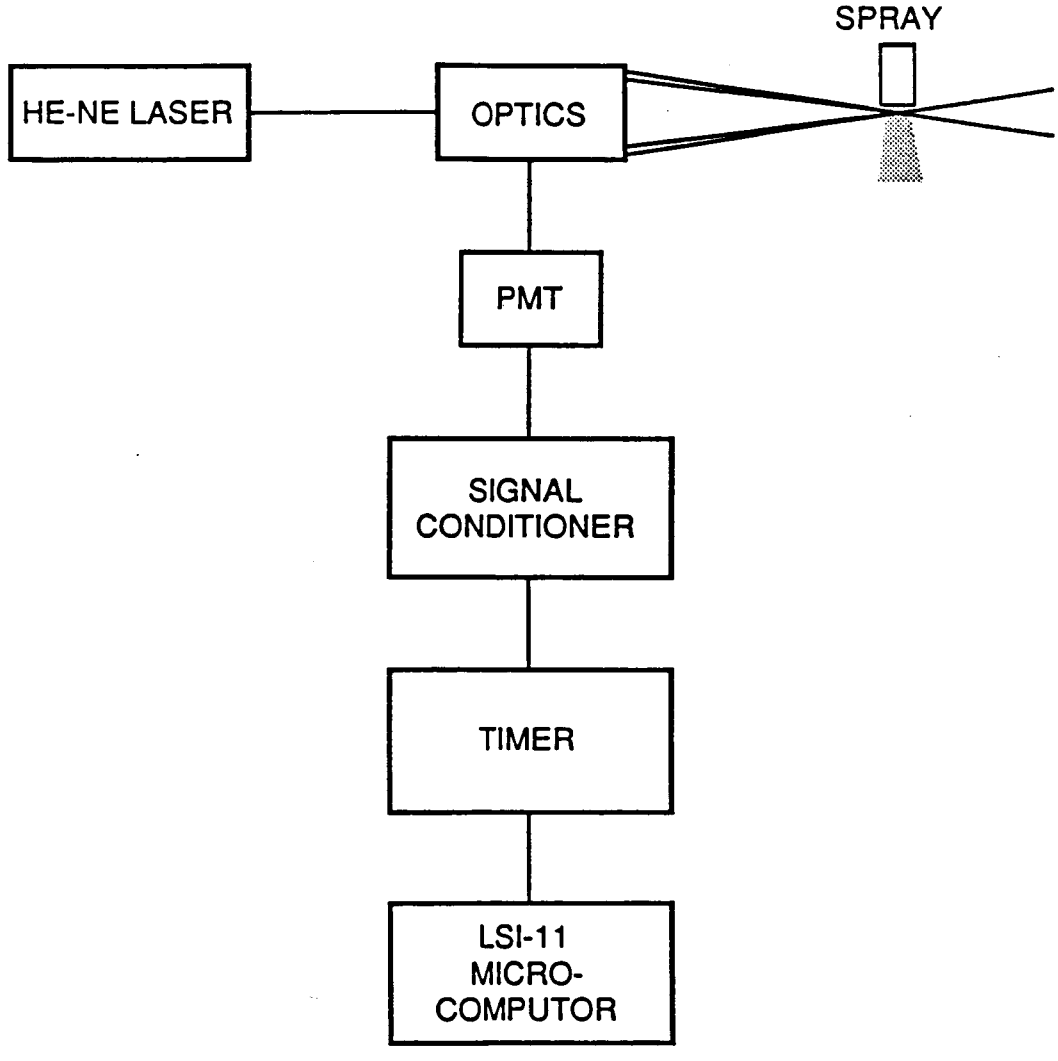

Figure 3.5 Schematic Diagram of the LDV Spray Characterization System

3.2.2 Spray Number Density and Stoichiometry

A spray characterization procedure was performed to specify the relative amounts of fuel and air in the spark gap region during ignition testing. The procedure involved making LDV measurements at points on a horizontal rectangular grid at the axial location of the ignition electrodes. Due to the difficulty in attempting LDV measurements through a cylindrical test section, a shorter test section cut off 3 mm above the laser beams was used for this procedure. This allowed LDV measurements to be made through air, with no obstruction from the test section. The basic procedure was as follows.

Droplet rate (N) and velocity (V_d) measurements were made in a 2 mm grid pattern over the entire cross section of the spray. The droplet number density (n) was determined locally in the sprays as follows:

$$n = N/V_a A_p \qquad (3\text{-}2)$$

where V_a is the air velocity and A_p is the probe area. V_a was measured as described in section 3.2.4. A_p was measured as described in Section 3.2.3. The number density was then converted to the local equivalence ratio by:

$$\phi = n(\rho_f \pi D_o^3/\rho_a)/3(f/a)_{m,st} \qquad (3\text{-}3)$$

where ρ_f and ρ_a are the densities of the liquid fuel and air respectively, D_o is the initial droplet diameter and $(f/a)_{m,st}$ is the stoichiometric fuel to air mass flow ratio.

The initial droplet diameter and not the local diameter was used in order to account for all of the fuel (liquid + vapor) present locally. It was

assumed that the evaporated fuel stayed in the radial vicinity of the droplets from which it evaporated, so that the radial profiles of fuel vapor matched the droplet number density profiles in the sprays. This was based on a characteristic mixing length analysis for a turbulent free jet (Hinze, 1981) from which radial mixing lengths of 1-2 mm were calculated for the sprays. Since these mixing lengths were very close to the average interdroplet spacings of the sprays (0.6-1.5 mm), this assumption was reasonable.

Typical radial profiles of number density and local equivalence ratio are given in Figure 3.6 for 50 μm methanol and n-heptane sprays with overall equivalence ratios of 0.51. Notice that while the equivalence ratio profiles of these sprays were very similar, the methanol number densities were roughly twice those of the n-heptane spray. This was because methanol, with fewer carbon atoms and a fuel-bound oxygen atom, required about twice the fuel to air ratio of n-heptane to achieve the same equivalence ratio. Equivalence ratio profiles for all sprays tested are shown in Appendix A.

The spark gap equivalence ratio (ϕ_g) was defined as the average value of the local equivalence ratio over the width of the electrode spacing. Values of ϕ_g are given in the next chapter in Tables 4.2 and 4.3 for all sprays tested, along with specific values of the spark gap widths used. Spark gap widths ranged from 2-7 mm, increasing with decreasing equivalence ratio. Due to the increasing amount of dilution air entrained into the dispersion jet, the equivalence ratio profiles became flatter in shape with decreasing overall equivalence ratio. This meant that larger gap widths corresponded to flatter equivalence ratio profiles. Therefore, the local equivalence ratio was relatively constant over the width of the spark gap for most cases.

Figure 3.7 shows spark gap equivalence ratio (based on a 2 mm gap width) plotted as a function of the overall equivalence ratio for n-heptane

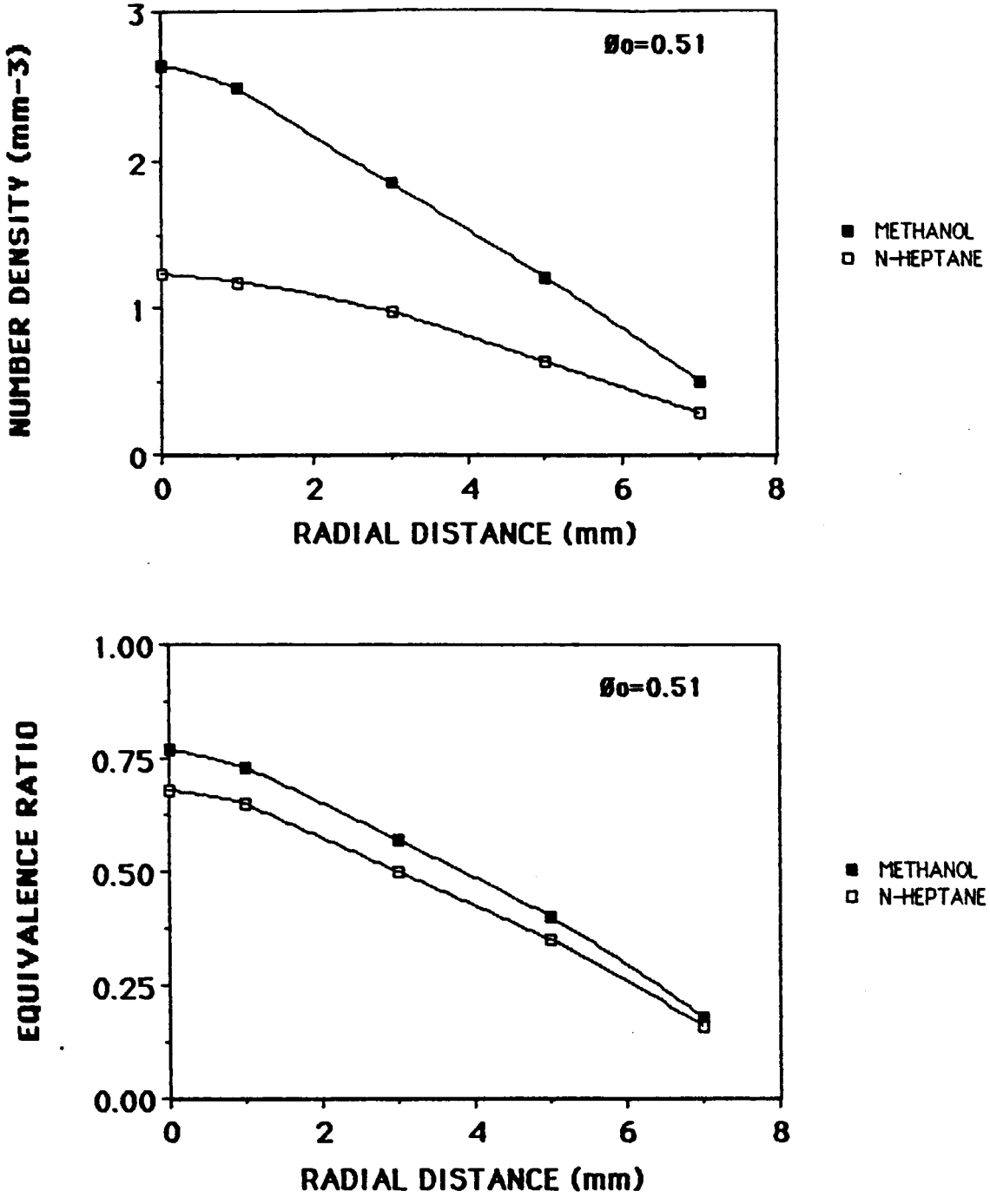

Figure 3.6 Radial Profiles of Droplet Number Density and Equivalence Ratio for Methanol and N-Heptane Sprays (D_0 = 50 μm; $Ø_0$ = 0.51; z = 10 cm)

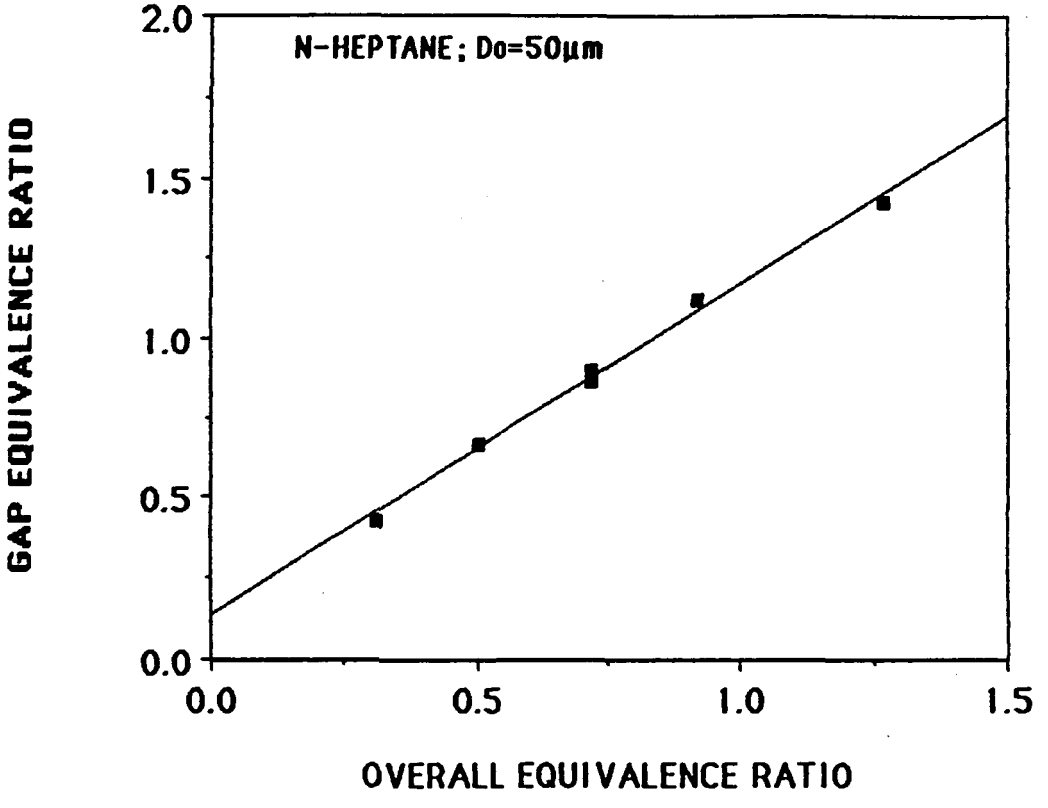

Figure 3.7 Variation of Spark Gap Equivalence Ratio with Overall Equivalence Ratio for N-Heptane Sprays (D_0 = 50 μm; z = 10 cm; Spark Gap = 2 mm)

sprays with 50 μm initial droplet diameters. As seen, ϕ_g was larger than and increased linearly with ϕ_o. These trends were observed for all sprays tested. The uncertainty in ϕ_g was determined from triplicate measurements of the same spray and found to be ± 5%. The symbol ϕ will be used interchangeably with ϕ_g subsequently, while the overall equivalence ratio will be denoted exclusively by ϕ_o.

At this point, a slight digression is in order to report an interesting phenomenon observed during the spray characterization procedures. As will be discussed more fully in Section 3.2.4, the droplet velocities were greater than the air velocities for most of the spray cases studied. For these cases, there existed an instantaneous droplet number density (n_{inst}) which differed from the previously defined droplet number density. The instantaneous number density was a measure of the number of droplets per volume of space (not air). It can be thought of as a snapshot (frozen in time) of the droplets in space. It was determined using an equation similar to that used for the previous number density, but based on the droplet velocity instead of the air velocity:

$$n_{inst} = N/V_d A_p \qquad (3\text{-}4)$$

where N is the LDV droplet rate, V_d is the mean droplet velocity and A_p is the LDV probe area.

A radial profile of the instantaneous droplet number density compared to the droplet number density is shown in Figure 3.8 for a 50 μm initial droplet diameter methanol spray with an overall equivalence ratio of 0.42. As seen in Figure 3.8, the instantaneous number densities are less than the spray number densities. In the time frame of an ignition spark (≈100 μs), the

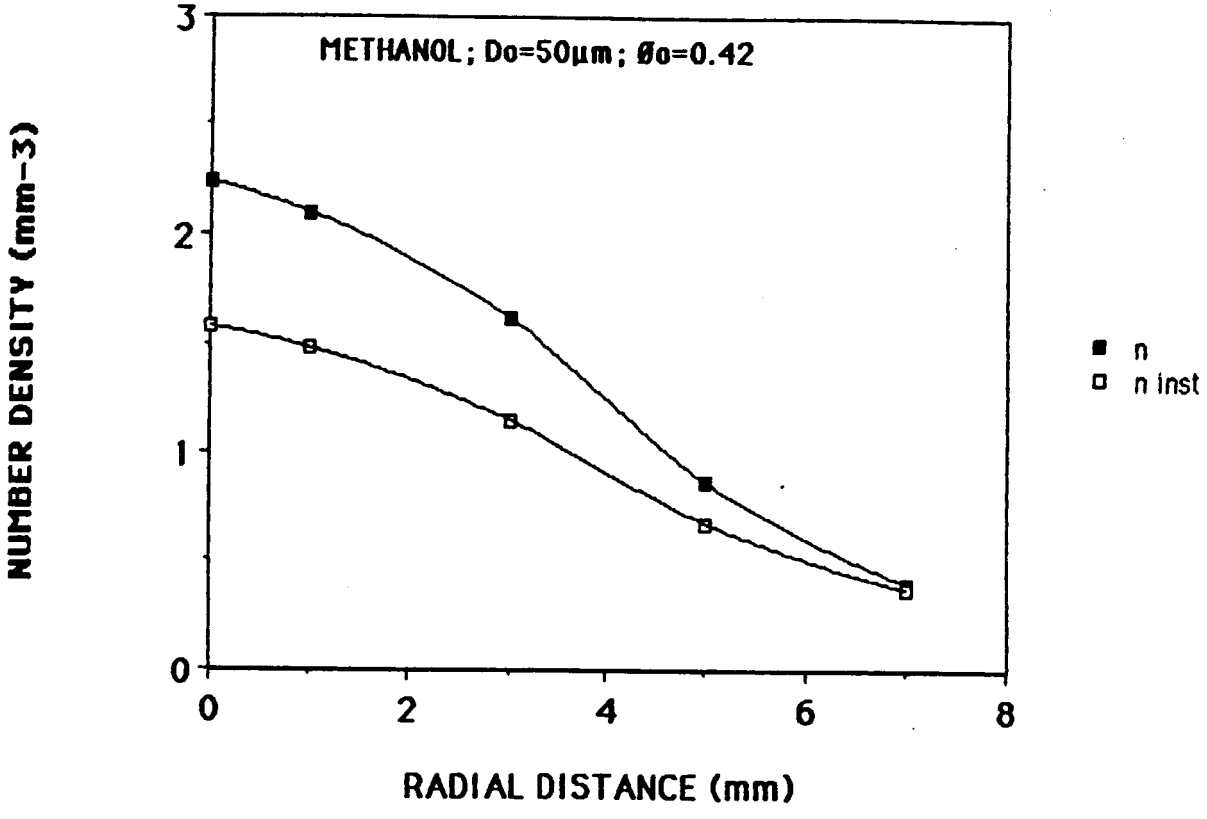

Figure 3.8 Radial Profiles of Instantaneous Droplet Number Density and Droplet Number Density for a Methanol Spray (D_0 = 50 µm; $Ø_0$ = 0.42; z = 10 cm)

instantaneous number density is the more relevant quantity of the two to consider when characterizing the spray. However, for ignition to occur, the spark kernel must propagate into the surrounding mixture. The time frame of this propagation, based on the flame speed and width of the test section, is on the order of several milliseconds. During this time, the flux of both fuel and air across the kernel boundary must be considered. Therefore, the droplet number density based on the air velocity (n) is more relevant to ignition and will be used exclusively to characterize the spray equivalence ratios in the subsequent reporting and analysis of ignition data.

3.2.3 LDV Probe Area

The LDV probe volume is the ellipsoidal region where the two laser beams cross, creating the fringe pattern which produces Doppler bursts when traversed by a droplet. These Doppler bursts are analyzed to determine the droplet velocity, and are counted to determine the droplet rate or frequency. The LDV probe area (A_p) is the projection of the probe volume normal to the spray direction. The size of the probe area is a function of: the diameter of the laser beams; the diameter of the droplets traversing it; the index of refraction of the droplets; the laser wavelength and power; the LDV optics; and the LDV processor electronics. A_p was determined in the following manner and subsequently used in the spray characterization procedure described in section 3.2.2.

Measurements of droplet rate (N) were made in a grid pattern over the entire cross section of the spray, as seen in Figure 3.9. The droplet rate measured in the center of each 4 mm^2 grid sector was assumed to represent the average droplet rate through the entire sector. The ratio of A_p to the sector area (A_i) was equal to the ratio of measured drop rate ($N_{p,i}$) to the

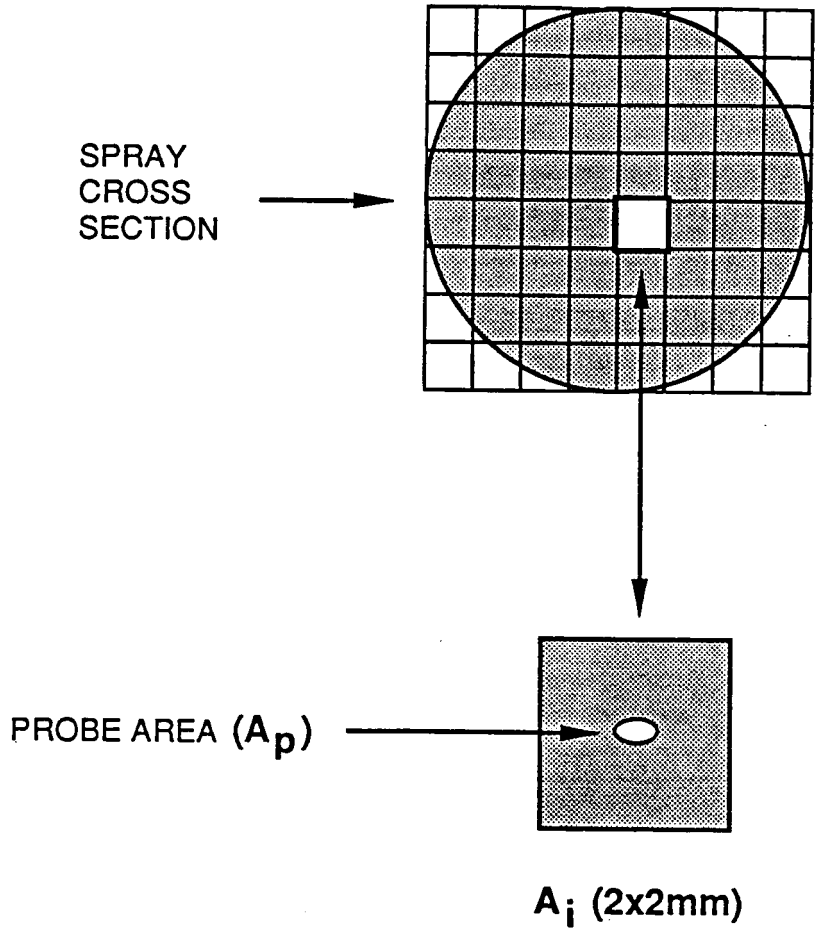

Figure 3.9 Schematic Diagram of Grid Measurement Pattern for Spray Characterization and Probe Area Calibration Procedures

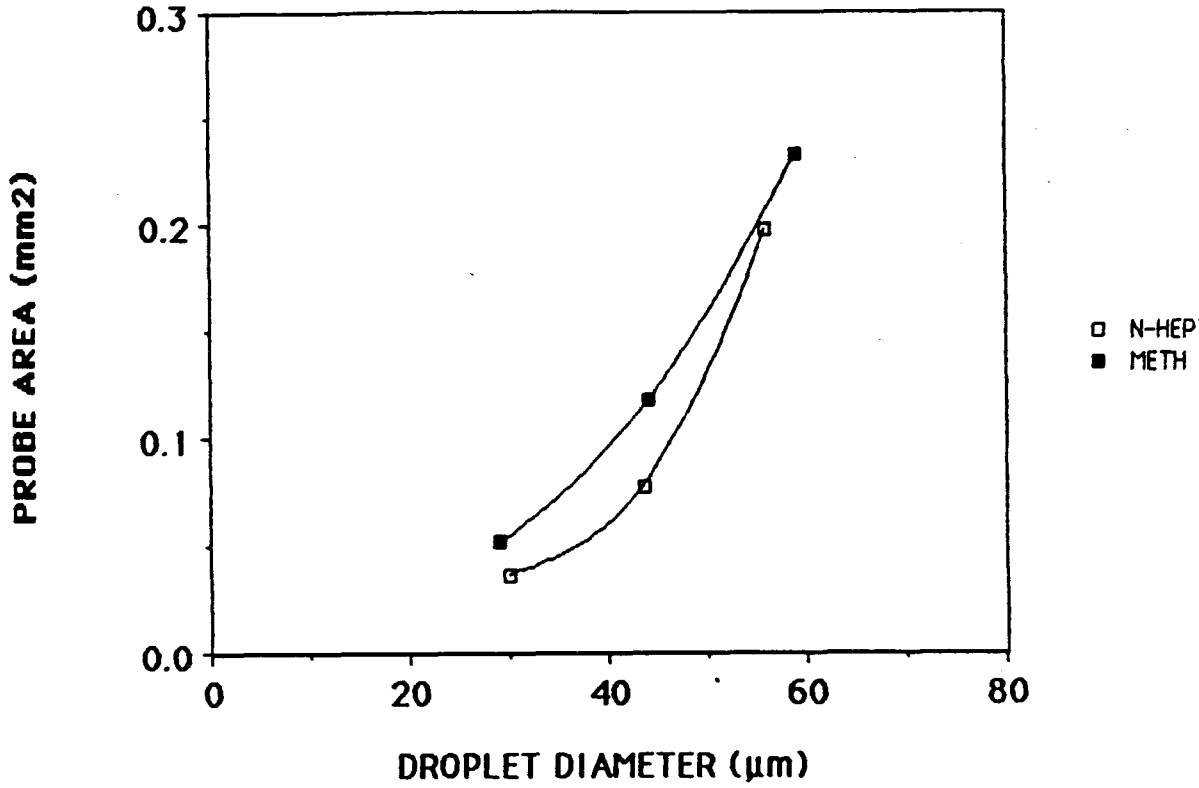

Figure 3.10 Effect of Droplet Diameter on the Effective Probe Area for N-Heptane and Methanol Sprays

total droplet rate (N_i) traversing A_i. From conservation of droplets, the sum of N_i over the entire spray was equal to the droplet generation rate (f_d). Therefore, the probe area was calculated by:

$$A_p = (\Sigma_i N_{p,i}) A_i / f_d \qquad (3\text{-}5)$$

These values were then used in Equations 3-2 and 3-4 to calculate the spray number densities. Measured values of the probe area are shown as a function of droplet diameter and fuel type in Figure 3.10. As seen, the probe area varied from about 0.03 to 0.23 mm^2, increasing with increasing droplet diameter. This was expected, since the intensity of scattered light increases with the diameter of the scattering particle squared.

3.2.4 Air and Droplet Velocity

For dilute sprays, such as those used in this study, it can be assumed that the fuel droplets have a negligible effect on the air flow (Faeth, 1979). Therefore, axial and radial air velocity profiles were measured initially over the entire range of air flow conditions and applied to all spray conditions tested in this study.

Mean air velocities were measured with the LDV using the smallest droplets attainable (17 μm initial droplet diameter) as the flow seed. Some justification for this is required, as a 17 μm particle may seem too large to follow the air flow. Figure 3.11 shows the effect of droplet size on droplet velocity over the range of air flow rates used in the study. These data were taken for n-heptane sprays at the centerline of the test section at an axial distance 10 cm downstream of the dispersion orifice. As seen, the droplet velocities asymptotically approached a constant value as the initial droplet

diameter decreased below 24 μm. This indicates that the smaller droplets have relaxed to the air velocity and can be used with the LDV to measure air velocities. It also indicates that the larger droplets (above 24 μm) are travelling faster than the air at this location in the test section. To further illustrate the difference in velocity between the droplets and the air in the sprays, Figure 3.12 compares axial velocity profiles of 17 and 70 μm initial diameter droplets as they proceed downstream from the dispersion orifice along the test section centerline (recall that the 17 μm droplets are following the air velocity). Because the 70 μm droplets are exiting from a larger diameter fuel orifice, they start out more slowly than the smaller droplets. Further downstream however, the larger droplets maintain a higher velocity due to their inertia, while the velocity of the smaller droplets and air relaxes more quickly. Therefore, by the time the spray has reached the ignition electrodes, the larger droplets are traveling faster than the air. Droplet Reynolds numbers in the sprays, based on the droplet diameter and slip velocity, ranged from 0.1-1.0, increasing with increasing droplet diameter.

Typical profiles of the radial variation of mean air and droplet velocities across the test section are shown in Figure 3.13. The droplet profiles were measured 10 cm axially downstream for methanol sprays with an overall equivalence ratio of 0.7 and initial droplet diameters of 35, 50 and 65 μm. Notice that both the air and droplet profiles are relatively constant across the center of the test section and tail off towards the edge. Again, the increase in droplet velocity with increasing size is clearly seen. It should be noted that the methanol sprays generally had higher droplet velocities than the n-heptane sprays. This is because methanol required roughly double the fuel flow rate of n-heptane to achieve the same equivalence ratio, as

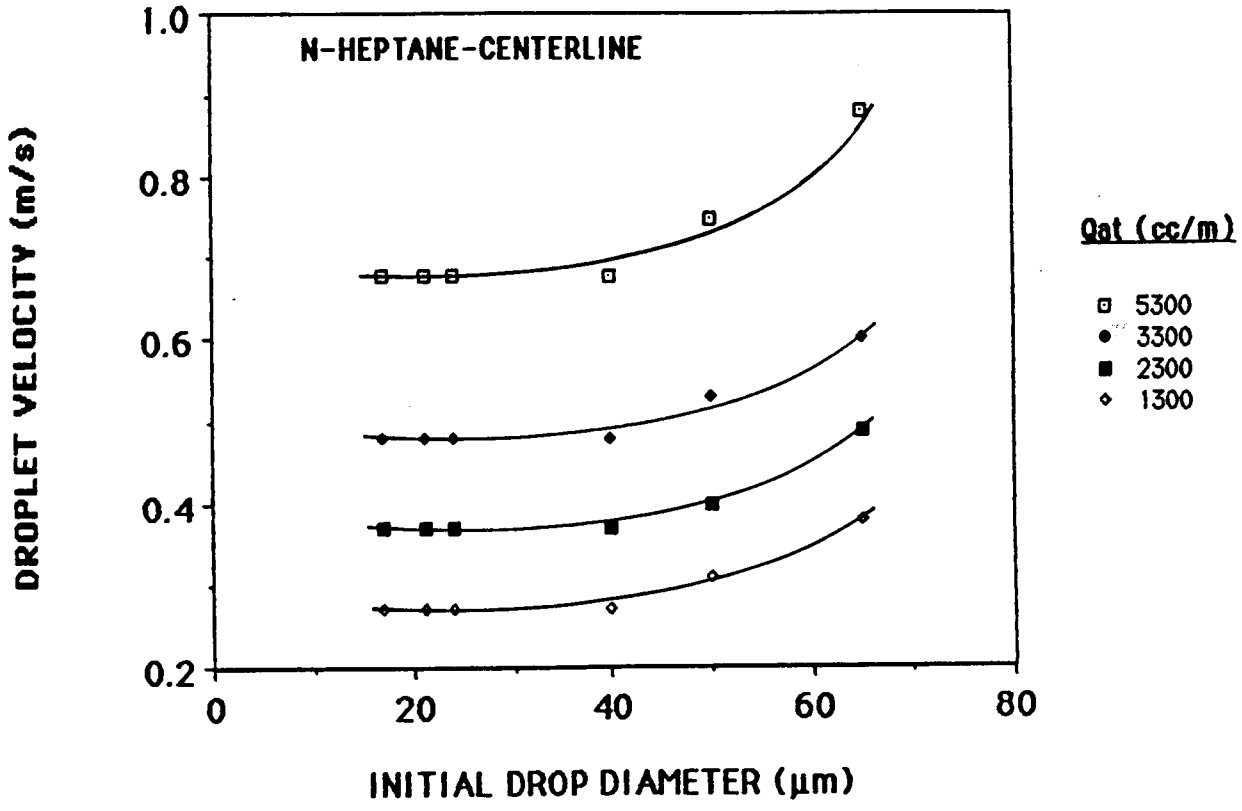

Figure 3.11 Effect of Initial Droplet Diameter on Mean Droplet Velocity for N-Heptane Sprays of Varying Total Air Flow Rates (z = 10 cm)

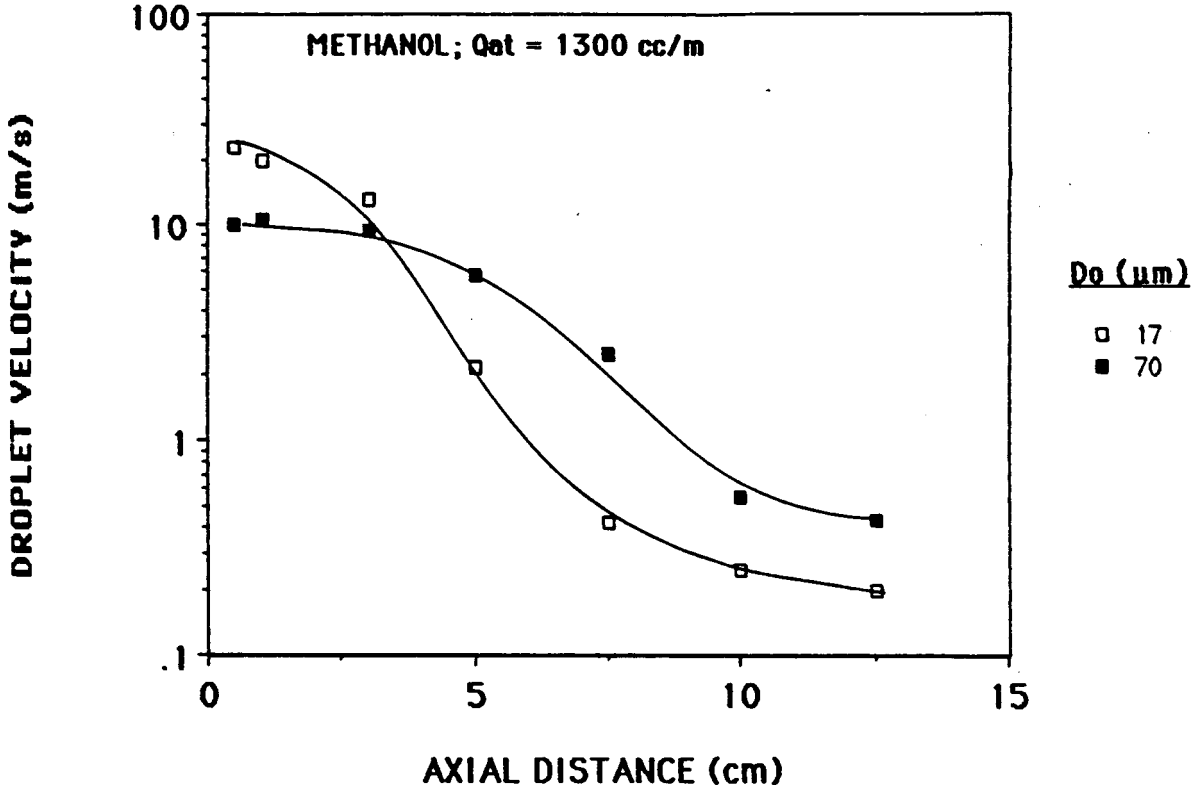

Figure 3.12 Axial Profiles of Mean Droplet Velocity for 17 and 70 µm Initial Droplet Diameter Methanol Sprays ($Ø_0$ = 1.27; r = 0 mm)

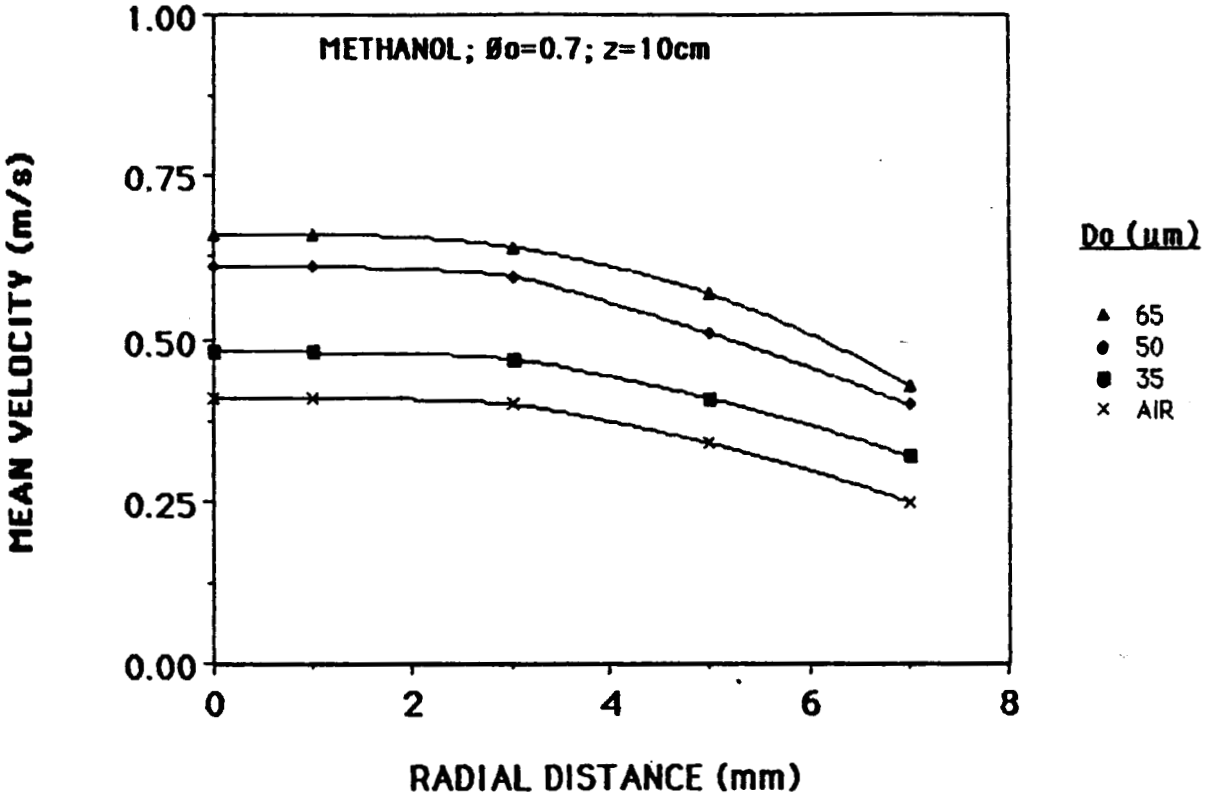

Figure 3.13 Radial Profiles of Mean Droplet and Air Velocity for Methanol Sprays of Varying Initial Droplet Diameter ($Ø_0$ = 0.7; z = 10 cm)

discussed previously. These higher fuel flow rates meant higher orifice exit velocities for the methanol droplets, which resulted in higher velocities downstream. It should also be noted that conservation of mass was obtained upon integrating the air velocity profiles across the section for all cases tested.

RMS velocities were measured using the LDV system and converted to turbulent intensity by dividing by the mean velocity. Values of turbulent intensity for the droplet velocities ranged from 20-25 % at the center of the sprays (r = 0-5 mm) and increased slightly towards the edges. In general, the turbulent intensity of the droplet velocities increased with decreasing velocity and decreasing droplet size.

3.3 Droplet Size Measurement

3.3.1 Droplet Sizing System

A Fraunhofer diffraction technique, based on a method developed by Dobbins et al. (1963) for polydisperse sprays, was used to measure the diameter of the droplets at the spark gap. A schematic of the droplet sizing system is given in Figure 3.14, and the method is described as follows. A collimated He-Ne laser beam was passed through the sprays, and the light diffracted by the droplets was focused by a 200 mm focal length collecting lens onto a photographic plate. If the diffracting droplets were monosized, the diffracted light appeared as a series of alternating light and dark concentric rings known as an Airy or Fraunhofer diffraction pattern (Dobbins et al., 1963). A photograph of the diffraction pattern produced by a 50 µm methanol spray is shown in Figure 3.15. The bright center of the pattern is due to the incident laser beam. Four sets of dark and light diffraction rings are clearly visible around the center. The intensity of the bright rings

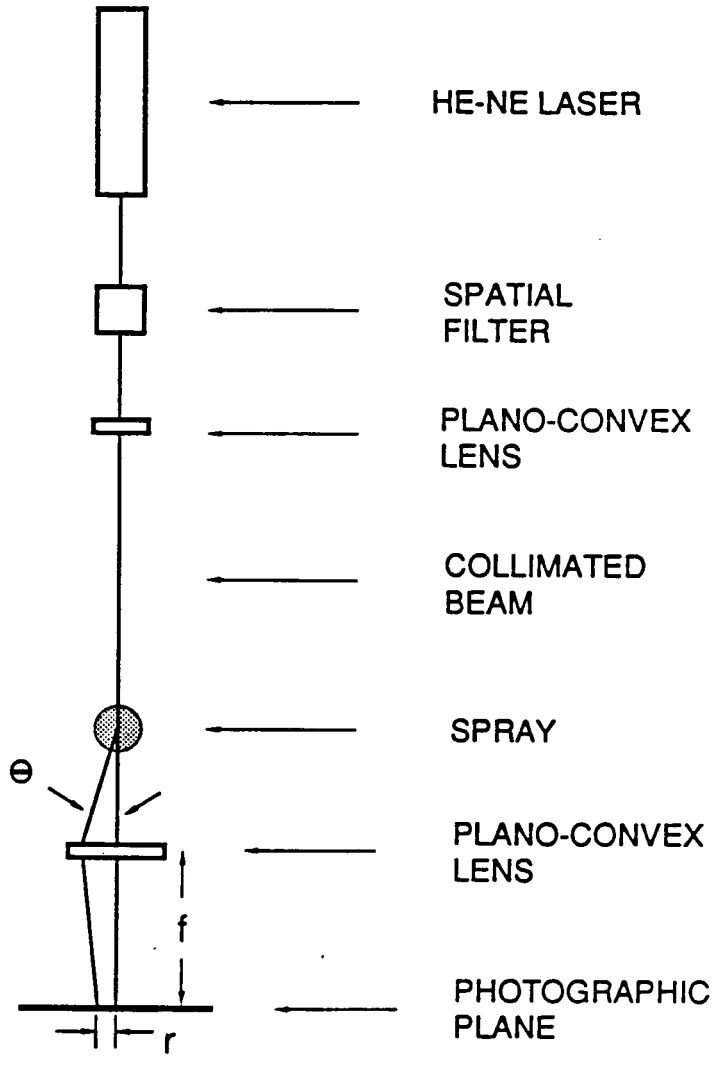

Figure 3.14 Schematic Diagram of the Droplet Sizing Apparatus

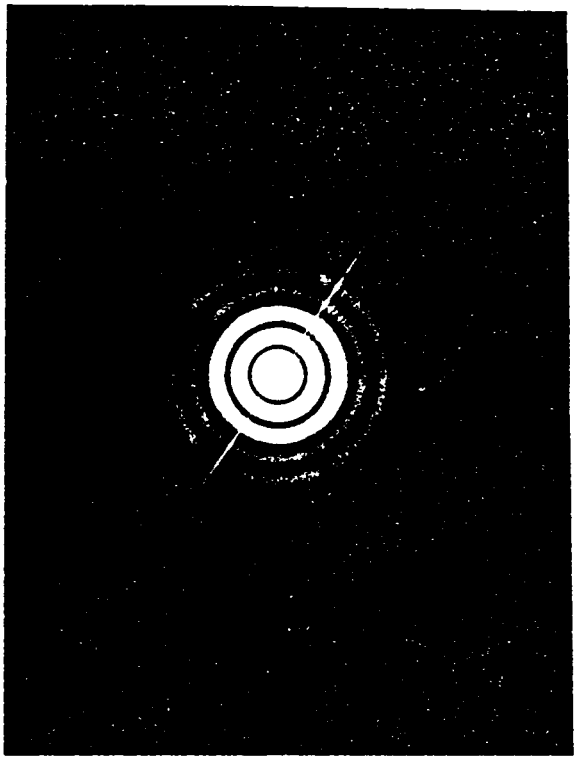

Figure 3.15 Photograph of a Fraunhofer Diffraction Pattern produced by a 50 μm Methanol Spray

decreased radially outward, so there were actually several sets of larger rings not observed due to the resolution of the film. The size of the spray droplets was obtained by measuring the radii of these light and dark rings, based on the following analysis.

The radial intensity distribution of a Fraunhofer diffraction pattern in the focal plane of the collecting lens is given by (Dobbins et al., 1963):

$$I(\theta)/I(0) = (2J_1(\alpha\theta)/\alpha\theta)^2 \qquad (3\text{-}6)$$

where $I(\theta)/I(0)$ is the ratio of the intensity of diffracted light at angle θ to the incident light intensity. J_1 is a Bessel function of the first kind. α is the particle size number given by: $\alpha = \pi D/\lambda$, where D is the diameter of the diffracting droplets and λ is the light wavelength (0.6328 μm). The collecting lens transforms the angular diffraction information to a radial coordinate system (with the small angle approximation) by the following relation: $\sin\theta \approx \theta \approx r/f$, where r is the radius on the focal plane of the lens of the light diffracted at an angle θ, and f is the focal length of the lens. This allows $\alpha\theta$ to be expressed as:

$$\alpha\theta = \pi D r/f\lambda \qquad (3\text{-}7)$$

The dark rings in the diffraction patterns occur when the diffracted light is zero, or at zeros of the Bessel function $J_1(\alpha\theta)$. These zeros occur at $\alpha\theta$ = 3.83, 7.02, 10.17, 13.32, 16.4, etc. The diameter of the diffracting droplets was directly determined by measuring the radius of the center of the dark rings and using the values of the Bessel function zeros above with Equation 3-7. The resulting equation for the droplet diameter is:

$$D = B_i \lambda f / \pi r_i \qquad (3\text{-}8)$$

where B_i is the i 'th zero of the Bessel function and r_i is the radius of the center of the i 'th dark ring. It can also be shown that the bright rings correspond to the zeros of a second Bessel function $J_2(\alpha\theta)$, occuring at $\alpha\theta$ = 5.14, 8.42, 11.62, 14.8, 17.96, etc. Therefore, the diameter of the spray droplets could also be determined with Equation 3-8 by measuring the radius of the light rings and using the zeros of $J_2(\alpha\theta)$.

The total number of rings measured for any given diffraction pattern varied from 4 to 8, increasing with increasing droplet diameter. The uncertainty in this droplet sizing technique was ± 1%, based on the variation in droplet diameter from multiple ring measurements.

Using this method, the droplet diameter at the spark gap (D_g) was measured for each of the sprays tested in this study. Representative photographs of the diffraction patterns obtained for the entire range of fuel and droplet size sprays tested are given in Appendix A. Comprehensive droplet sizing results are given in the next chapter in Tables 4.2 and 4.3. For a given fuel and droplet size spray, there was less than 5% variation in the measured spark gap droplet diameter over the entire range of equivalence ratios.

Figure 3.16 shows the axial variation in droplet diameter for methanol and n-heptane sprays of 50 μm initial droplet diameter and overall equivalence ratio of 1.0. The n-heptane droplets evaporated faster due to their greater volatility. The n-heptane sprays also had lower droplet velocities than the methanol sprays, as discussed in the previous section. This meant longer residence times between generation and ignition, which also led to enhanced evaporation.

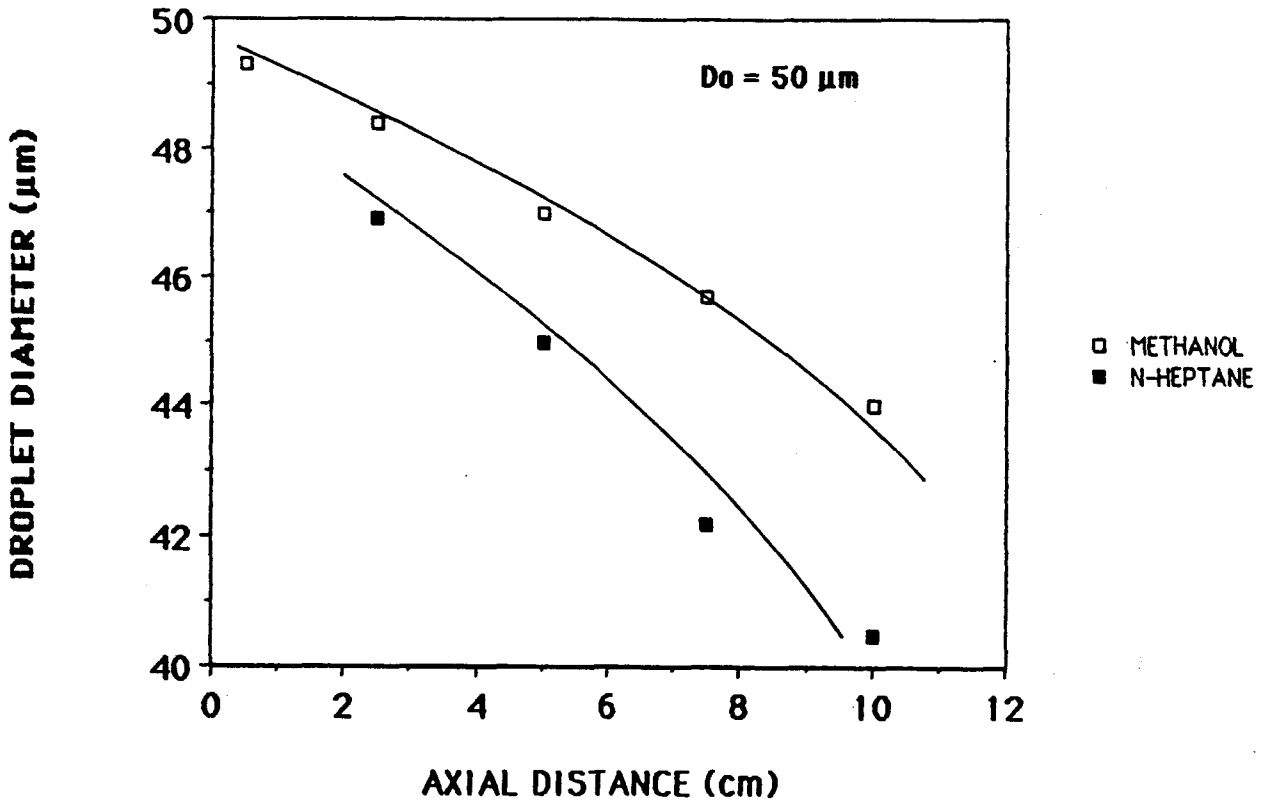

Figure 3.16 Axial Variation in Droplet Diameter for 50 µm Initial Droplet Diameter N-Heptane and Methanol Sprays (r = 0 mm)

Droplet size measurements were performed at the centerline of the test section. Since the droplet sizing technique made a line of sight average through the entire spray, no effect of radial position was expected. This was confirmed by measuring the drop size of a 50 μm n-heptane spray at three different radial positions (-4, 0 and 4 mm). The measured values were all within 1 %.

3.3.2 Extent of Prevaporization

The amount of evaporated fuel present in a spray is a critical factor in ignition (Ballal and Lefebvre, 1976). Increasing the extent of prevaporization not only decreases the energy required to evaporate the fuel droplets in the spark kernel, it also increases the rate of propagation, or growth, of the kernel into the unburned mixture. Therefore, an accurate measure of the extent of prevaporization was necessary for the sprays tested in this study.

The extent of prevaporization (Ω) was defined as the ratio of the mass of evaporated fuel to the mass of total fuel present. For the prevaporized, premixed cases, Ω was equal to one. For the sprays, Ω was determined at the spark gap based on the initial droplet diameter and the measured droplet diameter at the spark gap. Values of Ω are presented in the next chapter in Tables 4.2 and 4.3 for the sprays tested. Ω was kept relatively constant (within 5%) for each fuel. This was done by varying the axial location of the ignition electrodes. For example, the smaller droplet size sprays, which evaporated more quickly, were ignited at at smaller axial distance downstream.

3.4 Spray Ignition

3.4.1 Spark Generation System

Ignition sparks were delivered to the sprays by electrodes which protruded into the test section at axial distances 7.5, 10 and 12.5 cm below the dispersion orifice. The electrodes were placed with their axes normal to the spray direction, and were mounted on a micrometer traversing assembly which was used to adjust the spark gap width. The electrodes were 5 mm diameter stainless steel rods, with the spark producing ends machined to tips of 1 mm diameter and 6 mm length. The high voltage side electrode tip was pointed while the ground side tip was flat, as seen in Figure 3.17. The tips were bent upward approximately 15° to prevent accumulation of fuel droplets on them.

A capacitive discharge spark generation system produced the ignition sparks at the electrodes. The system was designed to provide independent control of the energy and duration of individual sparks, and consisted of a modified RC circuit as shown in Figure 3.18.

Sparks were generated in the following manner. The capacitor (0.5-50nF) was charged to 20 kV by closing the charging switch for 2 seconds. The charging switch was then opened. The spark was generated immediately afterward by closing the discharge switch, which caused the capacitor to discharge through the resistor (1-1000 kΩ) and across the electrode gap to ground. The two switches were high voltage solenoid switches, and were controlled by timing relays which allowed repetition of the charge/discharge cycle. The time interval between sparks could be varied from 3-15 seconds. The charging resistor was used to limit the current during charging, while the shunt resistor provided an alternative path to ground in cases where the discharging current could not jump the

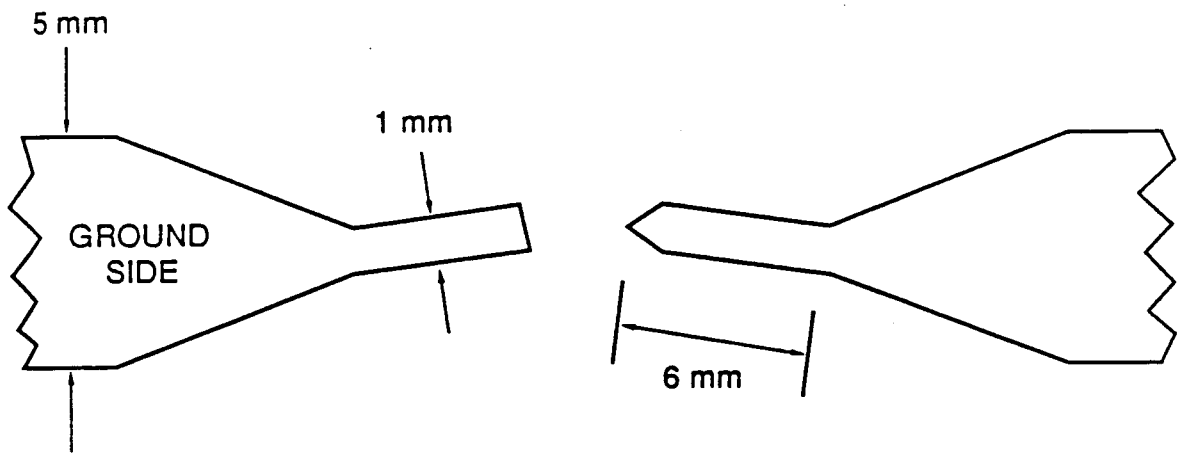

Figure 3.17 Ignition Electrode Tip Configuration

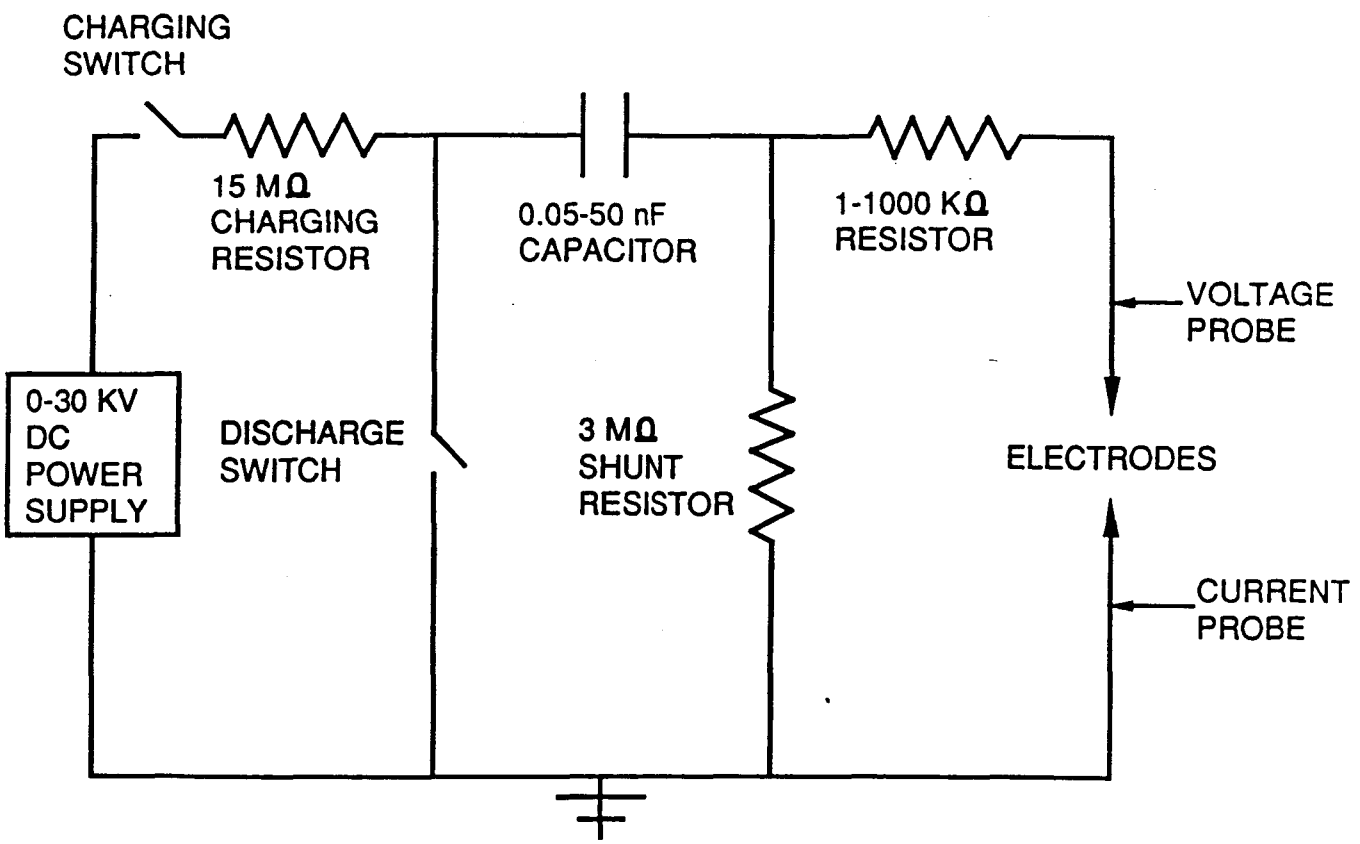

Figure 3.18 Schematic Diagram of the Spark Generation Circuit

spark gap.

The spark energy and duration were determined by the values of the capacitor and the resistor in the circuit. To measure the spark energy and duration, a high voltage probe was connected across the electrodes, and an inductive current probe was attached to the ground-side electrode. The resulting voltage and current traces of the spark were recorded on a two channel digital storage oscilloscope. Voltage, current and energy traces for a typical spark are shown in Figure 3.19. As seen, after the initial spike of the breakdown voltage, the spark voltage was relatively constant throughout the spark duration, while the spark current and energy decayed exponentially. The energy of a given spark was determined from:

$$E = \int_0^t V(t)\, I(t)\, dt \qquad (3\text{-}9)$$

where V is voltage, I is current, t is time. The spark duration, t, was taken as the time required for the spark current to decay to 5% of its initial value.

A series of calibration measurements was performed to determine the spark energy levels of the system described above. This spark energy calibration procedure was done over a wide range of spark gap widths (2-8 mm) and capacitance (0.1-50 nF) for three discreet values of spark duration (30, 60 and 100 µs). These durations were chosen to cover the range of optimum spark durations observed by previous researchers for similar spray conditions, including Rao and Lefebvre (1976), Ballal and Lefebvre (1978) and Chan and Polymeropoulos (1982). Typical results of these calibration measurements are given in Figure 3.20, which shows spark energy as a function of spark gap width for the range of capacitors and a duration of 60 µs. Each data point is the result of two sets of 15 spark energy

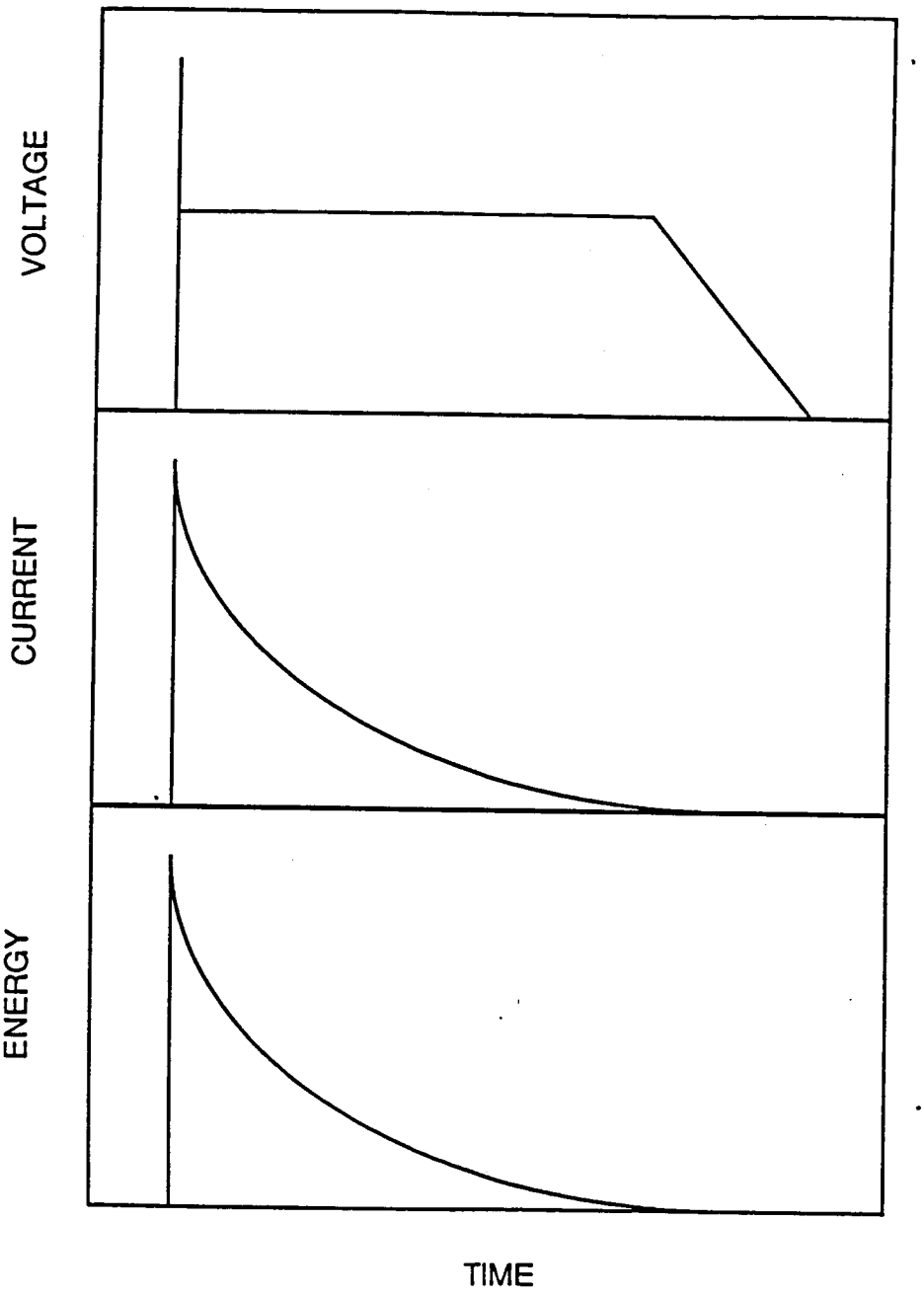

Figure 3.19 Typical Voltage, Current and Energy Traces of Ignition Sparks

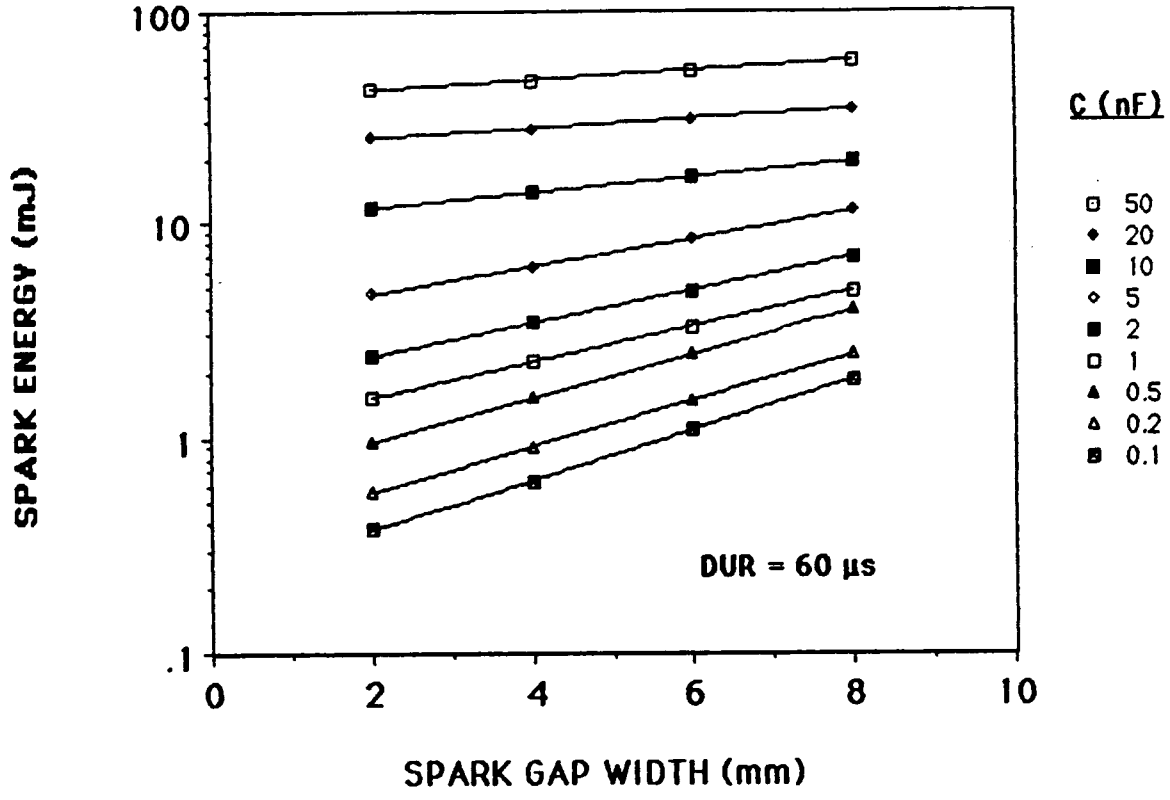

Figure 3.20 Effect of Spark Gap Width on Spark Energy for Varying Capacitor Values (Spark Duration = 60 µs)

measurements, taken on separate days. The standard deviation of each set of 15 measurements was less than 10% of the mean, while the day to day variation in the mean spark energy values was less than 5%. As seen in Figure 3.20, the spark energy varied logarithmically with the spark gap width for a given capacitance, which is seen as a linear relationship on the semi-log plots shown. This calibration procedure was performed in air, but it was subsequently observed that the composition of the mixture in the spark gap affected the measured spark energies by altering the resistance of the spark gap. Therefore, spark energy levels were measured for each individual ignition case studied, as will be described in the following section.

3.4.2 Minimum Ignition Energy Measurement

Spark ignition is a probabilistic phenomenon, as was discussed in Chapter 2. No sharp boundary was observed between spark energies which ignited a given mixture and those which did not. Rather, a range of spark energies was seen for which increasing the spark energy resulted in an increasing probability or frequency of ignition. An example of this is given in Figure 3.21, which shows the effect of spark energy on ignition frequency* for an n-heptane spray (ϕ_g=0.88, D_g=41 μm). Notice that the ignition frequencyrose sharply initially, then tailed off as it assymptotically approached an ignition frequency of 1.0 (100%). Similar behavior was observed for all of the spray and prevaporized ignition cases studied.

---

* The term 'ignition frequency' was employed based on previous usage in the literature. It should be noted, however, that this quantity is not a true frequency, but represents the incidence or probability of ignition.

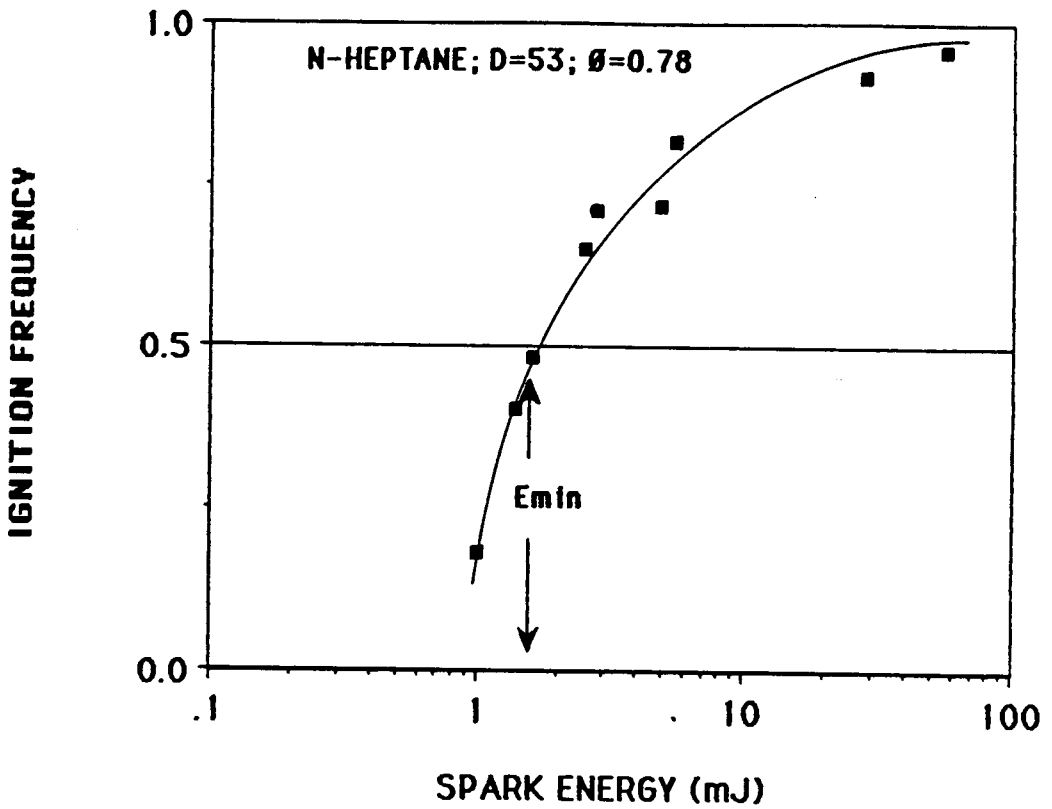

Figure 3.21 Effect of Spark Energy on Ignition Frequency for an N-Heptane Spray (D = 53 µm; Ø = 0.78; z = 12.5 cm)

Each point in Figure 3.21 was the result of ignition observations and spark energy measurements for one set of 50 single sparks. The interval between sparks varied from 5 to 20 seconds, increasing with decreasing equivalence ratio. This interval was always sufficient to allow the temperature and spray conditions in the test section to return to normal after a successful ignition. The criterion for ignition was that a visible flame propagate at least 5 cm into the mixture. The spark energy was measured simultaneously with the ignition observations and averaged for 20 of the 50 sparks, as described in the previous section. A minimum of two sets of 50 sparks was done at each energy level. The values of spark energy and ignition frequency for both sets were within 7% of the mean for all cases studied.

The minimum ignition energy (E_{min}) was defined as the spark energy level which produced an ignition frequency of 0.5 (50% ignition), as shown in Figure 3.21. The 50% level was chosen to account for the probabilistic effects of ignition, as will be described in Chapter 5. The uncertainty in E_{min} was calculated from the 95% confidence intervals of repeated sets of spark energy and ignition frequency measurements and found to be ± 10%.

3.4.3 Spark Parameter Optimization

The ignition frequency curve shown in Figure 3.21 was obtained with fixed values of spark gap width and spark duration. As discussed in Chapter 2, both of these parameters affect ignition. If the spark gap width is too small, excessive heat is lost to the electrodes through conduction. If it is too large, the spark kernel becomes larger than necessary for ignition, resulting in excessive heat lost to the surrounding mixture through convection. If the spark duration is too short, excessive energy is lost in the

accompanying shock wave, whose strength increases with decreasing spark duration. If the duration is too long, spark energy is still being input after ignition has occurred, resulting in convection losses to the mixture. Therefore, optimization of these spark parameters involves minimizing energy losses and must be done to obtain the lowest possible minimum ignition energy for each ignition case studied.

The procedure used to optimize the spark duration and gap width for a given spray case was as follows. The spark energy level (capacitor) which produced ignition frequencies in the 40% to 60% range was determined. With this capacitor, one set of 50 sparks was performed at each of three durations (30, 60 and 100 μs) over a range of gap widths. Starting at a small value, the gap width was increased in steps of 1 mm. For a given duration, the ignition frequency increased with increasing gap width, reached some maximum, then decreased. This was repeated for a larger (or smaller) capacitor in order to obtain ignition frequencies both above and below 50%. The optimum values of duration and gap width were then easily determined as those which resulted in the lowest 50% energy. For cases where the optimum duration was 30 or 100 μs, durations of 15 and 200 μs respectively were tested to confirm an optimum value.

CHAPTER 4

EXPERIMENTAL RESULTS AND DISCUSSION

The effects of droplet size, equivalence ratio and fuel properties on the minimum ignition energy of n-heptane and methanol sprays are reported in this chapter. Ignition energy results for prevaporized n-heptane and methanol mixtures are also reported to represent the lower limit of droplet size. Valuable insight into the ignition phenomenon is gained by comparing the spray and prevaporized results as a function of both equivalence ratio and droplet diameter.

4.1 Spray Ignition

4.1.1 Operating Conditions

The generation parameters and flow rates used to produce the n-heptane and methanol sprays ignited in this study are listed in Table 4.1. Also included are initial droplet diameters and overall equivalence ratios. As seen, air flow rates for the methanol and n-heptane sprays were similar, but methanol sprays required roughly double the fuel flow rates to achieve the same range of stoichiometry because of the fuel bound oxygen. For a given fuel and drop size spray, the dispersion air flow rate was set just high enough to adequately disperse the droplets. For a given drop size spray, the equivalence ratio was varied by adjusting the dilution air flow rate.

FUEL: N-HEPTANE

Do = 40 μm

Øo	Qf (cc/m)	fd (kHz)	O (μm)	Qadis(cc/m)	Qadil(cc/m)
1.04	0.18	89.6	17	1000	500
0.78	"	"	"	"	1000
0.52	"	"	"	"	2000
0.39	"	"	"	"	3000

Do = 50 μm

Øo	Qf (cc/m)	fd (kHz)	O (μm)	Qadis(cc/m)	Qadil(cc/m)
1.26	0.19	48.4	22	1300	0
0.94	"	"	"	"	450
0.75	"	"	"	"	900
0.55	"	"	"	"	1700
0.35	"	"	"	"	3400

Do = 65 μm

Øo	Qf (cc/m)	fd (kHz)	O (μm)	Qadis(cc/m)	Qadil(cc/m)
1.27	0.19	22.0	27	1300	0
0.92	"	"	"	"	500
0.72	"	"	"	"	1000
0.50	"	"	"	"	2000
0.34	"	"	"	"	3500

FUEL: METHANOL

Do = 35 μm

Øo	Qf (cc/m)	fd (kHz)	O (μm)	Qadis(cc/m)	Qadil(cc/m)
1.00	0.35	260.0	17	1500	0
0.80	"	"	"	"	500
0.67	"	"	"	"	1000
0.50	"	"	"	"	2000

Do = 50 μm

Øo	Qf (cc/m)	fd (kHz)	O (μm)	Qadis(cc/m)	Qadil(cc/m)
1.04	0.37	94.3	22	1500	0
0.84	"	"	"	"	500
0.60	"	"	"	"	1500
0.42	"	"	"	"	3000
0.30	"	"	"	"	5000

Do = 65 μm

Øo	Qf (cc/m)	fd (kHz)	O (μm)	Qadis(cc/m)	Qadil(cc/m)
1.17	0.38	43.6	27	1300	0
0.92	"	"	"	"	500
0.66	"	"	"	"	1500
0.44	"	"	"	"	3000
0.31	"	"	"	"	5000

Table 4.1 Spray Generation Parameters and Operating Conditions

Tables 4.2 and 4.3 contain values of the relevant spray parameters measured at the spark gap, as described in Chapter 3, for n-heptane and methanol sprays, respectively. Also included are the optimized ignition parameters and measured minimum ignition energies, which will be discussed in the next section.

While the tables are straightforward, several points should be noted. The axial location (z) of the ignition electrodes was varied as a function of droplet size, with the smallest sprays being ignited at the smallest axial distance. This was done for several reasons. The smallest droplets (30 and 33 μm) spread to a greater degree than the larger droplets as they progressed downstream. This resulted in droplet impaction, beginning about 10 cm downstream, on the test section walls. To solve this problem, the ignition electrodes were moved upward to an axial location of 7.5 cm where the sprays just filled the test section with no impaction. Conversely, the largest sprays (53 and 57 μm) did not spread sufficiently by the time they had reached 10 cm downstream. For these larger droplets the electrodes were moved to 12.5 cm where the sprays were more uniform across the test section. This variation in electrode positioning also had the effect of minimizing the difference in the extent of prevaporization between the different sized sprays. This resulted in values of Ω within 5% for a given fuel.

All sprays were generated with liquid fuel and air at 20 °C. The temperatures listed in Tables 4.2 and 4.3 were measured at the spark gap with a type K thermocouple and represent a bulk spray temperature. N-heptane sprays temperatures ranged from 8 to 10 °C while methanol spray temperatures ranged from -1 to 2 °C. The methanol sprays had lower temperatures because of methanol's higher latent heat of vaporization.

FUEL: N-HEPTANE

SPARK GAP SPRAY PARAMETERS:				IGNITION PARAMETERS:			
D = 33 µm Ω = 0.44 z = 7.5 cm							
Ø	Vd (m/s)	Va (m/s)	Red	T (°C)	DUR (µs)	GAP (mm)	Emin (mJ)
1.15	0.59	0.47	0.26	10	60	2	0.31
0.83	0.68	0.54	0.30	10	60	3	0.55
0.60	0.85	0.61	0.52	9	60	6	1.3
0.45	0.96	0.75	0.45	8	100	7	3.8
D = 41 µm Ω = 0.45 z = 10 cm							
Ø	Vd (m/s)	Va (m/s)	Red	T (°C)	DUR (µs)	GAP (mm)	Emin (mJ)
1.42	0.32	0.27	0.13	10	60	2	0.35
1.10	0.37	0.32	0.13	10	60	3	0.45
0.88	0.42	0.36	0.16	9	60	3	0.64
0.69	0.49	0.44	0.13	9	60	4	1.5
0.44	0.67	0.62	0.13	9	60	7	10.5
D = 53 µm Ω = 0.46 z = 12.5 cm							
Ø	Vd (m/s)	Va (m/s)	Red	T (°C)	DUR (µs)	GAP (mm)	Emin (mJ)
1.80	0.31	0.25	0.21	9	60	2	0.45
1.39	0.37	0.32	0.17	9	60	2	0.56
1.13	0.43	0.38	0.17	9	60	3	0.75
0.78	0.52	0.48	0.14	8	60	4	1.7
0.59	0.79	0.64	0.52	8	100	4	3.9

Table 4.2 N-Heptane Spray Characterization and Ignition Results

FUEL: METHANOL

SPARK GAP SPRAY PARAMETERS:				IGNITION PARAMETERS:			
D = 30 μm Ω = 0.37 z = 7.5 cm							
Ø	Vd (m/s)	Va (m/s)	Red	T (°C)	DUR (μs)	GAP (mm)	Emin (mJ)
1.15	0.70	0.47	0.45	2	60	4	1.0
0.94	0.83	0.49	0.67	1	60	4	1.2
0.82	0.94	0.56	0.75	0	60	5	1.6
0.63	1.01	0.63	0.75	0	100	6	3.2
D = 44 μm Ω = 0.32 z = 10 cm							
Ø	Vd (m/s)	Va (m/s)	Red	T (°C)	DUR (μs)	GAP (mm)	Emin (mJ)
1.17	0.45	0.28	0.50	1	60	5	2.1
0.99	0.53	0.33	0.59	0	60	5	2.3
0.79	0.69	0.43	0.75	-1	60	5	3.2
0.59	0.77	0.60	0.49	-1	100	6	8.3
0.45	1.10	0.75	1.01	-1	100	8	29
D = 57 μm Ω = 0.33 z = 12.5 cm							
Ø	Vd (m/s)	Va (m/s)	Red	T (°C)	DUR (μs)	GAP (mm)	Emin (mJ)
1.51	0.43	0.25	0.67	0	60	4	2.1
1.25	0.50	0.32	0.67	0	60	5	2.4
0.93	0.66	0.42	0.89	0	100	5	3.5
0.77	0.90	0.58	1.19	-1	100	5	6.2
0.65	1.10	0.80	1.12	-1	100	6	10.2

Table 4.3 Methanol Spray Characterization and Ignition Results

Greater heat transfer from the surrounding air to the droplet was required for evaporation, lowering the spray temperature. Both the lower spray temperatures and the higher latent heat decreased the volatility of the methanol sprays, resulting in their lower extent of prevaporization compared to n-heptane sprays.

Mean values of the spray number density at the spark gap varied from 0.5-4.1 mm^{-3} for n-heptane sprays and 1.0-13 mm^{-3} for methanol sprays, increasing with increasing equivalence ratio and decreasing droplet size. Mean values of the interdroplet spacing at the spark gap varied from 20-32 droplet diameters for n-heptane sprays and 15-25 droplet diameters for methanol sprays, increasing with decreasing equivalence ratio and decreasing droplet size.

4.1.2 Spark Duration and Gap Width

Minimum ignition energies were measured at optimum values of the spark duration and spark gap width for each spray tested, as described in Section 3.5.3. These optimum values are listed in Tables 4.2 and 4.3. Optimum values of both the spark duration and gap width decreased with increasing equivalence ratio. Optimum durations ranged from 60 to 100 µs for both n-heptane and methanol sprays. Optimum gap widths ranged from 2-7 mm for n-heptane sprays and 4-8 mm for methanol sprays. These values are in the same range found by previous researchers in similar studies (Rao and Lefebvre, 1976; Ballal and Lefebvre, 1978; Chan, 1982; and Singh, 1986).

Varying the spark gap width was found to have a large effect on E_{min}, while varying the spark duration had little effect. Figure 4.1 shows the effect of spark gap width and duration on the minimum ignition energy of a 41 µm n-heptane spray with an equivalence ratio of 0.69. As seen, varying the

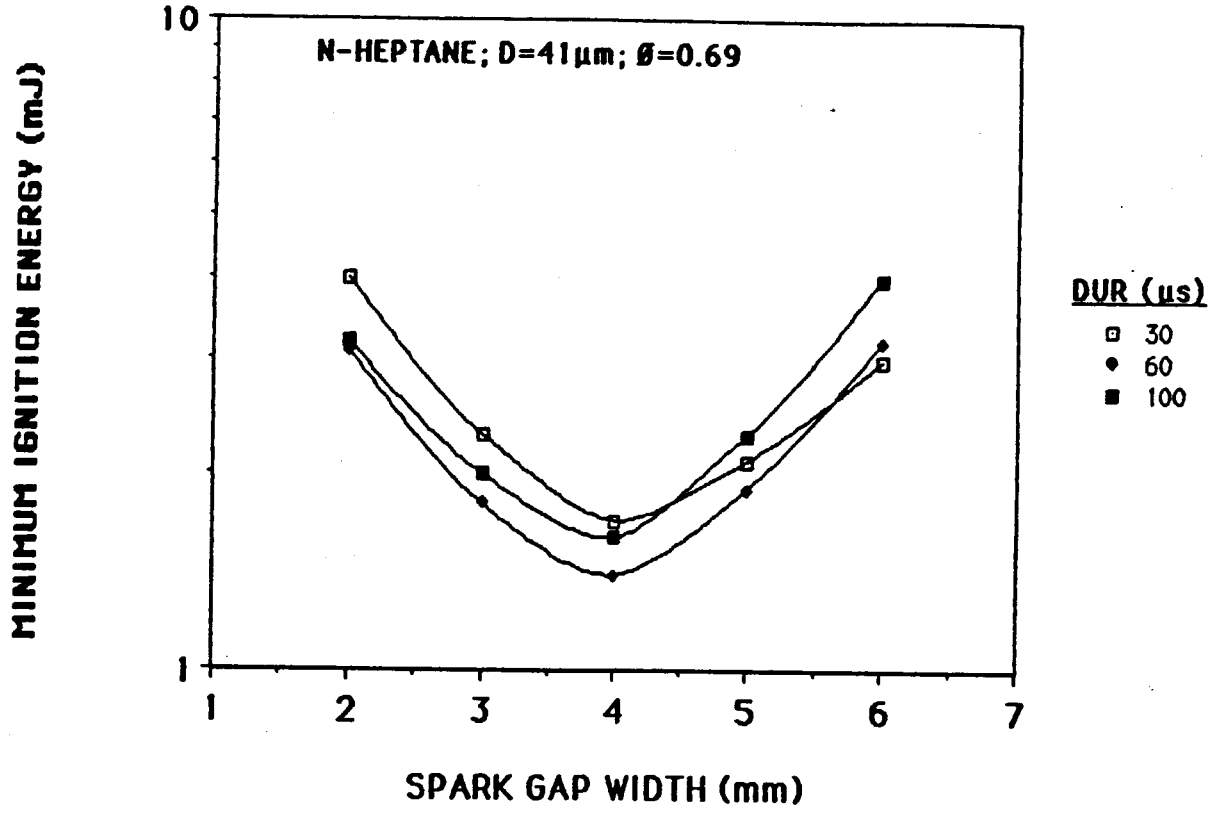

Figure 4.1 Effect of Spark Gap Width and Spark Duration on the Minimum Ignition Energy of an N-Heptane Spray (D = 41 µm; Ø = 0.69; z = 10 cm)

gap width from 2 to 6 mm had a pronounced effect on E_{min}, with an optimum value of 4 mm clearly evident for each duration. Varying the spark duration from 30 to 100 μs had a lesser effect on E_{min}, but an optimum duration of 60 μs was evident. Similar behavior was observed for all of the sprays tested.

4.1.3 Effect of Droplet Size and Equivalence Ratio

The variation in ignition frequency with spark energy was determined as described previously for the sprays listed in Tables 4.2 and 4.3 . Figure 4.2 shows typical ignition frequency curves for 56 μm n-heptane sprays ranging in equivalence ratio from 0.59 to 1.80. Notice that as Ø decreased from rich to lean, the curves became less vertical and began to tail off towards higher spark energies as they approached 100% ignition. Similar behavior was observed for all cases tested. Ignition frequency curves for all cases are shown in Appendix A.

The minimum ignition energy (E_{min} = 50% ignition) was determined from these ignition frequency curves as described in Section 3.5.2. The effect of equivalence ratio and droplet diameter on E_{min} is shown in Figure 4.3 for n-heptane and methanol sprays. As can be seen, both sets of curves are very similar qualitatively. For a given droplet size and fuel spray, E_{min} decreased sharply with increasing lean equivalence ratio, but began to level off as the sprays became richer. E_{min} continually decreased with increasing equivalence ratio and no optimum value of equivalence ratio for ignition was observed for any of the sprays tested. The lean ignition limit was determined to be about Ø = 0.4 for both n-heptane and methanol sprays. For any given equivalence ratio and fuel spray, E_{min} decreased with decreasing droplet size.

Similar behavior of E_{min} with respect to droplet size and equivalence

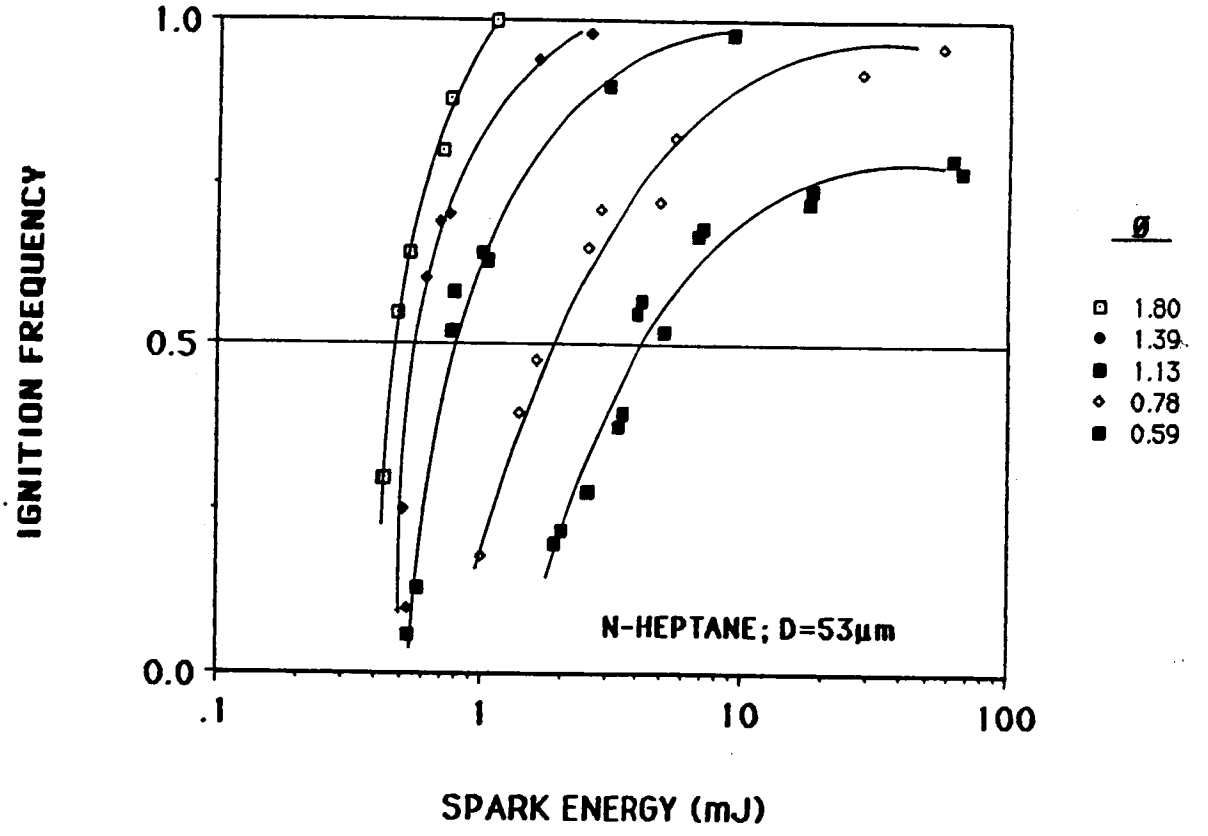

Figure 4.2 Effect of Spark Energy and Equivalence Ratio on the Ignition Frequency of N-Heptane Sprays (D = 53 µm; z = 12.5 cm)

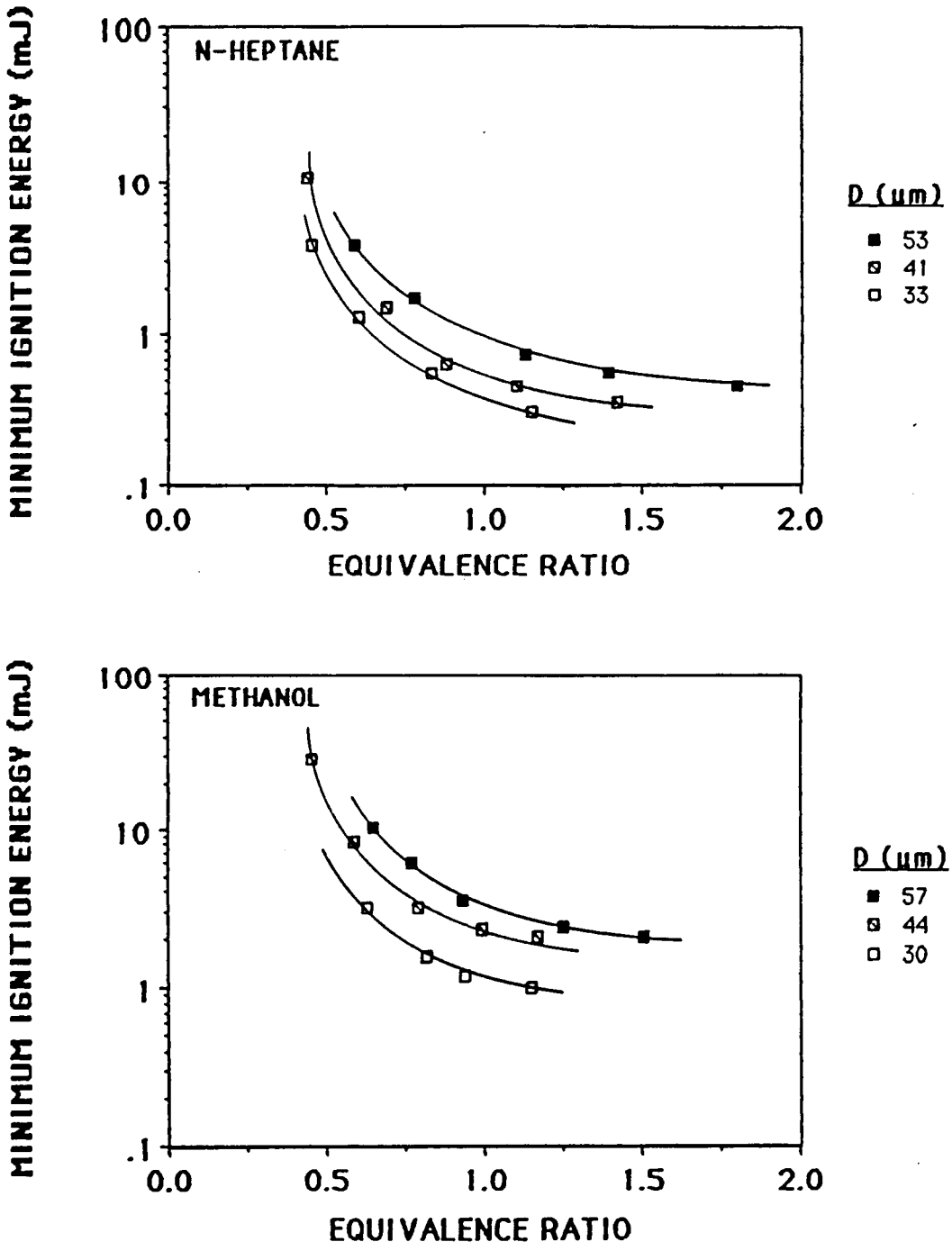

Figure 4.3 Effect of Equivalence Ratio and Droplet Diameter on the Minimum Ignition Energy of N-Heptane and Methanol Sprays

ratio has been observed in previous ignition studies with sprays in the same size range (Rao and Lefebvre, 1976; Ballal and Lefebvre, 1978 and 1981). The decrease in E_{min} with decreasing droplet size and increasing equivalence ratio can be explained as follows. For a given equivalence ratio, the smaller sprays had more total surface area of fuel which decreased the time required for the droplets to vaporize and burn in the spark kernel. The larger droplets took longer to vaporize and burn in the spark gap, resulting in energy losses to the unburned mixture. Therefore, more ignition energy was required for larger droplet size sprays. For a given droplet size, increasing the equivalence ratio improved ignition by increasing the amount of fuel in and around the spark kernel. This effect became less pronounced as the sprays became richer.

4.1.4 Effect of Fuel Properties

As seen in Figures 4.3, the methanol sprays required roughly 3 times more spark energy for ignition than the n-heptane sprays. This can be explained by examining the relative volatilities of the two fuels. Previous researchers (Ballal and Lefebvre, 1978; Peters and Mellor, 1980) have shown that fuel volatility is a critical factor in spray ignition, with E_{min} decreasing with increasing volatility. The volatility of the fuel in the spark kernel during ignition can be quantified in terms of a combustion mass transfer number (B) which may be defined as the ratio of the energy available for evaporation to the energy required for evaporation. Values of B (Kanury, 1975) were 5.82 and 2.70 for n-heptane and methanol, respectively. N-heptane's higher volatility, more than twice methanol's, accounted in a large part for the better ignitability of n-heptane sprays.

Increasing the extent of fuel prevaporization prior to ignition (Ω) has

also been shown to reduce ignition energy requirements (Ballal and Lefebvre, 1981). Values of Ω for the methanol sprays were about 25% lower than for the n-heptane sprays, as seen in Tables 4.2 and 4.3. This difference in Ω also accounted in some part for methanol's higher ignition energies. The relative importance of fuel prevaporization and volatility on ignition will be further examined analytically in Chapter 5.

Several differences between n-heptane and methanol combustion were observed in the types of flames produced by ignition. For very lean cases (Ø < 0.5) the n-heptane flames were faint blue in color. As Ø increased beyond 0.5, they became a brighter orange color. This indicated increasing soot formation and oxidation. In fact, the soot had to be cleaned from the electrodes often while testing n-heptane sprays. The methanol flames were a very faint blue color at lean equivalence ratios and became faint orange with increasing Ø, indicating very little sooting. This was confirmed by the fact that the electrodes showed no soot accumulation during methanol ignition.

4.2 Prevaporized Ignition

4.2.1. Operating Conditions

Ignition energy experiments were performed on prevaporized, premixed flowing n-heptane and methanol mixtures over the full range of equivalence ratios attainable. The fuel and air flow rates used to produce these mixtures are listed in Table 4.4, along with the measured minimum ignition energies and optimized spark parameters. The ignition electrodes were located 10 cm downstream axially for all prevaporized experiments. The mixture temperatures at the spark gap were 25 °C ± 1 for all cases. Equivalence ratios higher than 3.0 could not be tested for n-heptane mixtures because of

MIXTURE PARAMETERS:			IGNITION PARAMETERS:		
N-HEPTANE					
Ø	**Qf (cc/m)**	**Qa (cc/m)**	**DUR (μs)**	**GAP (mm)**	**Emin (mJ)**
0.6	0.19	2750	100	9	≈ 1000
0.65	"	2538	60	8	20
0.7	"	2357	30	7	2.9
0.8	"	2062	30	6	0.70
0.9	"	1833	30	5	0.40
1.0	"	1650	30	4	0.34
1.5	"	1100	-	-	< 0.2
2.0	"	825	-	-	< 0.2
2.5	"	660	30	4	0.43
3.0	"	550	30	7	2.0
METHANOL					
Ø	**Qf (cc/m)**	**Qa (cc/m)**	**DUR (μs)**	**GAP (mm)**	**Emin (mJ)**
0.6	0.38	3075	60	9	≈ 1000
0.65	"	2798	60	8	5.0
0.7	"	2559	30	5	0.93
0.75	"	2352	30	4	0.50
0.8	"	2171	30	3	0.34
0.85	"	2012	30	2	0.23
0.9	"	1870	30	2	0.20
1.0	"	1628	-	-	< 0.2

Table 4.4 Prevaporized Mixture Generation Parameters and Operating Conditions

fuel condensation in the dispersion cup. For the same reason, equivalence ratios above 1.0 could not be tested for methanol mixtures. However, the range of prevaporized mixtures tested was sufficient to provide a lower limit (D = 0) for the study of droplet size effects on ignition.

4.2.2. Spark Duration and Gap Width

The optimum values of spark duration and gap width are listed in Table 4.4 for prevaporized n-heptane and methanol mixtures. With the exception of the very lean cases (Ø = 0.6 and 0.65) the optimum duration was 30 μs for all mixtures. These durations were shorter than the comparable spray cases, which was expected since no time was required for fuel evaporation during ignition. The optimum spark gap widths varied from 4-9 mm and 2-9 mm for n-heptane and methanol mixtures, respectively. These values were comparable to those observed for spray ignition. The effect of varying spark duration and gap width on the minimum ignition energy of prevaporized mixtures was also similar to the behavior observed and reported for sprays.

4.2.3. Effect of Equivalence Ratio

The procedure for measuring the minimum ignition energy of the prevaporized mixtures was identical to the one used for sprays. The ignition frequency was determined as a function of spark energy and E_{min} was the spark energy which produced 50% ignition. Ignition frequency curves for all cases tested are presented in Figures 4.4, 4.5 and 4.6 for lean n-heptane, rich n-heptane and lean methanol mixtures, respectively. The prevaporized ignition frequency curves were very similar in shape to those observed for sprays.

For two of the lean cases (n-heptane and methanol, Ø = 0.6) E_{min} could

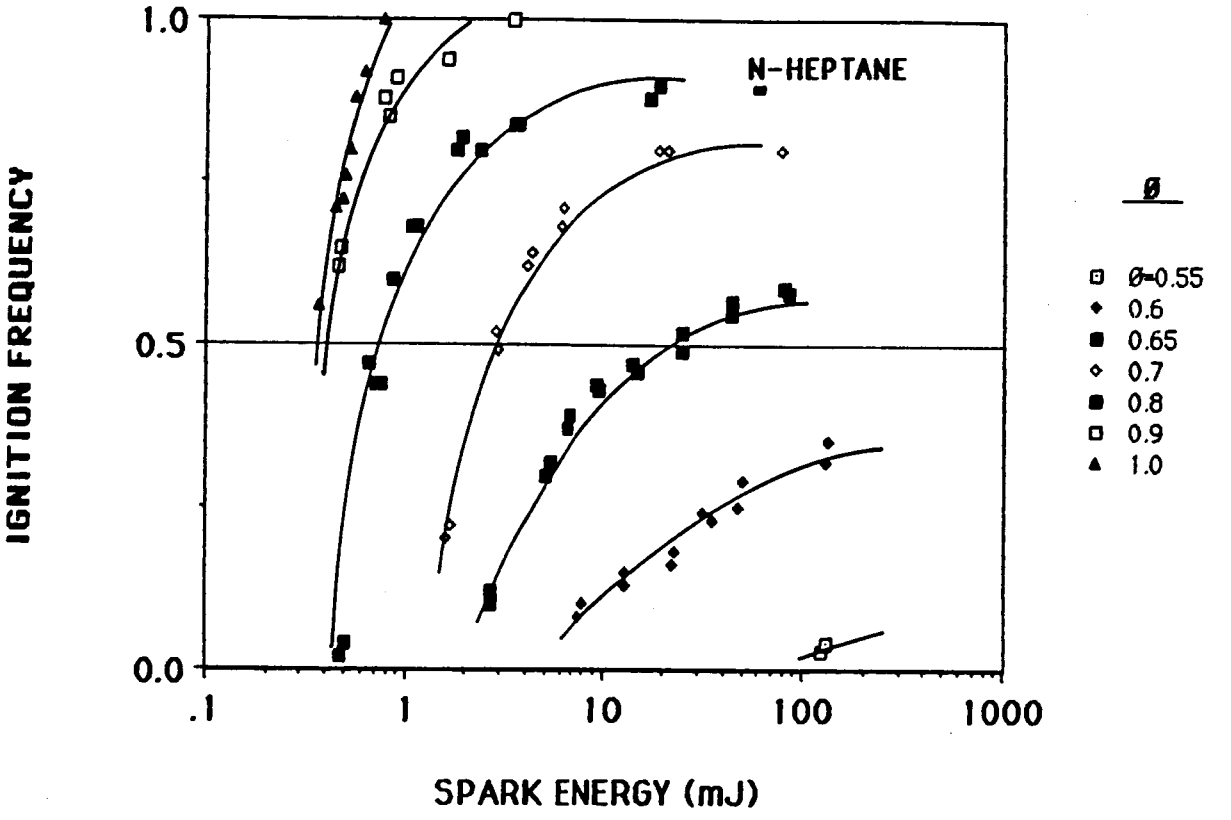

Figure 4.4 Effect of Spark Energy and Equivalence Ratio on the Ignition Frequency of Prevaporized, Premixed N-Heptane Under Fuel Lean and Stoichiometric Conditions

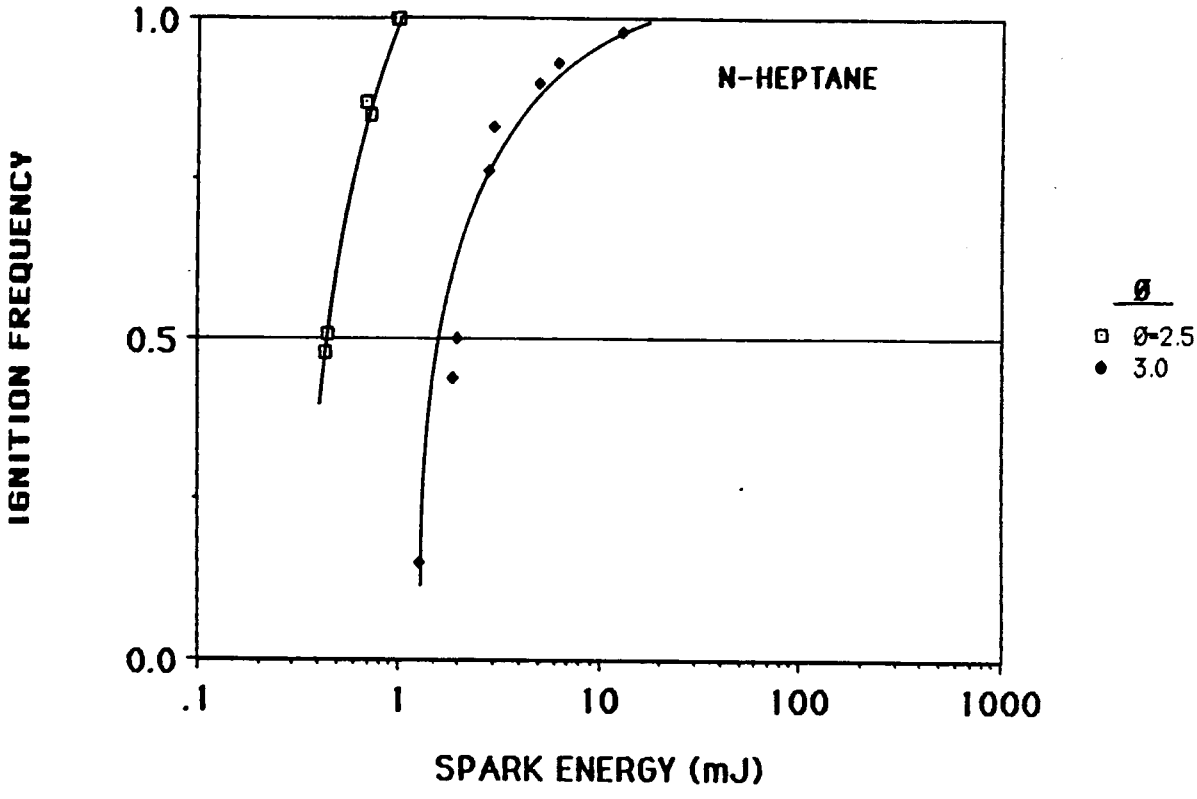

Figure 4.5 Effect of Spark Energy and Equivalence Ratio on the Ignition Frequency of Prevaporized, Premixed N-Heptane Under Fuel Rich Conditions

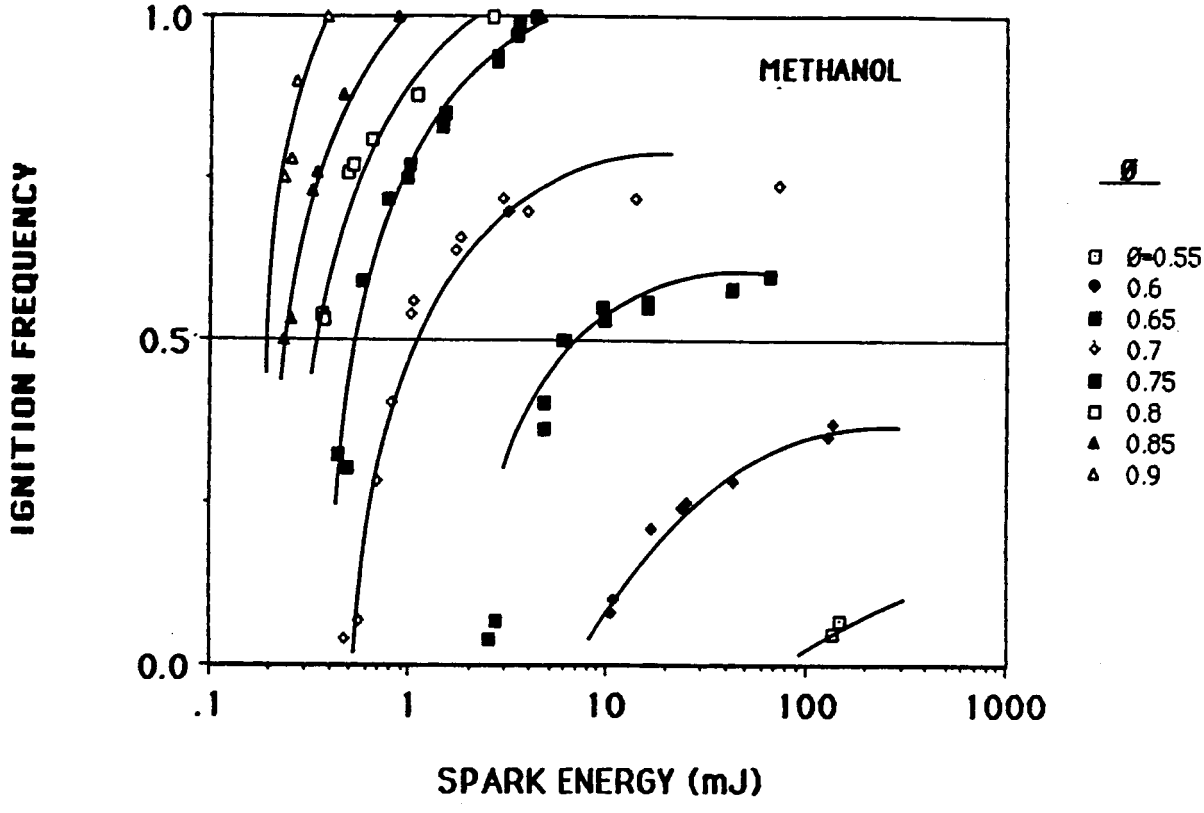

Figure 4.6 Effect of Spark Energy and Equivalence Ratio on the Ignition Frequency of Prevaporized, Premixed Methanol Under Fuel Lean Conditions

only be estimated because the highest spark energies attainable with the ignition circuit, about 100 mJ, resulted in ignition frequencies less than 50%. Therefore only partial ignition frequency curves were obtained. E_{min} was estimated by extrapolating these partial curves to the 50% line based on the shapes of the other curves. E_{min} was estimated to be 1000 ± 300 mJ for both cases. For three of the richer cases (n-heptane, Ø = 1.5, 2.0 and methanol, Ø = 1.0) only an upper limit could be determined for E_{min} because the lowest spark energies attainable, about 0.2 mJ, produced 100% ignition. E_{min} is reported as < 0.2 mJ for these mixtures .

The variation in minimum ignition energy with equivalence ratio is shown in Figure 4.7 for prevaporized, premixed n-heptane and methanol. An optimum equivalence ratio for n-heptane ignition, between Ø = 1.5 and Ø = 2.0, is evident from this figure. This is in very good qualitative and quantitative agreement with data presented by Lewis and Von Elbe (1961), who reported an optimum equivalence ratio of about 1.8 corresponding to a minimum ignition energy of about 0.23 mJ for prevaporized n-heptane. Rich mixtures of methanol could not be tested due to the condensation problem mentioned previously, so no optimum equivalence ratio for methanol was observed. Prevaporized lean ignition limits were observed at equivalence ratios of 0.55 for n-heptane and 0.5 for methanol.

4.2.4. Effect of Fuel Properties

As seen in Figure 4.7, prevaporized methanol was easier to ignite than prevaporized n-heptane. This may seem to contradict the spray results, which showed that n-heptane sprays were more ignitable. However, the reason the methanol sprays were more difficult to ignite was because they needed more spark energy for fuel vaporization due to their lower volatility.

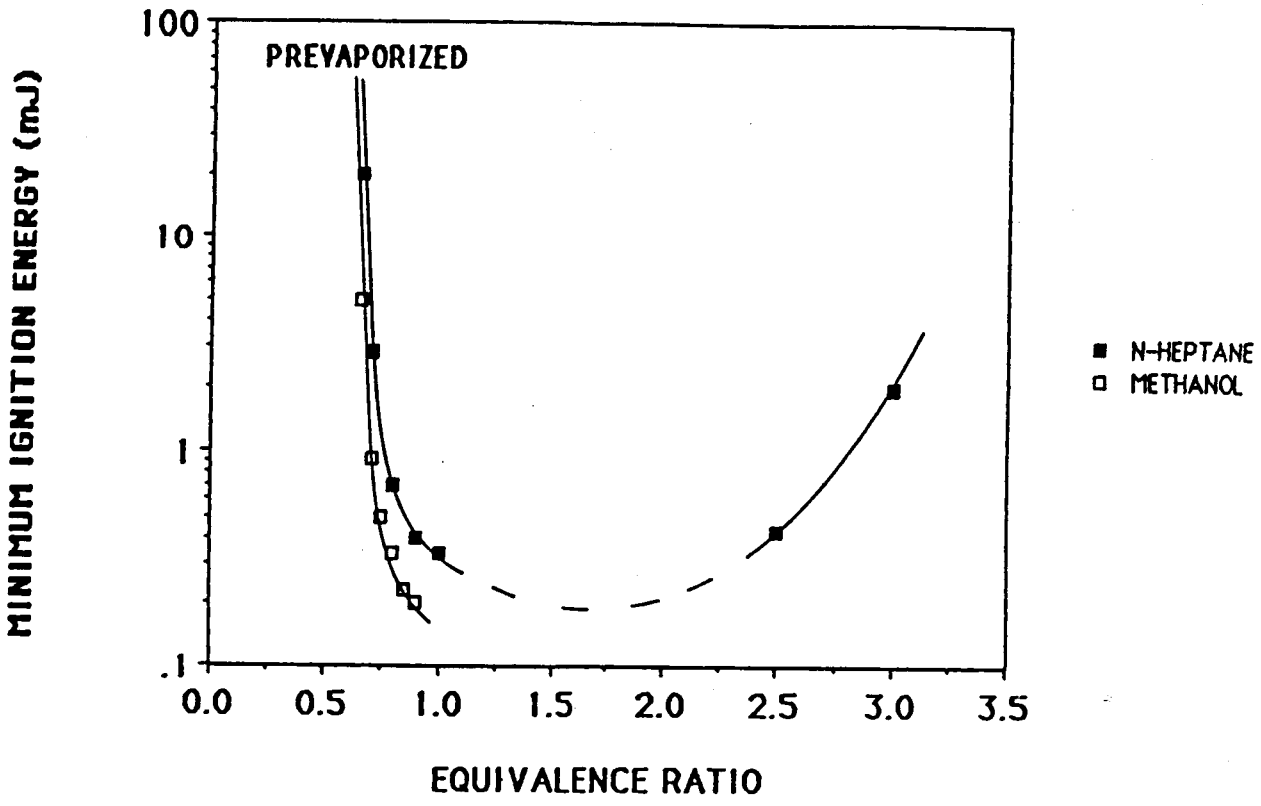

Figure 4.7 Effect of Equivalence Ratio on the Minimum Ignition Energy of Prevaporized, Premixed N-Heptane and Methanol

Volatility is not a factor in the prevaporized case, and activation energy is the critical fuel property. Methanol has a lower activation energy than n-heptane, 41.3 cal/gmol as opposed to 60.5 cal/gmol (Kanury, 1975), which accounted for its better ignitability in the vapor state.

4.3 Spray and Prevaporized Comparison

4.3.1. Extension of Lean Ignition Limits

Figure 4.8 shows the spray and prevaporized ignition data plotted together for n-heptane and methanol. Extension of the prevaporized lean ignition limit to lower equivalence ratios was evident for both n-heptane and methanol sprays. This extension can be explained as follows. When the ignition spark occurs, temperatures in the spark path reach several thousand degrees Kelvin (Maly, 1978). Fuel droplets present in the immediate vicinity of the spark vaporize and burn, along with the prevaporized fuel, to form the spark kernel. Successful ignition occurs if the spark kernel is able to propagate into the unburned mixture surrounding it. In spray ignition, the kernel is surrounded by fuel droplets and a vaporized fuel/air mixture with a range of equivalence ratios. Even at lean overall gap equivalence ratios, localized regions that are richer and easier to ignite exist around the droplets. These regions of favorable stoichiometry accelerate the growth of the spark kernel into the surrounding mixture. Thus, the presence of fuel droplets enhances lean spray ignition. In contrast, prevaporized premixed mixtures have a uniform distribution of fuel vapor, so kernel growth is limited by the ignitability of the stoichiometry being tested.

Similar extension of lean flammability limits has been observed in previous spray studies. For example, Burgoyne and Cohen (1954) found that the flammability limits were extended leanward for tetralin sprays with

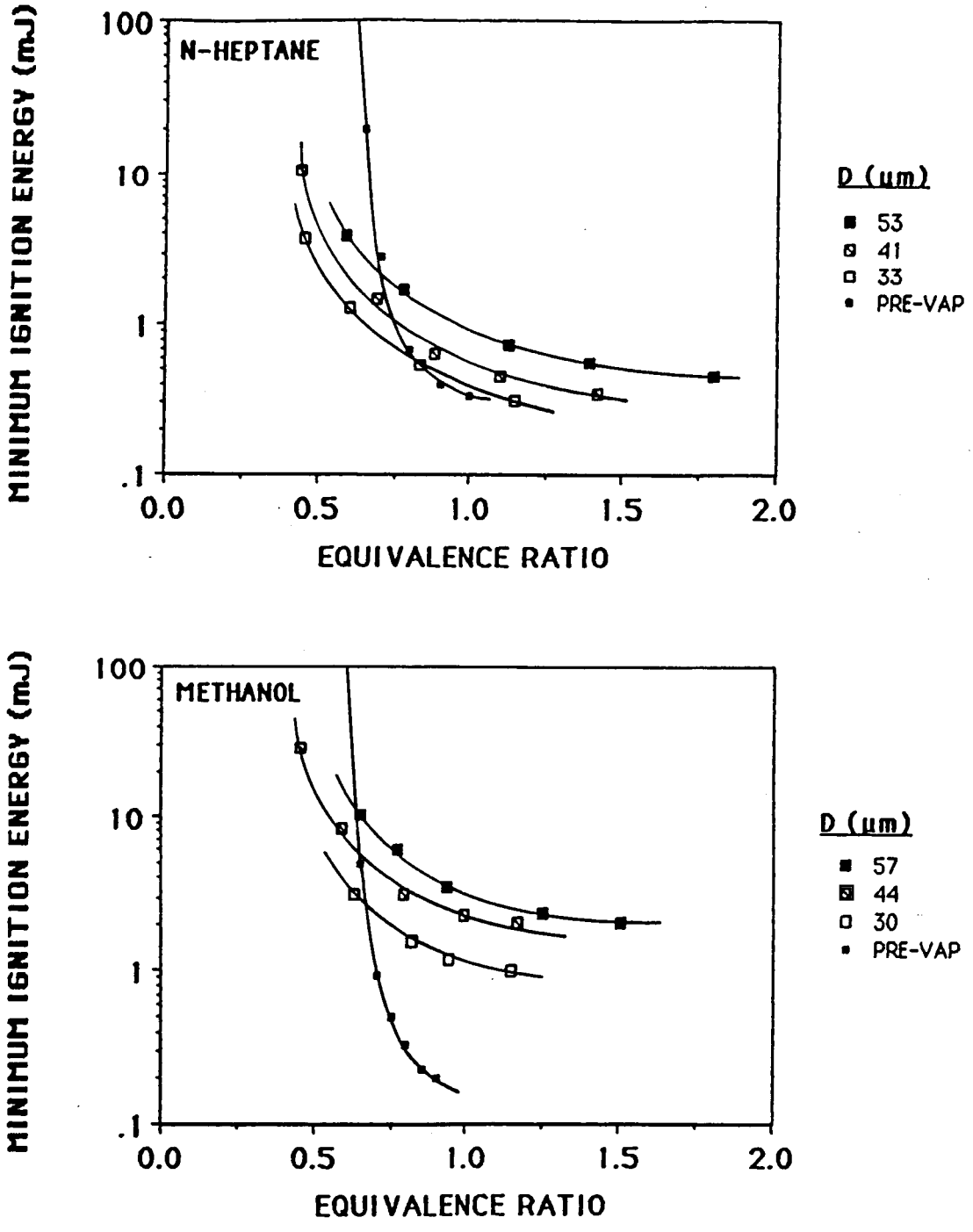

Figure 4.8 Effect of Equivalence Ratio and Droplet Diameter on the Minimum Ignition Energy of N-Heptane and Methanol Sprays and Prevaporized Mixtures

droplets in the 10-40 μm range. Also, Mizutani and Nakajima (1973) obtained extension of the flammability limits by the addition of kerosine droplets to a propane air mixture.

4.3.2. Optimum Droplet Size for Ignition

The spray and prevaporized ignition energy data are given as a function of droplet size for various equivalence ratios in Figure 4.9 for n-heptane and methanol. Prevaporized data were plotted at zero diameter, the lower limit of drop size. The dashed lines are an extrapolation from the lowest drop size studied to the prevaporized case. The minima in the extrapolated region of the ignition curves suggest the existence of an optimum droplet size for ignition of lean sprays, occuring below 30 μm for both fuels. The existence of this optimum droplet size was indicated over a larger range of lean equivalence ratios for n-heptane (0.4-0.8) than for methanol (0.4-0.65). The optimum diameter could not be quantified from this study, obviously.

The existence of an optimum droplet diameter for ignition can be explained as follows. A successful spark ignition event can be considered as two separate processes. Initially, the spark has to vaporize and burn the fuel in its path to create a spark kernel. Secondly, this kernel has to propagate into the unburned mixture. The amount of energy needed to vaporize and burn a given amount of fuel in the spark gap decreases monotonically as the droplet size decreases to zero, due to the enhanced evaporative quality of the fuel. Therefore, the existence of an optimum drop size for ignition must be explained in terms of the second process, flame propagation.

Flame propagation studies (Burgoyne and Cohen, 1954; Polymeropoulos and Das, 1976; Hayashi et al., 1976; Mizutani and Nakajima, 1973) have shown

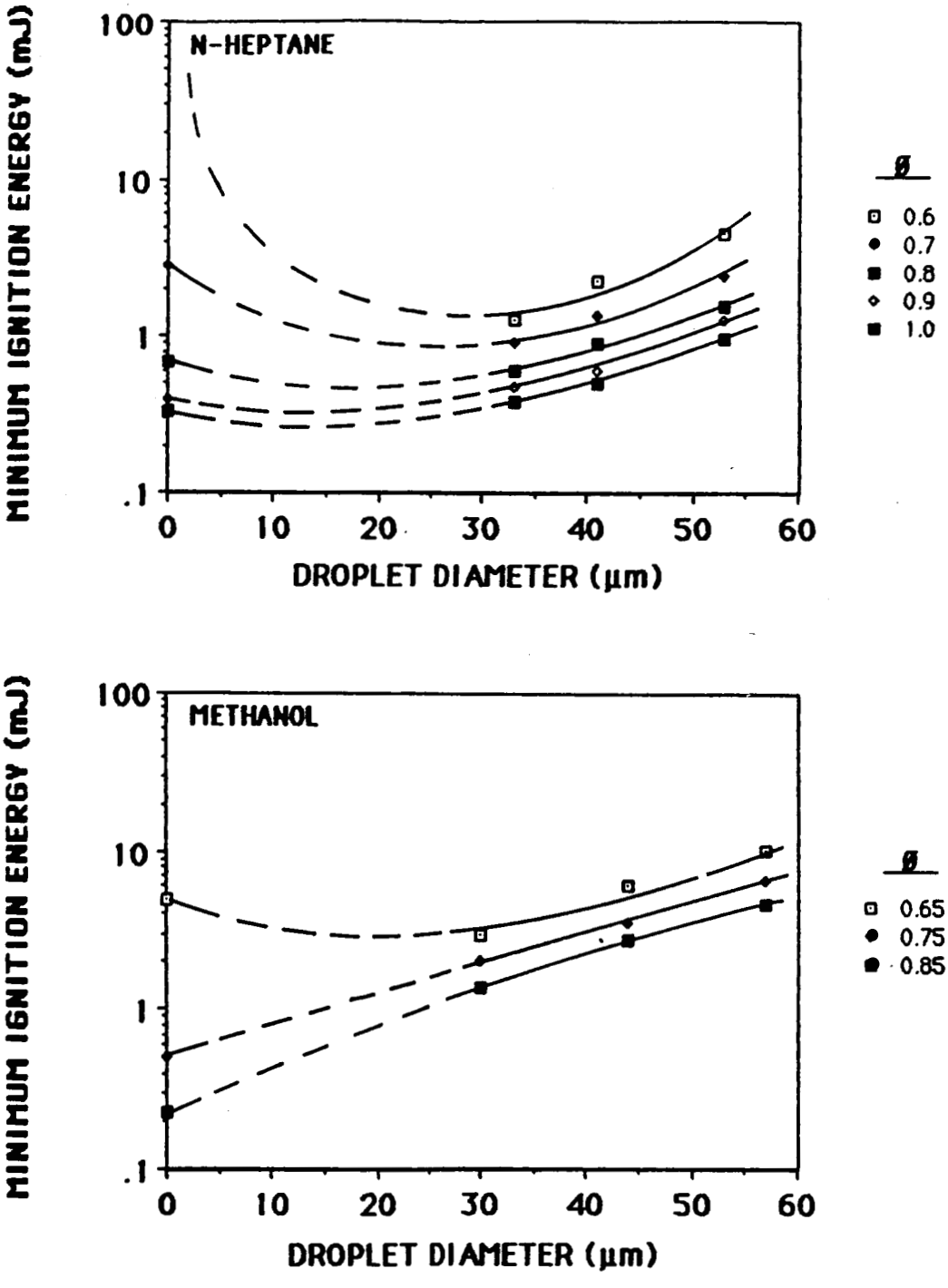

Figure 4.9 Effect of Droplet Diameter and Equivalence Ratio on the Minimum Ignition Energy of N-Heptane and Methanol Sprays

that as drop sizes are decreased from large values to zero, sprays in the transition region (10-40 μm) achieve the maximum flame speed. This enhanced flame speed would also enhance spark kernel propagation rates, and ignition. Therefore, the optimum in drop size for ignition is probably caused by the increased flame propagation rates in the transition region, and should occur at the drop size where the flame speed is maximized.

Previous researchers also have observed optimum droplet sizes for ignition. Chan (1982) and Singh (1986) found optimum sizes of 15 μm and 22-26 μm respectively for ignition of tetralin aerosols at lean equivalence ratios, which agrees with the current findings. A numerical thermal ignition study by Aggarwal and Sirignano (1984) predicted an optimum droplet size for ignition, which increased with increasing equivalence ratio. This optimum was attributed to the distribution of fuel vapor in the ignition zone, which is affected by the total droplet surface area.

4.4 Summary of Experimental Results

To briefly summarize the major experimental results:

1) Ignition was improved (required ignition energies were lowered) by decreasing the droplet size, increasing the equivalence ratio and increasing the fuel volatility of the sprays.

2) An optimum equivalence ratio for ignition of prevaporized n-heptane was observed between 1.5 and 2.0; no optimum equivalence ratio was seen for spray ignition.

3) An optimum droplet size for spray ignition, less than 30 μm, was suggested for lean sprays of both fuels. This optimum was related to the maximum flame speeds observed by previous researchers for sprays in this

transition region size range.

4) Extension of the lean prevaporized ignition limit was observed for all sprays tested. This was attributed to interdroplet regions of gas-phase stoichiometry more favorable to ignition created by the evaporating droplets.

CHAPTER 5

ANALYTICAL SPARK IGNITION STUDIES

It has been shown that many factors affect the minimum ignition energy of fuel sprays. Droplet size, equivalence ratio, extent of prevaporization and fuel properties are parameters that will be examined by two analytical models which are described in this Chapter. The models will be used to predict minimum ignition energies based on these and other parameters using a characteristic time approach. The results will give insight into the relative importance of these parameters on the spark ignition process, as well as the ability of characteristic time models to accurately predict ignition energies. One of the models will also be extended to simulate the randomness of the spray ignition process in order to explain the probabilistic nature of the experimental results.

5.1 Spray Ignition Model (Ballal and Lefebvre)

The ignition model developed by Ballal and Lefebvre (1981) takes a characteristic time approach, with the criterion for ignition being that the time required for the fuel to evaporate and chemically react in the spark kernel must be less than or equal to the time it takes the kernel to be quenched by thermal conduction and turbulent diffusion. A critical quenching diameter was calculated from this. The minimum ignition energy was the amount of energy required to raise this critically sized kernel to the stoichiometric adiabatic flame temperature. The fuel and air properties used

in the model are listed in Table 5.1.

5.1.1 Model Formulation

The ignition model was developed to be used over a wide range of flow conditions. To correlate the present ignition data, the heterogeneous, quiescent and monodisperse case was used. (The model criterion for quiescent conditions was $Re_d \ll 16$. The droplet Reynolds numbers for the present sprays varied from 0.3-1.2.)

The basic assumptions of the model were as follows. A spherical spark kernel was formed by the ignition spark. The temperature in this kernel was the stoichiometric, adiabatic flame temperature of the fuel. The air properties in the kernel were evaluated at a mean temperature of 1300 K. The basic premise of the model was given by:

$$t_q = t_e + t_c \qquad (5\text{-}1)$$

which equated the time required for droplet evaporation (t_e) and chemical reaction (t_c) to the quenching time (t_q) of the spherical spark kernel.

The quenching time was defined as the ratio of the heat capacity of the spark kernel divided by the average rate of heat loss from the kernel by conduction. This was given by:

$$t_q = c_{pa}\rho_a \Delta T(\pi/6)d^3 / 1.33\pi d k_a \Delta T_{st} \qquad (5\text{-}2)$$

where d is the diameter of the spark kernel, ΔT_{st} is the temperature difference between the stoichiometric, adiabatic flame temperature of the kernel and the ambient spray and ρ_a, c_{pa} and k_a are the density, specific

FUEL PROPERTIES:

PROPERTY	SYMBOL	UNITS	N-HEPTANE	METHANOL
Density	p	(kg/m3)	6.88E+02	7.96E+02
Flame Temperature	Tst	(°K)	2266	2152
Boiling Temperature	Tb	(°K)	371	337
Latent Heat of Vaporization	L	J/kg	3.65E+05	1.10E+06
Activation Energy	Eact	(kcal/mole)	60.5	41.3
Combustion Transfer Number	B	-	5.82	2.70

AIR PROPERTIES:

PROPERTY	SYMBOL	UNITS	VALUE	TEMP.
Density	p	(kg/m3)	2.71E-01	(1300°K)
Specific Heat	cpa	(J/kg°K)	1.20E+03	(1300°K)
Thermal Conductivity	ka	(J/sm°K)	8.37E-02	(1300°K)
Thermal Diffusivity	α	(m2/s)	2.58E-04	(1300°K)

Table 5.1 Fuel and Air Properties Used for Ignition Modeling

heat and thermal conductivity of air evaluated at 1300 K. This reduced to:

$$t_q = d^2/8\alpha \qquad (5\text{-}3)$$

where α is the thermal diffusivity of air.

The evaporation time was defined as the ratio of the mass of fuel contained within the spark kernel to the rate of fuel evaporation and was given by:

$$t_e = (1-\Omega)\rho_f c_{pa} D^2/8k_a \phi \ln(1+B_{st}) \qquad (5\text{-}4)$$

where Ω is the fraction of fuel in vapor form, D is the droplet diameter, ϕ is the equivalence ratio and B_{st} is the stoichiometric combustion mass transfer number. The $(1-\Omega)$ term was included to account for fuel vapor in the ignition zone prior to the spark. This fuel vapor was assumed to have reduced the evaporation time by the time it would have taken to produce that vapor had it been present initially in the form of fuel droplets the same size as those present. Values of B_{st} were taken from Kanury (1970).

The chemical reaction time was defined in terms of the laminar flame speed (S_L) and was given by:

$$t_c = 12.5\alpha/S_L^2 \qquad (5\text{-}5)$$

Using relations 5-3 to 5-5 in equation 5-1, the critical quenching distance was determined, and was given by:

$$d_q = \left[(1-\Omega)\rho_f D^2/\rho_a \phi \ln(1+B_{st}) + (10\alpha/S_L)^2\right]^{0.5} \qquad (5\text{-}6)$$

The minimum ignition energy was defined as the energy required to raise the critical diameter kernel to the stoichiometric adiabatic flame temperature (T_{st}), and E_{min} was given by:

$$E_{min} = c_{pa}\rho_a\Delta T_{st}(\pi/6)d_q^3 \qquad (5\text{-}7)$$

5.1.2 Minimum Ignition Energy Predictions

Initial attempts to model n-heptane spray ignition were unsuccessful because the chemical times calculated with equation 5-5 were an order of magnitude higher than the evaporation times. This resulted in predicted ignition energies an order of magnitude higher than the experimental values. The chemical times were expected to be less than the evaporation times, since evaporation has been shown to be the rate controlling factor in ignition (Ballal and Lefebvre, 1978; Peters and Mellor, 1981). For this reason, the chemical time (t_c) was neglected for further modeling attempts. (Values of the laminar flame speed (Warnatz, 1984) used in Equation 5-5 varied from 30 to 40 cm/s, with maximum values occuring at $\Phi = 1.1$.)

The spark ignition model, neglecting chemical times, was used to predict minimum ignition energies for the experimental spray cases reported previously. Figure 5.1 compares the predicted values of E_{min} with the measured values for n-heptane and methanol sprays. Several observations can be made about the model from these results. The predicted effect of equivalence ratio matched the experimental results well for $\Phi > 0.8$, as seen by the similarity of the slopes in this region. For equivalence ratios decreasing below 0.8, however, the model failed to predict the sharper increase in E_{min} observed experimentally. This was expected since the

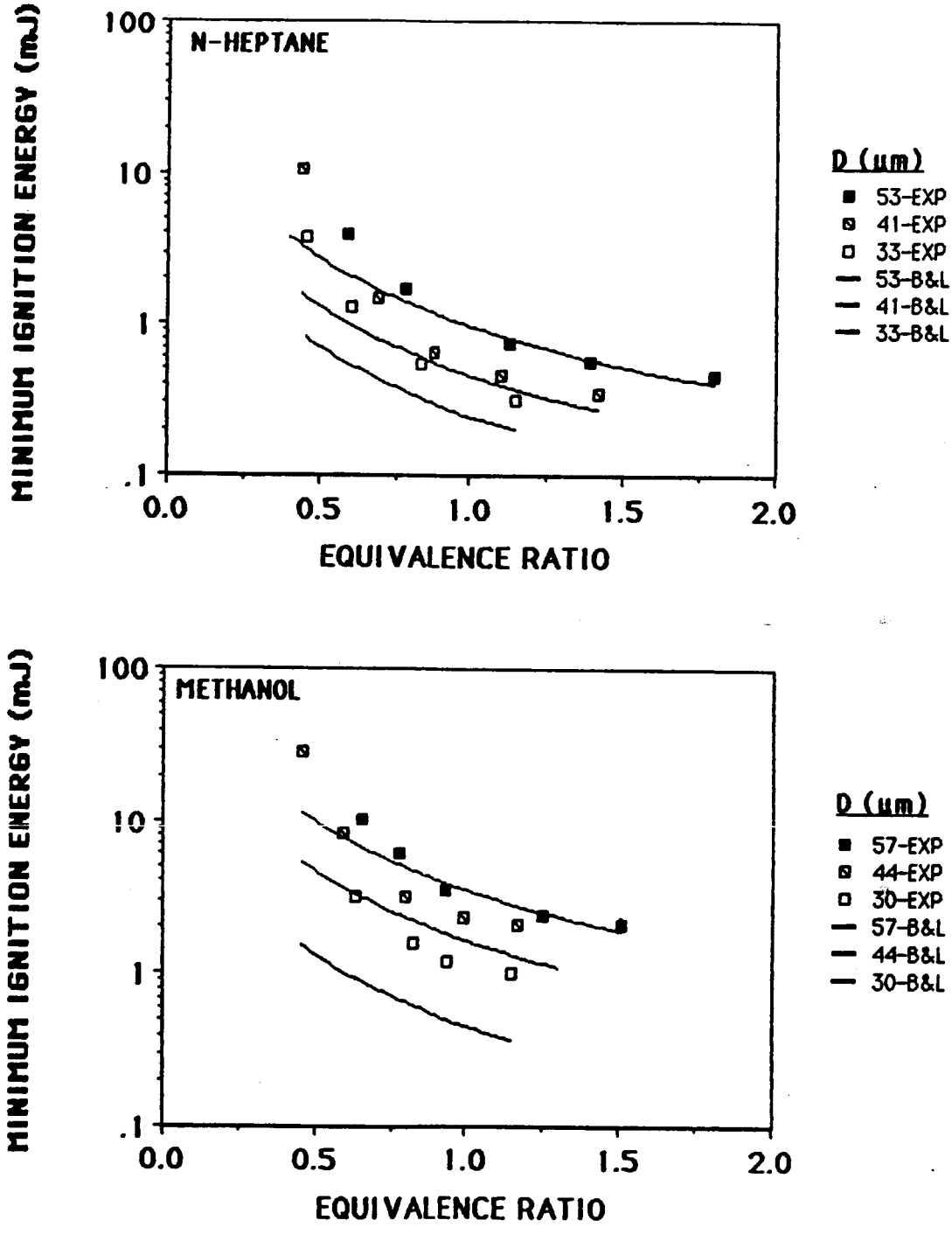

Figure 5.1 Predictions of Minimum Ignition Energy using Ballal and Lefebvre's Ignition Model for N-Heptane and Methanol Sprays

model didn't include chemical times, which would become larger as the lean ignition limit was approached. For equivalence ratios above 0.8, the quantitative agreement between the predicted and experimental ignition energies was very good for the largest drop sizes. As droplet size decreased, however, the model increasingly underpredicted E_{min}. This was partially explained by the exclusion of chemical times. As the droplet size decreased, the evaporation times decreased also and the chemical times became relatively more important. Furthermore, equation 5-6, without the chemical time, predicts a monotonic decrease in quenching distance and ignition energy, approaching zero for zero drop size (vapor). Therefore, the model also breaks down as droplet size decreases because it cannot account for the transition region fuel distribution effects which result in the optimum droplet size for ignition observed experimentally.

In summary, the spark ignition model developed by Ballal and Lefebvre was not able to account for spray ignition behavior as the equivalence ratio approached the lean limit or as the droplet diameter dropped below 40 μm. However, the general agreement between the model predictions and the experimental data is quite good considering the global nature of the model compared to the complex nature of the spark ignition process.

5.1.3 Effect of Extent of Prevaporization

The effect of fuel prevaporization on ignition was also studied using the ignition model of Ballal and Lefebvre. This was done to address a question raised in Chapter 4 concerning the fact that ignition energies were measured for n-heptane and methanol sprays with different values of Ω. It was not clear how much of the difference in ignition energy between the n-heptane and methanol sprays could be attributed to their difference in Ω, and how much

was due to the difference in their volatilities. To examine this, E_{min} was predicted for sprays of the two fuels with the same value of $\Omega = 0.39$. This was done for n-heptane sprays with D = 41 μm and methanol sprays with D = 44 μm.

Figure 5.2 shows the effect of varying Ω on the predicted ignition energies for these sprays. The experimental values of Ω (n-heptane = 0.45; methanol = 0.32) are included as a reference. As seen, using a mean value of Ω (0.39) decreased the difference in E_{min} between the n-heptane and methanol sprays by about 25%. This indicates that the majority of the difference in ignition energies was due to the difference in volatility of the fuels.

5.2 Characteristic Time Model for Ignition (Peters and Mellor)

The second ignition model used to evaluate the experimental data was the characteristic time model (CTM) for ignition of quiescent fuel sprays, which was developed by Peters and Mellor (1980) based on an earlier model for flame stabilization. This model associated specific times with the physical processes occuring during spark ignition and stated that the ignition limit was reached when the mixing rate of the spark kernel with its environment equalled the fuel evaporation rate.

5.2.1 Model Formulation

The basic assumptions of the model were similar to those presented for the previous model of Ballal and Lefebvre. A spherical spark kernel was formed by the ignition spark and the temperature in this kernel was the stoichiometric, adiabatic flame temperature of the fuel. The air properties in the kernel were evaluated at a mean temperature of 1300 K. In addition,

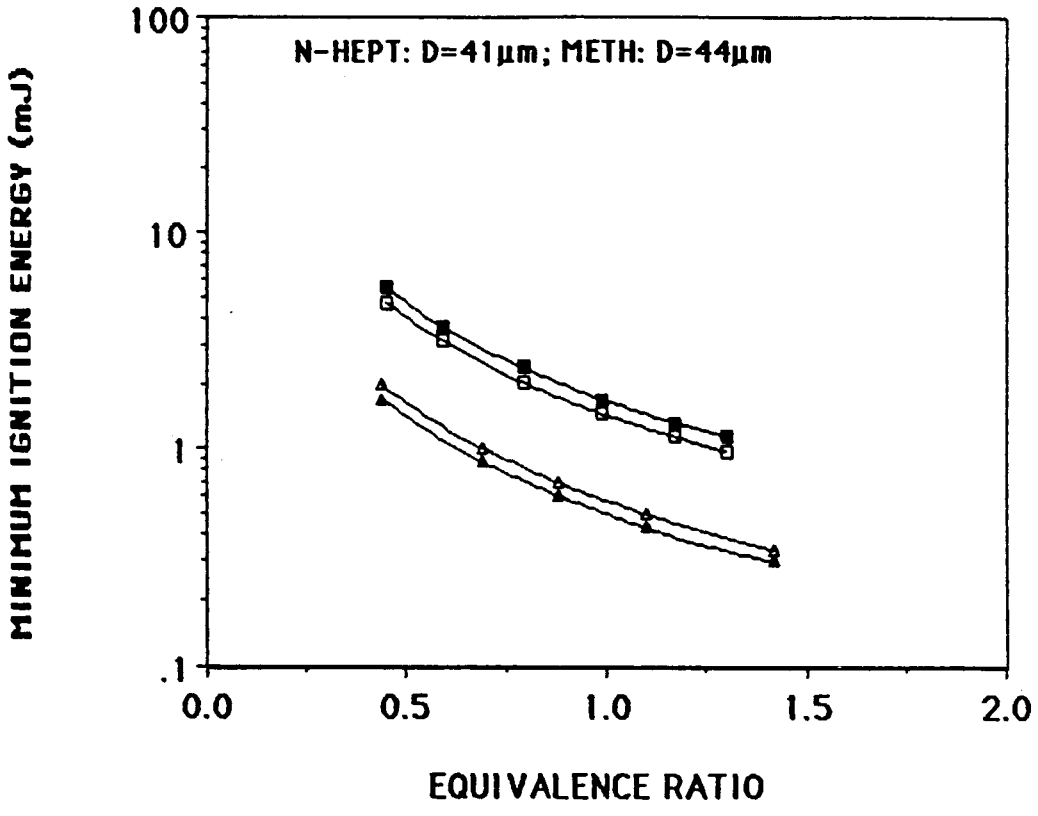

Figure 5.2 Effect of Extent of Prevaporization on the Predicted Minimum Ignition Energies of Ballal and Lefebvre's Ignition Model for N-Heptane and Methanol Sprays (D = 41 and 44 µm, respectively)

ignition was assumed to be controlled by evaporation. That is, the time required for evaporation of the fuel in the spark kernel was very much larger than the time required for chemical reaction. Therefore, chemical times were neglected. The basic premise of the model was given by:

$$t_{sl} \sim t_{eb}/\emptyset \qquad (5\text{-}8)$$

where t_{sl} is the time required for the heat to be removed from the kernel by conduction, t_{eb} is the time required for evaporation of a fuel droplet in the kernel and $\emptyset$ is the equivalence ratio at the spark gap. Since the total amount of fuel being vaporized contributed to the ignition process, t_{eb} was divided by the equivalence ratio, which was proportional to the total number of droplets present.

Note that the CTM differed from the previously described model of Ballal and Lefebvre in that it only assumed proportionality between the relevant characteristic times, not absolute equality. The model was applied by evaluating t_{sl} and t_{eb} from the measured ignition energies and experimental conditions to determine the proportionality in equation 5-8. E_{min} was then predicted based on this proportionality. The fuel and air properties used in these calculations were identical to those used in the previous model, and are listed in Table 5.1.

For a quiescent mixture, the relevant mode of heat transfer from the spark kernel was conduction. Therefore, the time required for heat loss from the kernel was given by:

$$t_{sl} = A/\alpha_a \qquad (5\text{-}9)$$

where A is the surface area of the kernel and α_a is the thermal diffusivity. For a spherical spark kernel, this became:

$$t_{sl} = \pi d^2 \rho_a c_{pa} / k_a \qquad (5\text{-}10)$$

where d is the diameter of the spark kernel and ρ_a, c_{pa} and k_a are the density, specific heat and themal conductivity of air evaluated at 1300 K. To evaluate d, the minimum ignition energy was defined as the energy required to heat a spherical volume of air with diameter d to the stoichiometric, adiabatic flame temperature:

$$d_q = (E_{min} / \pi/6 \rho_a c_{pa} \Delta T_{st})^{1/3} \qquad (5\text{-}11)$$

where d has been replaced by d_q, the quenching distance, and ΔT_{st} is the temperature difference between the stoichiometric, adiabatic flame temperature of the kernel and the ambient spray.

The time required for evaporation of a fuel droplet in the spark kernel was derived from the "d^2 law" of Godsave, given by:

$$t_{eb} = D_o^2 / \beta \qquad (5\text{-}12)$$

where D_o is the droplet diameter and β is the evaporation coefficient. This expanded to:

$$t_{eb} = D_o^2 \rho_f c_{pa} / 8 k_a \ln(1+B_{st}) \qquad (5\text{-}13)$$

where B_{st} is the stoichiometric mass transfer number, taken from Kanury

(1970).

Using the experimental conditions and measured ignition energies, t_{sl} and t_{eb} were calculated with equations 5-10, 5-11 and 5-13. A simple linear regression analysis was then performed with these values to determine the proportionality in equation 5-8. Results of this are given in Figure 5.3, which shows t_{sl} plotted as a function of t_{eb}/ϕ for the experimental data of this study. The least-squares fit was:

$$t_{sl} = 15.8t_{eb}/\phi - 0.7 \qquad (5\text{-}14)$$

The coefficient of correlation (r) for this fit was 0.89 and the y-intercept was well within the standard error of estimate (13.6) of zero. The scatter in the correlation was not excessive considering only 26 data points were modeled.

This correlation was very close to the one obtained by Peters and Mellor (1980) using the CTM with experimental data of Ballal and Lefebvre (1978):

$$t_{sl} = 14.2t_{eb}/\phi + 2.29 \qquad (5\text{-}15)$$

Equation 5-15 was the result of ignition energy measurements made for iso-octane, diesel oil and heavy fuel oil sprays with SMD ranging from 20 to 170 μm and equivalence ratios ranging from 0.43 to 1.0. The agreement between the two correlations is very good considering t_{sl} and t_{eb} only ranged from 0-120 ms and 0-7 ms respectively for the present study, while the corresponding ranges for the data in Peters and Mellor's correlation were 0-1000 ms and 0-70 ms.

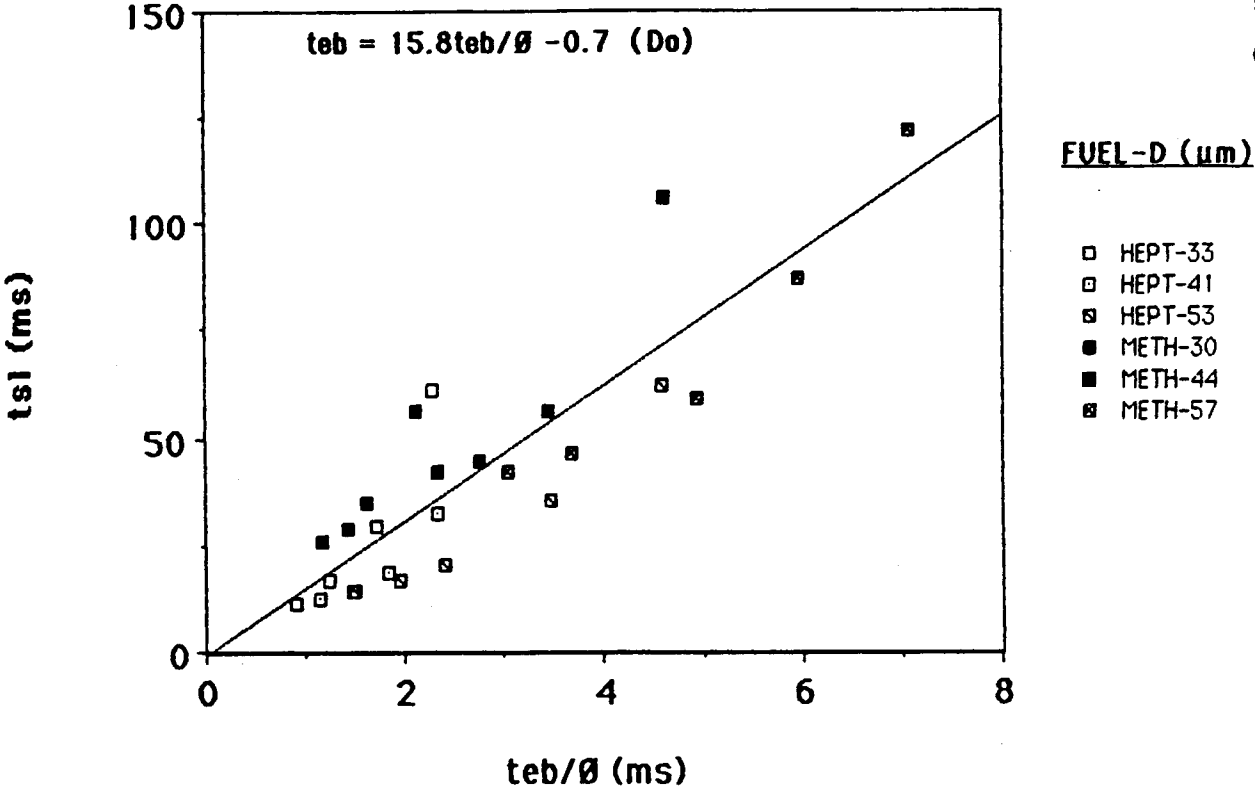

Figure 5.3 Characteristic Time Correlation for N-Heptane and Methanol Sprays (using Initial Droplet Diameters)

5.2.2 Minimum Ignition Energy Predictions

Using the correlation obtained for the present data (5-14) and neglecting the small y-intercept, E_{min} was calculated with equations 5-10, 5-11 and 5-13 as:

$$E_{min} = 0.261 c_{pa} \rho_a^{-0.5} \Delta T_{st} D_0^3 \left(\rho_f / \phi \ln(1+B) \right)^{1.5} \quad (5\text{-}16)$$

Comparisons of the minimum ignition energies predicted by 5-16 and the experimentally measured values are shown in Figure 5.4 for n-heptane and methanol sprays. As seen, the CTM qualitatively predicted the effects of droplet size and equivalence ratio on ignition quite accurately. Quantitatively however, the predicted ignition energies were about 50% higher than the measured values for n-heptane sprays of all sizes. For methanol sprays, the model overpredicted E_{min} for the 57 μm sprays and underpredicted E_{min} for the 30 μm sprays by about 30%, while the 44 μm predictions were very close to the experimental values. As in Ballal and Lefebvre's model, the agreement between the measured and predicted values of E_{min} deteriorated with decreasing equivalence ratio, suggesting the need for chemical kinetic times in modeling lean sprays.

5.2.3 Effect of Initial Versus Spark Gap Droplet Diameter

The CTM was developed to model ignition energies based on initial spray conditions, since detailed information about spray parameters at the ignition location is not always available. (It was not clear whether CTM the correlation obtained by Peters and Mellor for Ballal and Lefebvre's quiescent data (Eq. 5-15) was obtained using initial or spark gap diameters.) In this study, however, measurements of droplet diameter were made directly at

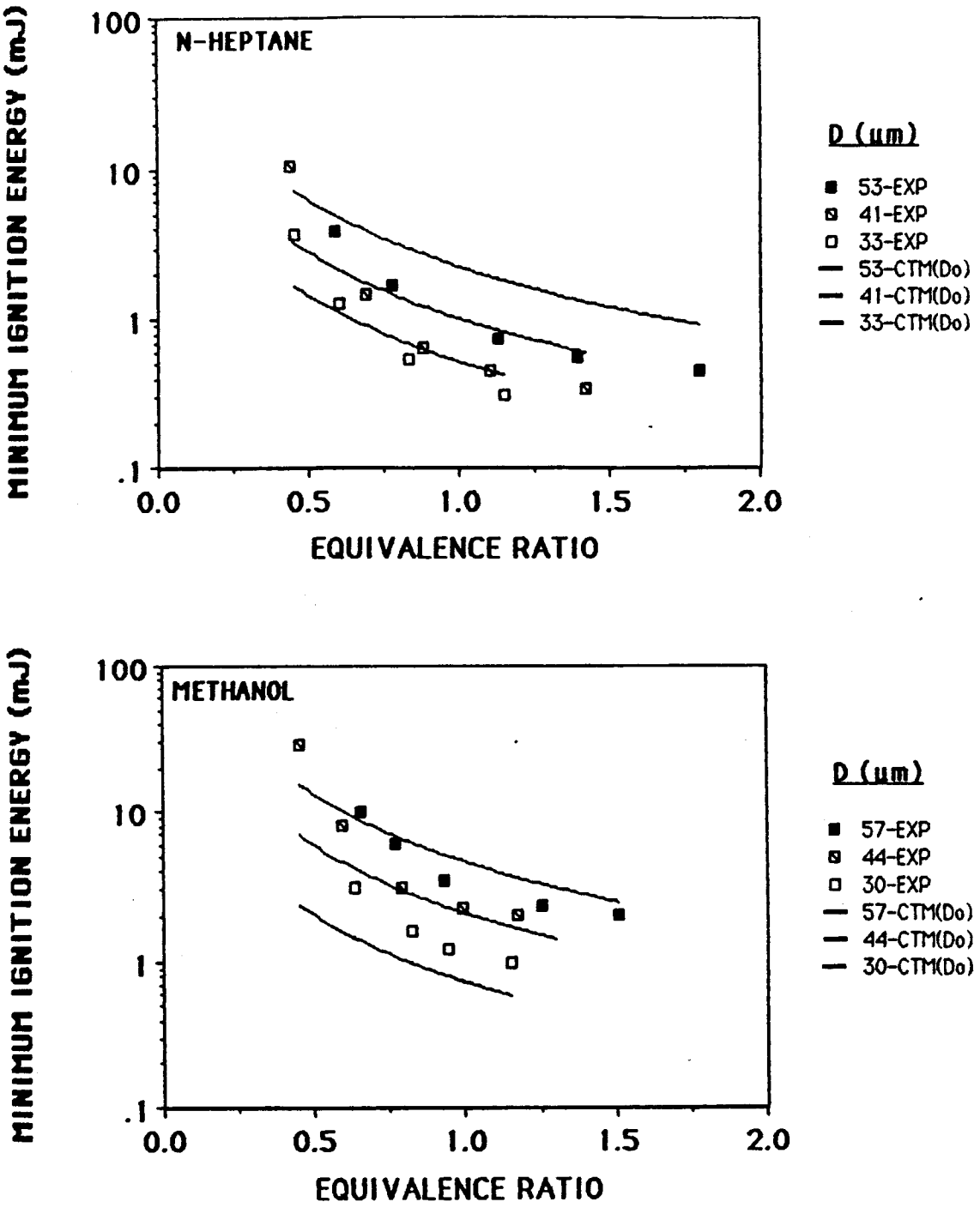

Figure 5.4 CTM Minimum Ignition Energy Predictions for N-Heptane and Methanol Sprays (using Initial Droplet Diameters)

the spark gap. Therefore, the droplet evaporation term in the CTM was modified to use these measured values, instead of the initial droplet diameters used previously. This gave a more realistic estimate of the time required for evaporation in the spark kernel. With this modification the droplet evaporation time became:

$$t_{eb} = D^2\rho_f c_{pa}/8k_a \ln(1+B_{st}) \qquad (5\text{-}17)$$

where D is the droplet diameter measured at the spark gap. The correlation between t_{sl} and t_{eb} was determined as before and found to be:

$$t_{sl} = 20.6t_{eb}/\emptyset + 1.7 \qquad (5\text{-}18)$$

Figure 5.5 shows a plot of t_{sl} as a function of $t_{eb}/\emptyset$ for this case. The correlation coefficient (r) of this least squares fit was 0.9 and the y-intercept was within the standard error of estimate (12.9) of zero. As seen in Figure 5.5, the evaporation times were decreased by about a factor of one-third compared to the initial diameter case (Figure 5.3), which increased the slope of the correlation by about 30%.

Using this correlation, the minimum ignition energy was given by:

$$E_{min} = 0.389c_{pa}\rho_a^{-0.5}\Delta T_{st}D_o^3\left(\rho_f/\emptyset \ln(1+B)\right)^{1.5} \qquad (5\text{-}19)$$

Values of E_{min} predicted by this equation are compared to the experimentally measured values in Figure 5.6 for n-heptane and methanol sprays. As seen, this modification had no qualitative effect on the predicted ignition energies. Using the spark gap droplet diameter improved the n-heptane predictions but

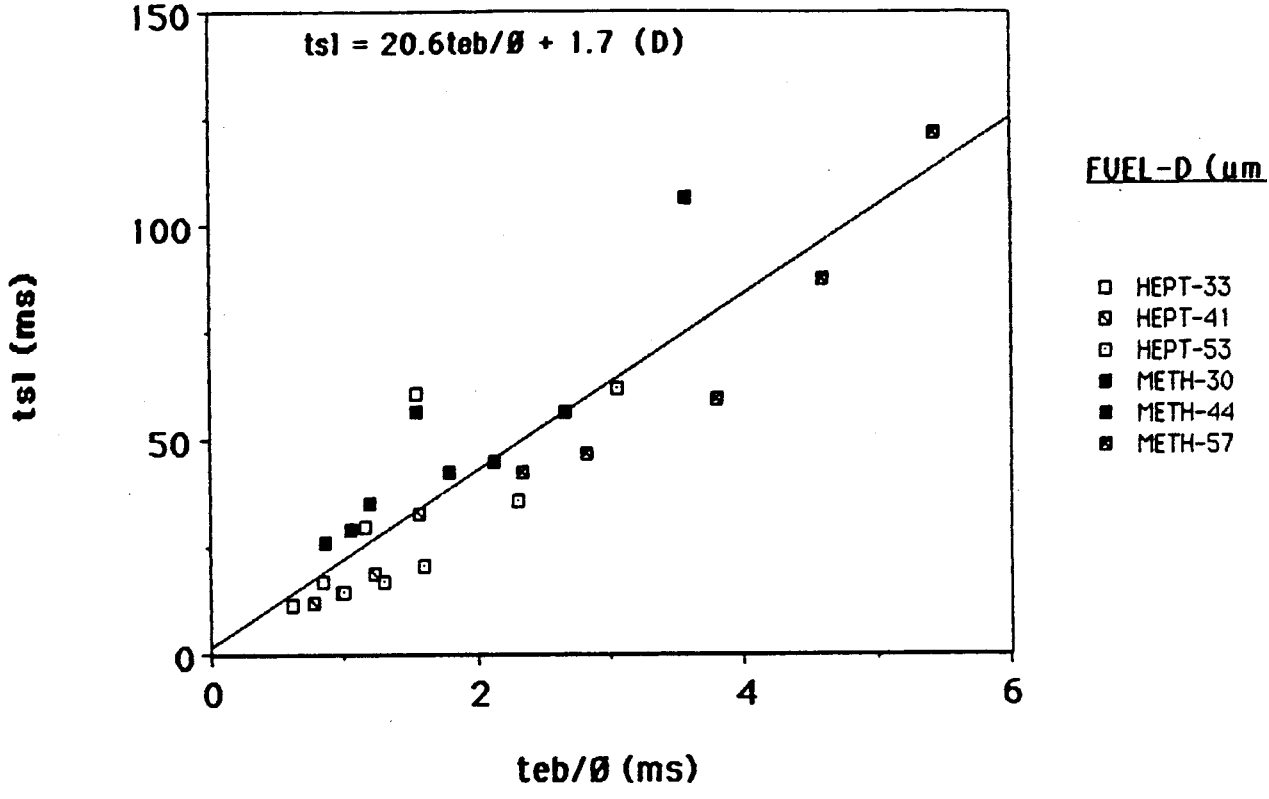

Figure 5.5 Characteristic Time Correlation for N-Heptane and Methanol Sprays (using Spark Gap Droplet Diameters)

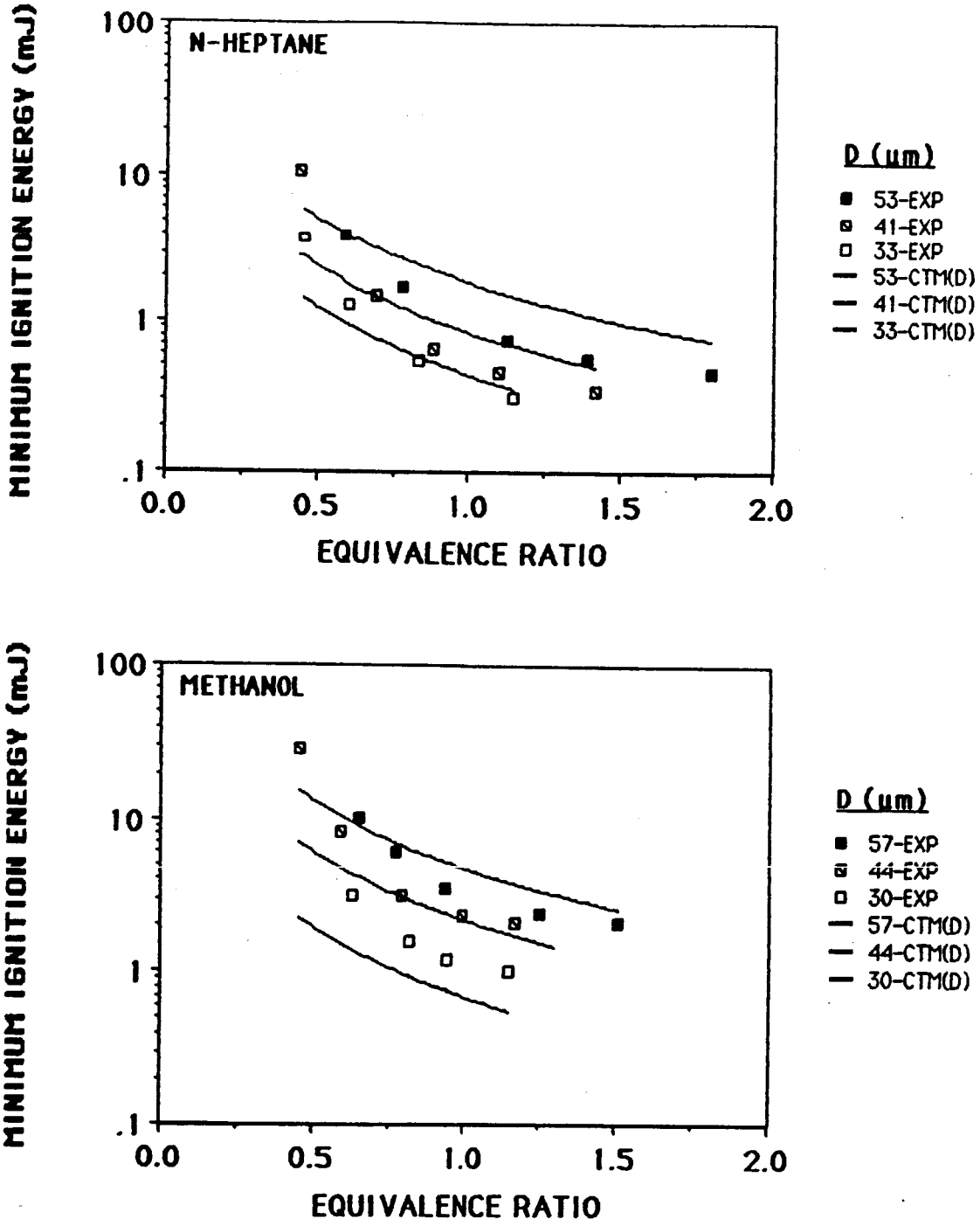

Figure 5.6 CTM Minimum Ignition Energy Predictions for N-Heptane and Methanol Sprays (using Spark Gap Droplet Diameters)

had very little effect on the methanol predictions. This was expected since n-heptane's greater volatility resulted in larger differences between the initial and spark gap droplet diameters than for methanol sprays.

5.2.4 Effect of Extent of Prevaporization

The CTM was further modified to include the effects of prevaporized fuel in the ignition zone prior to sparking. This fuel vapor was assumed to have reduced the evaporation time by the time it would have taken to produce that vapor had it been present initially in the form of fuel droplets (Ballal and Lefebvre, 1981). The droplet evaporation time became:

$$t_{eb} = (1-\Omega)D^2\rho_f c_{pa}/8k_a \ln(1+B_{st}) \qquad (5\text{-}20)$$

where Ω is the fraction of fuel in vapor phase and D is the droplet diameter measured at the spark gap. The correlation between t_{sl} and t_{eb} was determined as before and found to be:

$$t_{sl} = 29.8t_{eb}/\phi + 5.5 \qquad (5\text{-}21)$$

Figure 5.7 shows a plot of t_{sl} as a function of t_{eb}/ϕ for this case. The correlation coefficient (r) of this least squares fit was 0.9 and the y-intercept was within the standard error of estimate (12.6) of zero. The evaporation times were decreased by about a factor of two compared to the initial diameter case, which nearly doubled the slope of the correlation.

Using this correlation, the minimum ignition energy was given by:

$$E_{min} = 0.676c_{pa}\rho_a^{-0.5}\Delta T_{st}D^3\left((1-\Omega)\rho_f/\phi\ln(1+B)\right)^{1.5} \qquad (5\text{-}22)$$

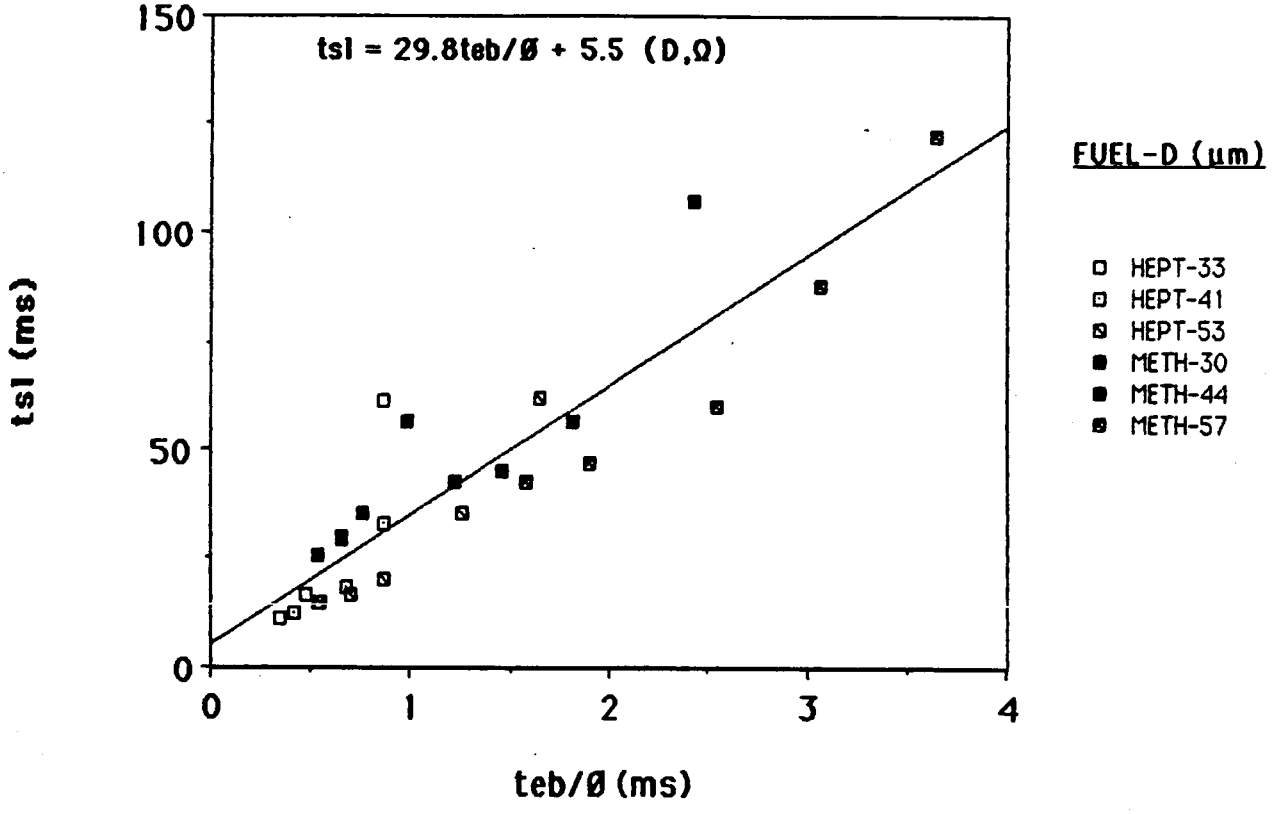

Figure 5.7 Characteristic Time Correlation for N-Heptane and Methanol Sprays (using Spark Gap Droplet Diameters and Extent of Prevaporization)

Values of E_{min} predicted by this equation are compared to the experimentally measured values in Figure 5.8 for n-heptane and methanol sprays. As seen, the qualitative agreement was again quite good with the exception of equivalence ratios approaching the lean limit. In addition, the quantitative agreement between the predicted and measured ignition energies improved significantly for the n-heptane sprays, while little change was seen for methanol. Again, this was expected due to n-heptane's greater volatility, which resulted in smaller drop sizes and more prevaporized fuel than methanol.

In general, the CTM was shown to be quite reliable in predicting the ignition energies of the sprays examined in this study. It appears that use of local (spark gap) spray parameters, such as droplet size and extent of prevaporization, results in more accurate predictions compared to use of initial parameters. Inclusion of chemical times, while not attempted in this study, might also improve model performance for lean and smaller droplet size sprays.

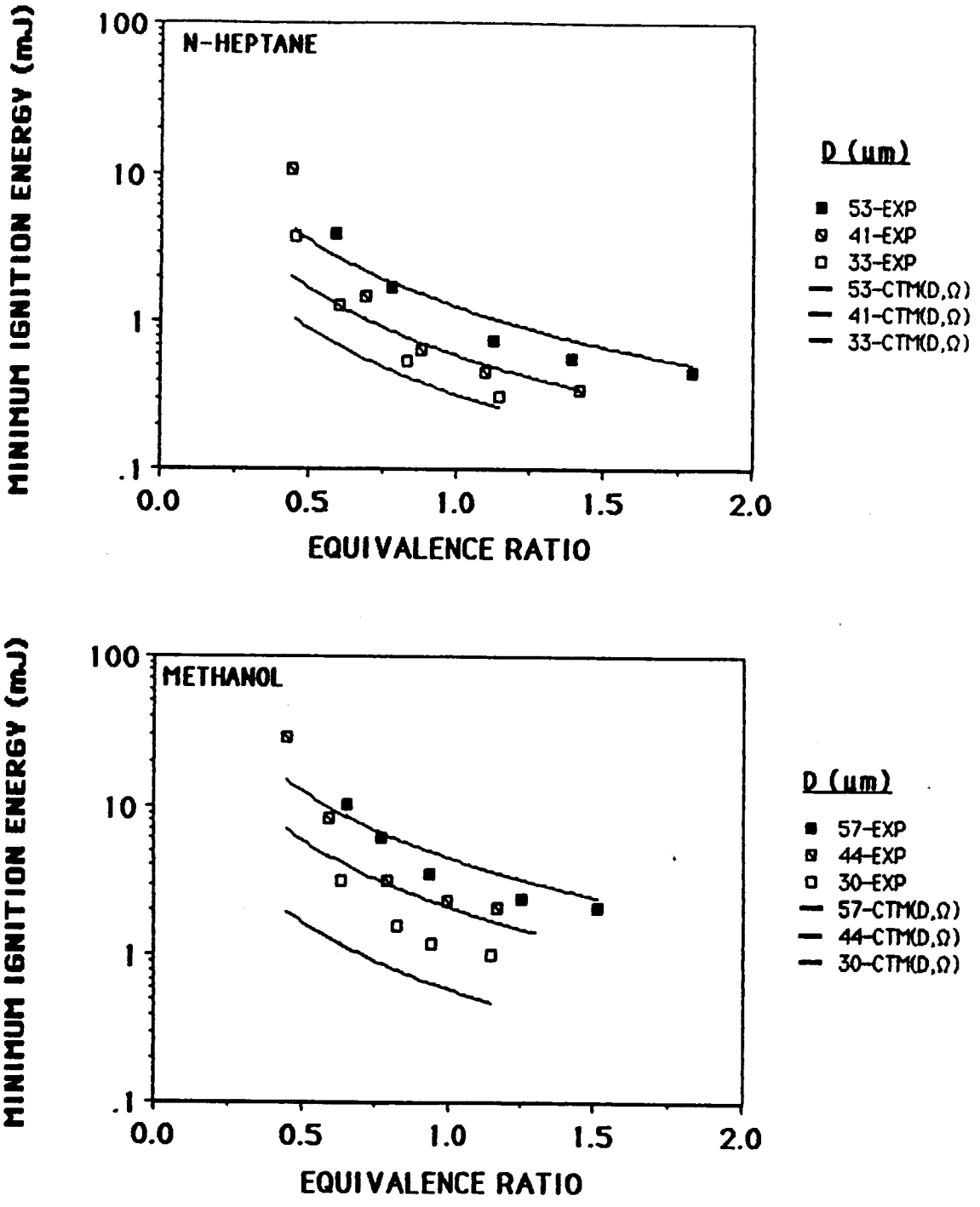

Figure 5.8 CTM Minimum Ignition Energy Predictions for N-Heptane and Methanol Sprays (using Spark Gap Droplet Diameters and Extent of Prevaporization)

5.3 Ignition Frequency Model

The experimental ignition energy results illustrate the probabilistic nature of spray ignition. This was seen in the variation in ignition frequency with spark energy. An ignition frequency model (IFM) was developed to account for these probabilistic effects by assuming that the randomness of spray ignition is caused entirely by variations in two of the main parameters affecting ignition, the spark energy and the equivalence ratio in the spark gap. Random normal distributions were simulated for these parameters, and these distributuions were used in conjunction with the previously described CTM for ignition (modified to use the spark gap droplet diameter and the extent of prevaporization) to predict the ignition frequency for a given spark energy and spray. The model was formulated as described below.

The probability distribution functions of the equivalence ratio (number density) in the spark gap and the spark energy were quantified experimentally in terms of their standard deviations. The standard deviation of the number density measurements was 50%, and was determined by statistically analyzing number density measurements taken for a time period of 10 ms (the average time a typical droplet or group of droplets spent in the spark gap). The standard deviation of the spark energy measurements was 10%. This information was used by a Monte Carlo random normal distribution simulator to generate arrays of 50 probable values of equivalence ratio (ϕ_i) and spark energy ($E_{sp,i}$) for a given mean equivalence ratio and mean spark energy case. $E_{min,i}$ was calculated for each value of ϕ_i, using the CTM, and compared to $E_{sp,i}$. If $E_{min,i}$ was less than or equal to $E_{sp,i}$, successful ignition occured. If $E_{min,i}$ was greater than $E_{sp,i}$, no ignition occured. The ignition frequency for that spark energy was the number of successful ignitions divided by fifty. This was repeated over a full range of spark

energies to generate an ignition frequency curve for a given mean equivalence ratio spray. A complete listing of the APL program used to run this program is given in Appendix C.

Typical results of the model are given in Figure 5.9, which shows ignition frequency curves generated by the IFM compared to the ignition frequencies obtained experimentally for representative n-heptane and methanol sprays. As seen, the IFM predicted quite accurately the observed variation in ignition frequency with spark energy for these cases.

Figure 5.10 shows IFM predictions for both rich (Ø = 1.42) and lean (Ø = 0.44) 41 μm n-heptane sprays. Several things can be observed from these results. For the very lean case, the IFM substantially underpredicted the 50% ignition energy, or E_{min}. This was because the ignition frequency predictions were based on minimum ignition energies calculated with the CTM. Where the CTM underpredicted E_{min}, such as lean cases approaching the ignition limit, the IFM overpredicted the ignition frequency for a given spark energy. The ignition frequency model, then, is limited by the accuracy of the ignition energy model (CTM) used. For the rich case in Figure 5.10, the 50% ignition energy predicted by the IFM was within 5% of the experimentally observed value. The slope of the predicted curve was less steep than the slope of the experimental curve, however. This issue will be addressed in the following paragraph. The ignition frequency modeling results shown in Figures 5.9 and 5.10 were representitive of results obtained for both fuels over the entire range of droplet sizes and equivalence ratios tested.

The slope of the ignition frequency curves predicted by the IFM were a function of the standard deviations of the spark energy and equivalence ratio used in the model. Smaller standard deviations would have resulted in steeper slopes, and vice-versa. This is illustrated in Figure 5.11, which

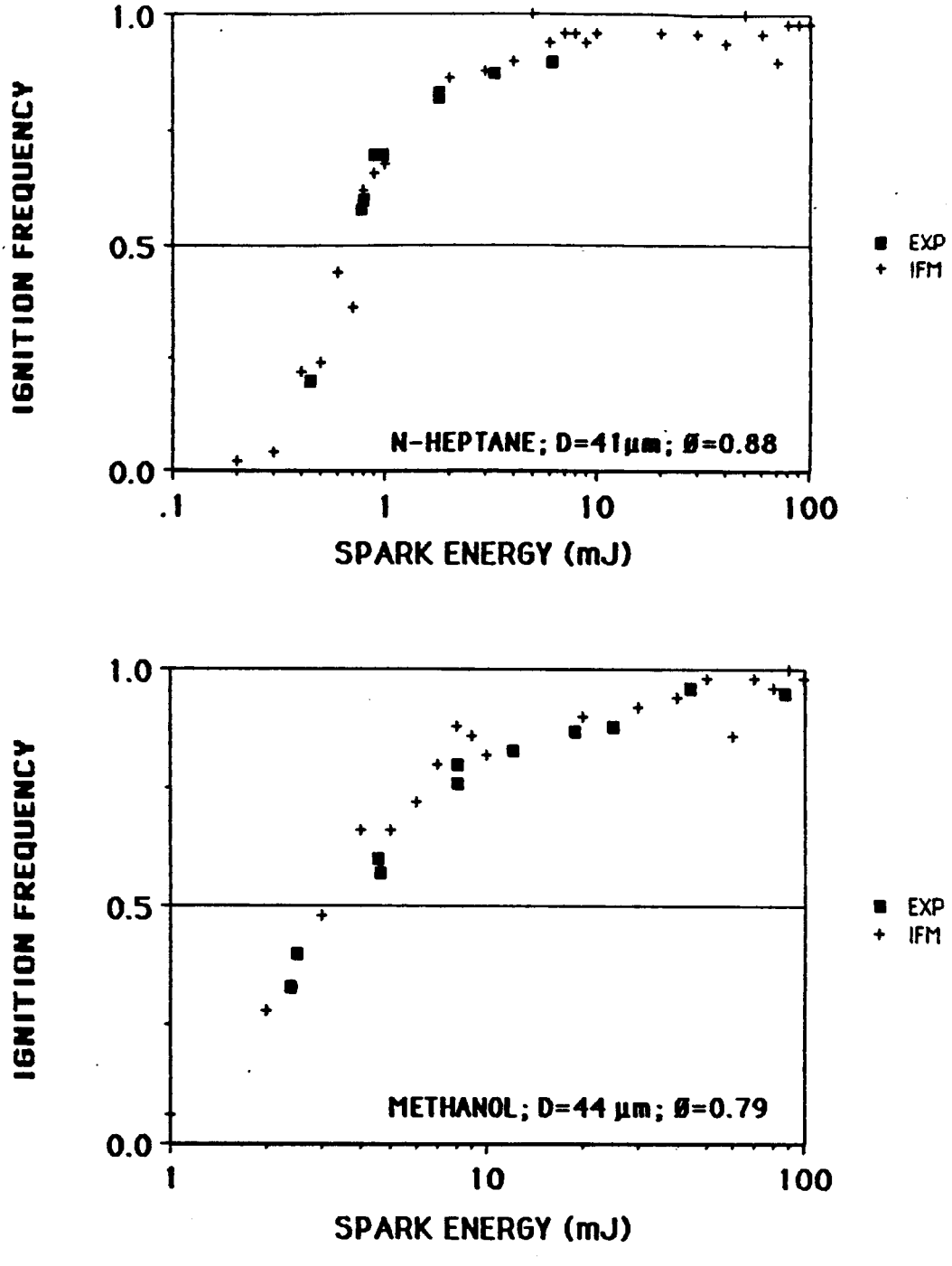

Figure 5.9 IFM Ignition Frequency Predictions for N-Heptane and Methanol Sprays (D = 41,44 µm; Ø = 0.88,0.79)

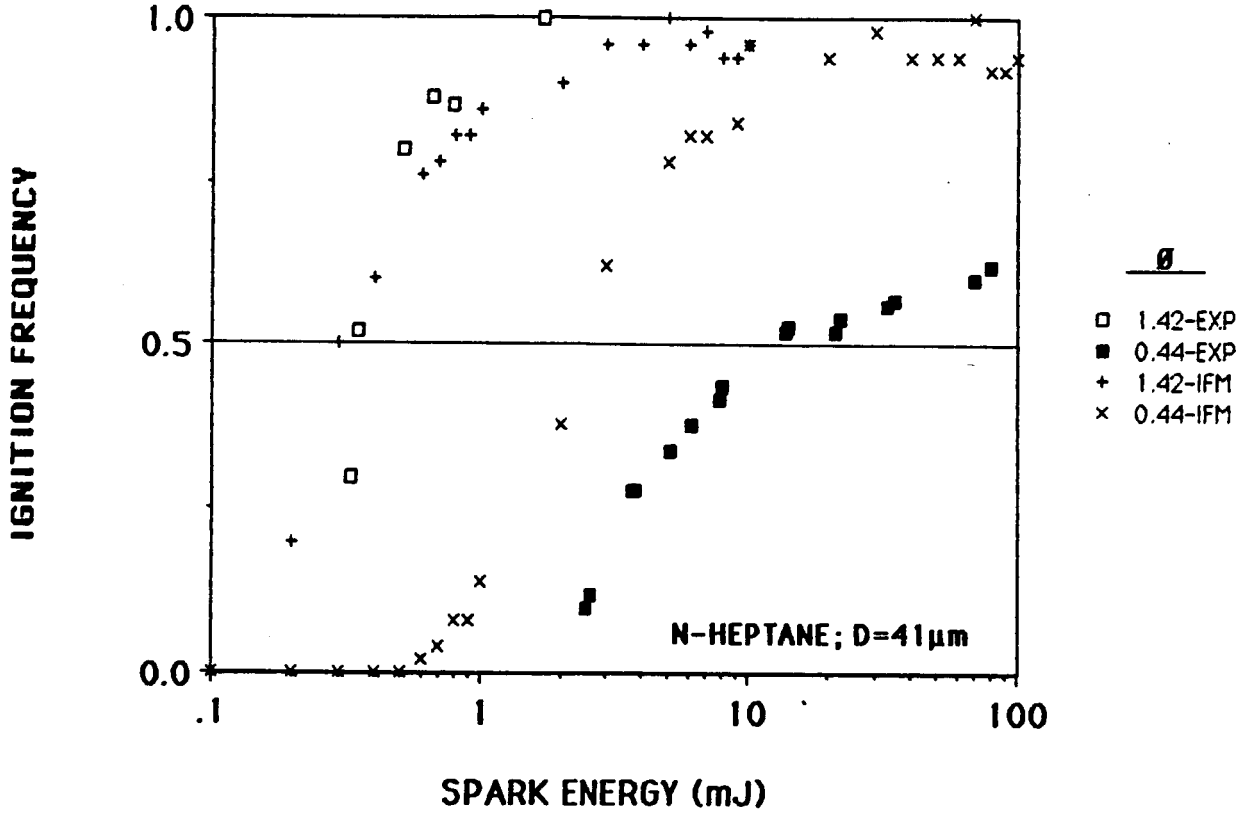

Figure 5.10 IFM Ignition Frequency Predictions for N-Heptane Sprays (D = 41 µm; Ø = 1.42 and 0.44)

shows the predicted ignition frequency curves for a 41 μm n-heptane spray with equivalence ratio of 1.42 using standard deviations of 50%, 30% and 10% for the equivalence ratio. The standard deviation of the spark energy was held constant at 10%. From Figure 5-11 it appears that by using a standard deviation of about 30% for the equivalence ratio in the IFM, the slope of the corresponding experimental ignition frequency curve in Figure 5.10 would have been predicted quite accurately. However, no decrease in the standard deviation of the number density with increasing equivalence ratio was observed experimentally to warrant this.

Finally, note in Figure 5.11 that all three curves cross the 50% ignition line at approximately the same spark energy. This is because the probability distribution functions used in the IFM for both the equivalence ratio and the spark energy are symmetric about the mean value. If the standard deviations of the distributions were zero (i.e. if ignition was deterministic), the ignition frequency curve would collapse to a straight vertical line which would also cross the 50% ignition line at the same energy. This illustrates that while spark ignition of sprays is probabilistic, choosing 50% ignition as the criterion for the minimum ignition energy accounts for these probabilistic effects.

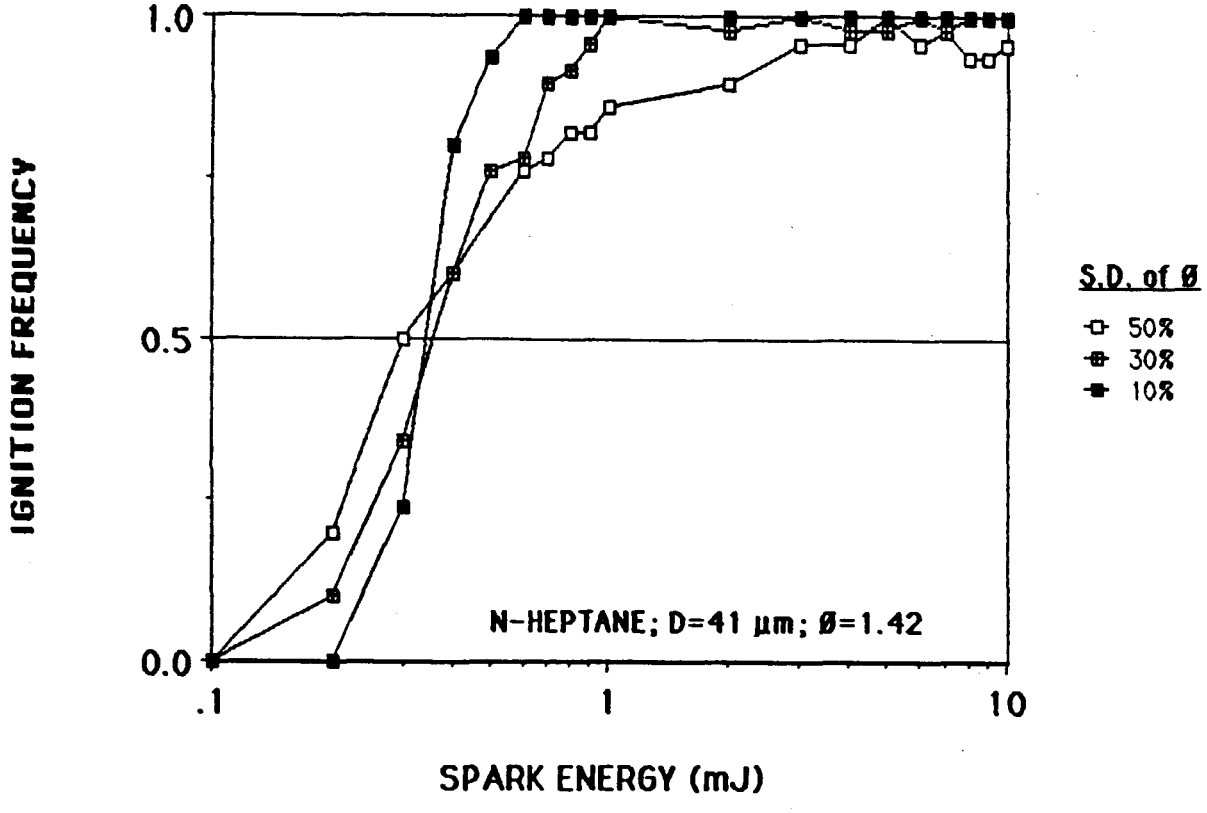

Figure 5.11 Effect of Varying the Standard Deviation of Equivalence Ratio on IFM Ignition Frequency Predictions for an N-Heptane Spray (D = 41 µm; Ø = 1.42)

CHAPTER 6

CONCLUSIONS AND RECOMMENDATIONS

6.1 Conclusions

A monodisperse spray ignition system was developed and used to study the spark ignition behavior of fuel sprays over a wide range of operating conditions. A criterion based on the probabilistic nature of ignition was determined for the minimum ignition energy, which was measured over a 30-57 μm droplet range and a wide range of equivalence ratios for n-heptane and methanol fuels. The sprays were characterized in terms of their number density, drop size, extent of prevaporization and velocity at the ignition spark gap. The spray droplet size was an important factor in spray ignition. Ignition was enhanced in all cases by decreasing the droplet diameter, which increased the total surface area of fuel in the ignition zone. Increasing the spray equivalence ratio also enhanced ignition in all cases, so the optimum amount of fuel in the ignition zone was never reached. Fuel volatility was the critical fuel property in correlating spray ignition behavior for a given fuel droplet size.

Minimum ignition energy measurements were made for prevaporized, premixed n-heptane and methanol to provide ignition data for the lower limit of droplet size. The optimum vapor phase equivalence ratio for ignition was also determined from these measurements for n-heptane. Activation energy was the critical fuel property for correlating prevaporized ignition behavior.

Flame propagation was closely related to ignition. The importance of

transition region effects on flame propagation rates in sprays of this size range and smaller was exhibited by the existence of an optimum droplet size for ignition at lean equivalence ratios for both fuels. This optimum size could not be quantified due to limitations of the spray generator, but it was attributed to the maximum flame speeds achieved by sprays in the transition region. Extension of the lean ignition limits was observed for sprays of both fuels, and attributed to the enhancing effect of the fuel vapor supplied by evaporating droplets.

Two models using a characteristic time approach were applied to correlate the spray ignition results. Both models predicted quite accurately, qualitatively and quantitatively, the observed ignition behavior. The models underpredicted ignition energies as the spray equivalence ratios approached the lean limit and as the droplet sizes decreased below 40 μm. This was because they did not account for the importance of kinetic times for lean mixtures and smaller droplets, nor did they account for transition region effects in smaller sprays.

The random nature of the spray ignition process was explained with a probabilistic model which took into account the distributions of spray number densities and spark energies during ignition. This model predicted ignition frequency curves which were in very good agreement with the observed variation in ignition frequency with spark energy. The success of the model indicated that the probabilistic nature of spray ignition is due in a large part to the random positioning of droplets in a spray.

6.2 Recommendations for Future Work

While this study points out important factors for optimizing ignition and minimizing ignition energies for spray combustors, further experimental and theoretical advancements are needed before the knowledge acquired here can be applied to such systems. Suggested experimental studies and their objectives are listed below:

1) Modification of the spray system should be done to generate droplets in the 10-30 μm range to quantify the optimum drop size for ignition and to determine the effects of equivalence ratio, prevaporization and fuel properties on this optimum.

2) Ignition studies should be performed with the prevaporizing system to add vapor to the interdroplet spacing of the sprays. Ω should be varied for fixed values of D and Ø to quantify the importance of prevaporization to ignition and to evaluate ignition models which use Ω.

3) Ignition studies should be performed with sprays formed using the dispersion jet only (no dilution air) to reduce the levels of turbulence in the sprays. A larger diameter test section should also be used to eliminate the problem of droplet impingement on the walls.

4) The prevaporizing apparatus should be modified to generate rich methanol mixtures in order to quantify the optimum equivalence ratio for prevaporized methanol mixtures. This could possibly be done by heating the entire flow system from the vaporizing chamber to the test section, or by

increasing the fuel and air flow rates for the existing set-up.

5) Modifications should be made with the spray system to generate bi-modal distributions of droplets to quantify their ignition behavior relative to monodisperse sprays. Such a study would begin to provide a link between monodisperse and polydisperse ignition studies. This information could also be used to assess the relative importance of size correlation parameters, such as SMD and D_{20}, for ignition modelling.

Improvements in modeling of the spark ignition process can be achieved in several ways:

1) A more detailed chemical kinetic term is needed to account for the sharp increase in ignition energies observed experimentally as the lean ignition limit is approached. The use of a non-unity exponent for Ø in the t_{hc} term developed by Peters and Mellor (1982) could improve the CTM performance in this respect.

2) Attention should be given to modelling the observed transition region effects, i.e. the flame propagation and fuel distribution effects resulting in an optimum droplet size for ignition. Both ignition models presently predict a monotonic decrease in ignition energy with decreasing droplet size, thus underpredicting E_{min} for smaller droplets ($D < 35\ \mu m$).

3) Statistical methods for determining the actual distributions of number density and equivalence ratio for sprays over a range of conditions should be developed in order to verify the IFM assumptions in this respect.

LIST OF REFERENCES

Adelman, H. G.,
1981, "A Time Dependent Theory of Spark Ignition", Eighteenth Symposium (International) on Combustion, p.1333, The Combustion Institute, Pittsburgh, PA.

Aggarwal, S. K. and Sirignano, W. A.,
1985, "Ignition of Fuel Sprays: Deterministic Calculations for Idealized Droplet Arrays", Twentieth Symposium (International) on Combustion, p.1773, The Combustion Institute, Pittsburgh, PA.

Aggarwal, S. K. and Sirignano, W. A.,
1986, "Ignition of Polydisperse Sprays: Importance of D_{20}", Combustion Science and Tecnology 46, p.289.

Aggarwal, S. K. and Nguyen, K.,
1987, "Numerical Simulation of the Ignition of Combustible Fuel-Air Mixtures Flowing in a Tube", Presented at the Spring Technical Meeting, Central States Section/ The Combustion Institute.

Ballal, D. R. and Lefebvre, A. H.,
1975, "The Influence of Flow Parameters on Minimum Ignition Energy and Quenching Distance", Fifteenth Symposium (International) on Combustion, p.1473, The Combustion Institute, Pittsburgh, PA.

Ballal, D. R. and Lefebvre, A. H.,
1975, "The Influence of Spark Discharge Characteristics on Minimum Ignition Energy in Flowing Gases", Combustion and Flame, 24, p.99.

Ballal, D. R. and Lefebvre, A. H.,
1977, "Ignition and Flame Quenching in Flowing Gaseous Mixtures," Proceedings of the Royal Society of London, A357, p.163.

Ballal, D. R. and Lefebvre, A. H.,
1978, "Ignition and Flame Quenching of Quiescent Fuel Mists", Proceedings of the Royal Society of London, A364, p.277.

Ballal, D. R. and Lefebvre, A. H.,
1978, "Ignition of Liquid Sprays at Subatmospheric Pressure", Combustion and Flame, 31, p.115.

Ballal, D. R. and Lefebvre, A. H.,
1978, "Ignition and Flame Quenching of Flowing Heterogeneous Fuel-Air Mixtures", Combustion and Flame, 35, p.155.

Ballal, D. R. and Lefebvre, A. H.,
1981, "A General Model of Spark Ignition for Gaseous and Liquid Fuel-Air Mixtures", Eighteenth Symposium (International) on Combustion, p.1737, The Combustion Institute, Pittsburgh, PA.

Bellan, J. and Cuffel, R.,
1983, "A Theory of Nondilute Spray Evaporation Based upon Multiple Drop Interactions", Combustion and Flame, 51, p.55.

Bellan, J. and Cuffel, R.,
1986, "Ignition of Nondilute Clusters of Drops in Convective Flows", Paper No. WSS-86-24, Western States Section/ The Combustion Institute, Pittsburgh, PA.

Berglund, R. N., and Liu, B. Y. H.,
1973, "Generation of Monodisperse Aerosol Standards", Environmental Science and Technology, 7, 2, 147.

Bradley, D. and Lung, F. K-K.,
1987, "Spark Ignition and the Early Stages of Turbulent Flame Propagation", Combustion and Flame, 69, p.71.

Blanc, M. V., Guest, P. G., Von Elbe, G., and Lewis, B.,
1948, "Minimum Ignition Energies and Quenching Distances of Mixtures of Hydrocarbons and Ether with Oxygen and Inert Gases", Third Symposium on Combustion, Flame and Explosion Phenomena, The Combustion Institute, Pittsburgh, PA.

Burgoyne, J. H. and Cohen, L.,
1954, "The Effect of Drop Size on Flame Propagation in Liquid Aerosols", Proceedings of the Royal Society of London, Series A: Mathematical and Physical Sciences, 225, No. 1162, p.375.

Chan, K. K. and Polymeropoulos, C. E.,
1981, "An Experimental Investigation of the Minimum Ignition Energy of Monodisperse Sprays", Paper No. 81-21, Fall Technical Meeting, Eastern States Section, The Combustion Institute, Pittsburgh, PA.

Chan, K. K.
1982, "An Experimental Investigation of the Minimum Ignition Energy of Monodisperse Fuel Sprays", Doctoral Thesis, Rutgers University, New Brunswick, NJ.

Dixon-Lewis, G. and Shepherd, I. G.,
1975, "Some Aspects of Ignition by Localized Sources, and of Cylindrical and Spherical Flames", Fifteenth Symposium (International) on Combustion, p.1483, The Combustion Institute, Pittsburgh, PA.

Dobbins, R. A., Crocco, L. and Glassman, I.,
1963, "Measurement of Mean Particle Size of Sprays from Diffractively Scattered Light", AIAA Journal, 1, p.1882.

DOE/EIA - 0219(85),
1985, "International Energy Annual", U. S. Department of Energy.

Faeth, G. M.,
1979, "Spray Combustion Models - a Review", Proceedings of the Seventeenth Aerospace Sciences Meeting, Paper No. 79-0293, AIAA.

Hayashi, S. and Kumagai, S.,
1974, "Flame Propagation in Fuel Droplet-Vapor-Air Mixtures", Fifteenth Symposium (International) on Combustion, 445-452, The Combustion Institute, Pittsburgh, PA.

Hayashi, S., Kumagai, S. and Sakai, T.,
1976, "Propagation Velocity and Structure of Flames in Droplet-Vapor-Air Mixtures", Combustion Science and Technology, 15, 169.

Hayashi, S., Ohtani, T. and Iinuma, K.,
1981, "Limiting Factor of Flame Propagation in Low Velocity Fuel Clouds", Eighteenth Symposium (International) on Combustion, p.361, The Combustion Institute, Pittsburgh, PA.

Kanury, A. M.,
1975, "Introduction to Combustion Phenomena", Gordon and Breach Science Publications Inc., N.Y., N.Y.

Kono, M., Kumagai, S. and Sakai, T.,
1977, "The Optimum Condition for Ignition of Gases by Composite Sparks", Sixteenth Symposium (International) on Combustion, p.757, The Combustion Institute, Pittsburgh, PA.

Law, C. K. and Chung, S. H.,
1978, "Theory of Thermal Ignition in Fuel Droplet Burning", Combustion and Flame, 31, p.285.

Law, C. K. and Chung, S. H.,
1980, "An Ignition Criterion for Droplets in Sprays", Combustion Science and Technology, 22, p.17.

Lewis, B. and von Elbe, G.,
1987, "Combustion, Flames and Explosions of Gases", Third Edition, Acedemic Press, Orlando, FL.

Litchfield, E. L.,
1960, U. S. Bureau of Mines, Rep. Inv. 5671.

Maly, R. R. and Vogel, M.,
1978, "Initiation and Propagation of Flame Fronts in Lean CH_4-Air Mixtures by the Three Modes of the Ignition Spark", Seventeenth Symposium (International) on Combustion, p.821, The Combustion Institute, Pittsburgh, PA.

Maly, R. R.,
1981, "Ignition Model for Spark Discharges and the Early Phase of Flame Front Growth", Eighteenth Symposium (International) on Combustion, p.1747, The Combustion Institute, Pittsburgh, PA.

Mizutani, Y. and Nakajima, A.,
1973, "Combustion of Fuel Vapor-Drop-Air Systems: Part 1 - Open Burner Flames", Combustion and Flame, 21, p.343.

NACA Report No. 1300,
1959, "Basic Considerations in the Combustion of Hydrocarbon Fuels with Air", Table XXXII, Appendix, by the Propulsion Chemistry Division, Lewis Flight Propulsion Laboratories.

Nizami, A. A., Singh, S. and Cernansky, N. P.,
1982, "Formation of Oxides of Nitrogen in Monodisperse Spray Combustion of Hydrocarbon Fuels", Combustion Science and Technology, 28, p.97.

Peters, J. E. and Mellor, A. M.,
1980, "An Ignition Model for Quiescent Fuel Sprays", Combustion and Flame, 38, p.65.

Peters, J. E.,
1981,"An Ignition Model for Gas Turbine Engines", Doctoral Thesis, Purdue University, West Lafayette, IN.

Peters, J. E. and Mellor, A. M.,
1982, "A Spark Ignition Model for Liquid Fuel Sprays Applied to Gas Turbine Engines", AIAA Journal of Energy, 6,4, p.272.

Polymeropoulos, C. E. and Das, S.,
1975, "The Effect of Droplet Size on the Burning Velocity of Kerosine-Air Sprays", Combustion and Flame, 25, p.247.

Polymeropoulos, C. E.,
1984, "Flame Propagation in Aerosols of Fuel Droplets, Fuel Vapor and Air", Combustion Science and Technology, 40, p.217.

Rao, H. N. S. and Lefebvre, A. H.,
1973, "Ignition of Kerosine Fuel Sprays in a Flowing Air Stream", Combustion Science and Technology, 8, p.95.

Rao, K. V. L. and Lefebvre, A. H.,
1976, "Minimum Ignition Energy in Flowing Kerosine-Air Mixtures", Combustion and Flame, 27, p.1.

Rose, H. E. and Priede, T.,
1958, "Ignition Phenomena in Hydrogen-Air Mixtures", Seventh Symposium (International) on Combustion, p.436, The Combustion Institute, Pittsburgh, PA.

Rose, H. E. and Priede, T.,
1958, "Investigation of Characteristics of Spark Discharges as Employed in Ignition Experiments", Seventh Symposium (International) on Combustion, p.454, The Combustion Institute, Pittsburgh, PA.

Roth, W. R., Guest, P. G., von Elbe, G. and Lewis, B.,
1951, "Heat Generation by Electric Spark and Rate of Heat Loss to the Spark Electrodes", Journal of Chemical Physics, 19,12, p.1530.

Saitoh, T., Ishiguro, S. and Niioka, T.,
1982, "An Experimental Study of Droplet Ignition Characteristics Near the Ignitible Limit", Combustion and Flame, 48, p.27.

Sangiovanni, J. J. and Kesten, A. S.,
1978, "Effect of Droplet Interactions on Ignition in Monodispersed Droplet Streams", Sixteenth Symposium (International) on Combustion, p.577, The Combustion Institute, Pittsburgh, PA.

Sarv, H.,
1985, "Oxides of Nitrogen Emissions from the Combustion of Monodisperse Liquid Fuel Sprays", Doctoral Thesis, Drexel University, Philadelphia, PA.

Sirignano, W. A.,
1984, "Fuel Droplet Vaporization and Spray Combustion Theory", Progress in Energy and Combustion Science, 9, p.291.

Singh, A. K., and Polymeropoulos, C. E.,
1985, "Spark Ignition of Monodisperse Aerosols", presented at the Fall Technical Meeting, Eastern Section of the Combustion Institute.

Singh, A. K.,
1986, "Spark Ignition of Monodisperse Aerosols", Doctoral Thesis, Rutgers University, New Brunswick, NJ.

Stevenson, W. H.,
1976, "Principles of Laser Velocimetry", Proceedings of the Fourteenth Aerospace Sciences Meeting, p.307, AIAA.

Swett, Jr., C. C.,
1956, "Spark Ignition of Flowing Gases using Long Duration Discharges", Sixth Symposium (International) on Combustion, p.523, The Combustion Institute, Pittsburgh, PA.

Warnatz, J.
1984, "Chemistry of High Temperature Combustion of Alkanes up to Octane", Twentieth Symposium (International) on Combustion, p.845, The Combustion Institute, Pittsburgh, PA.

Ziegler, G. F. W., Wagner, E. P. and Maly, R. R.,
1984, "Ignition of Lean Methane-Air Mixtures by High Pressure Glow and Arc Discharges", Twentieth Symposium (International) on Combustion, p.1817, The Combustion Institute, Pittsburgh, PA.

APPENDIX A

COMPREHENSIVE SPRAY CHARACTERIZATION AND IGNITION RESULTS

For brevity, only representitive results of the spray characterization and ignition measurements were reported in the main body of text. Comprehensive results are given in this appendix. Figures A.1 and A.2 show radial profiles of the local equivalence ratio for all of the sprays tested in this study. Figure A.3 shows Fraunhofer diffraction patterns from each of the fuel and droplet size sprays tested at an overall equivalence ratio of 0.7. Finally, Figures A.4 and A.5 report the experimental ignition energy measurements, showing the variation in ignition frequency with spark energy for each of the sprays tested.

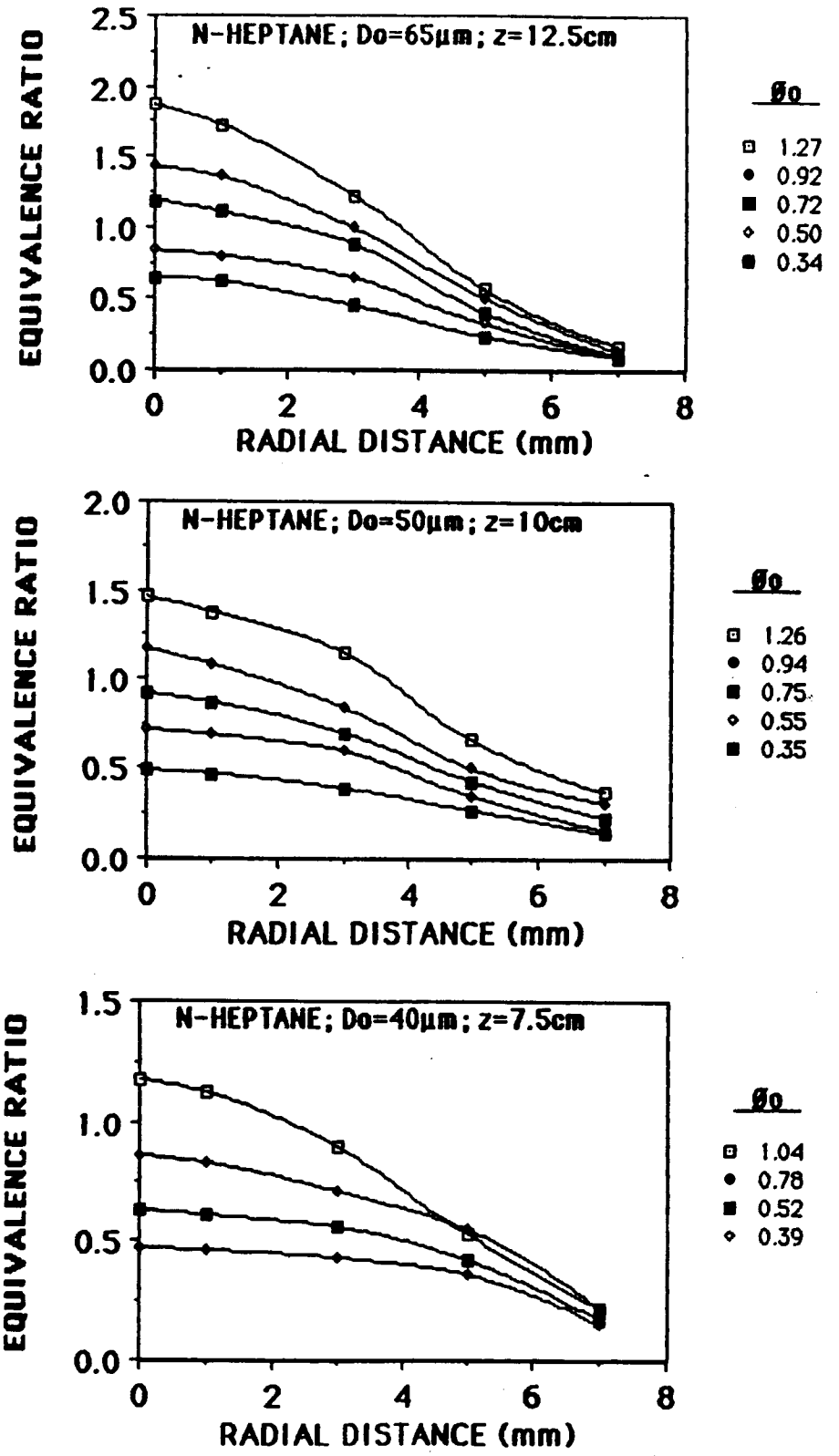

Figure A.1 Radial Profiles of Local Equivalence Ratio for N-Heptane Sprays of Varying Overall Equivalence Ratio (D_0 = 65, 50 and 40 µm)

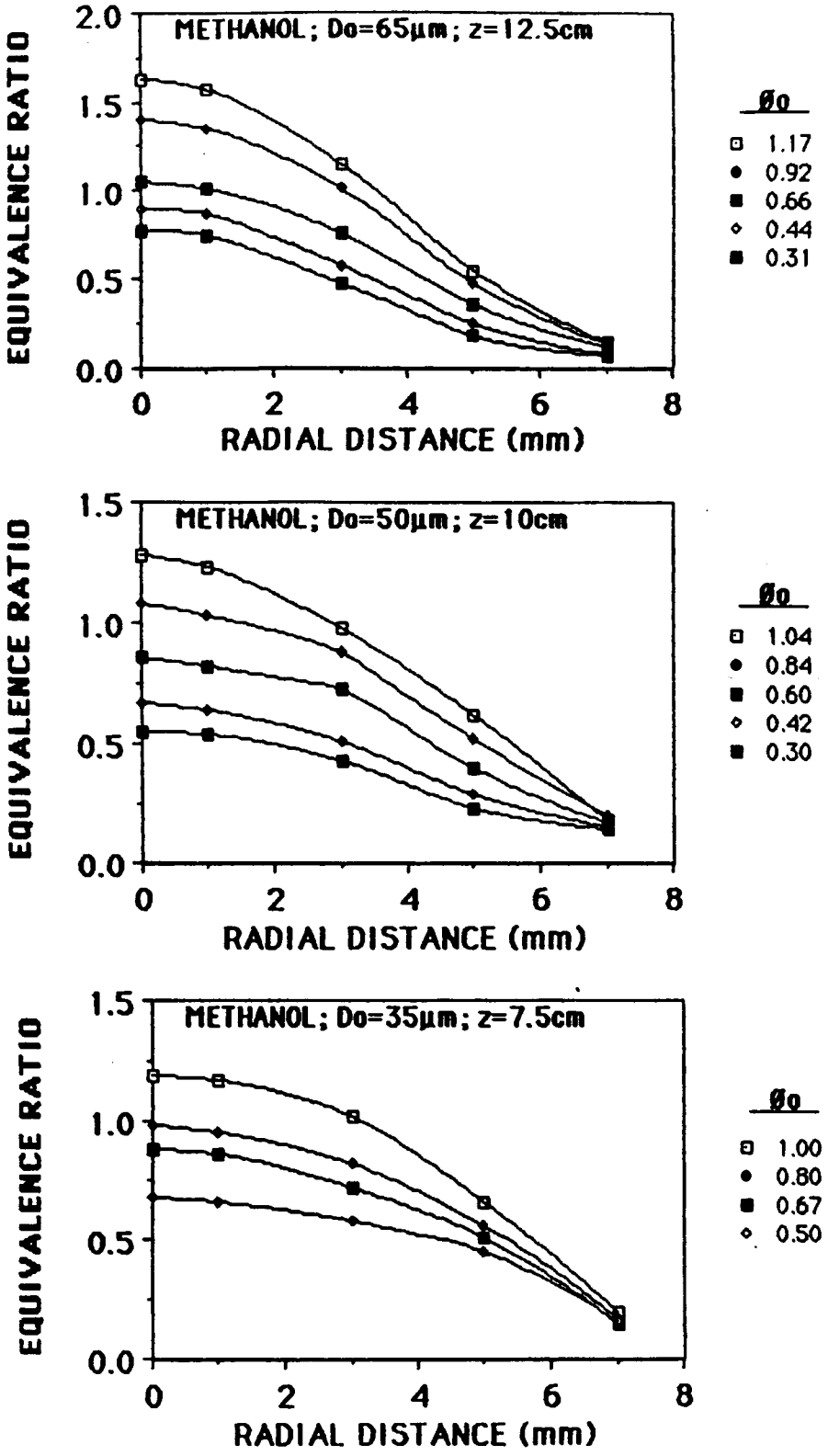

Figure A.2 Radial Profiles of Local Equivalence Ratio for Methanol Sprays of Varying Overall Equivalence Ratio (D_o = 65, 50 and 35 µm)

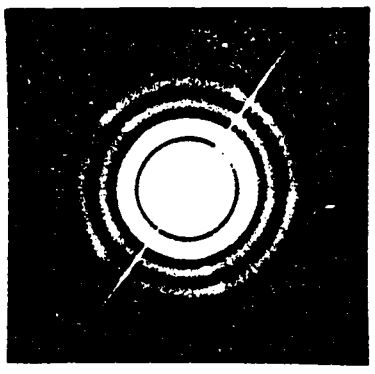

H – 53

M – 57

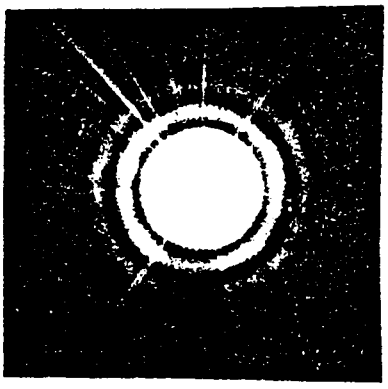

H – 41

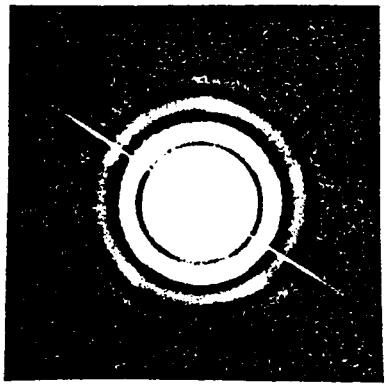

M – 44

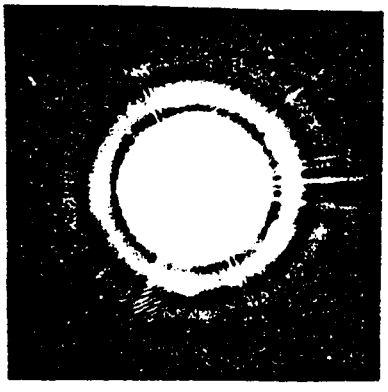

H – 33

M – 30

Figure A.3 Fraunhofer Diffraction Patterns produced by N-Heptane (D = 53, 41 and 33 μm) and Methanol (D = 57, 44 and 30 μm) Sprays ($\emptyset_o = 0.7$)

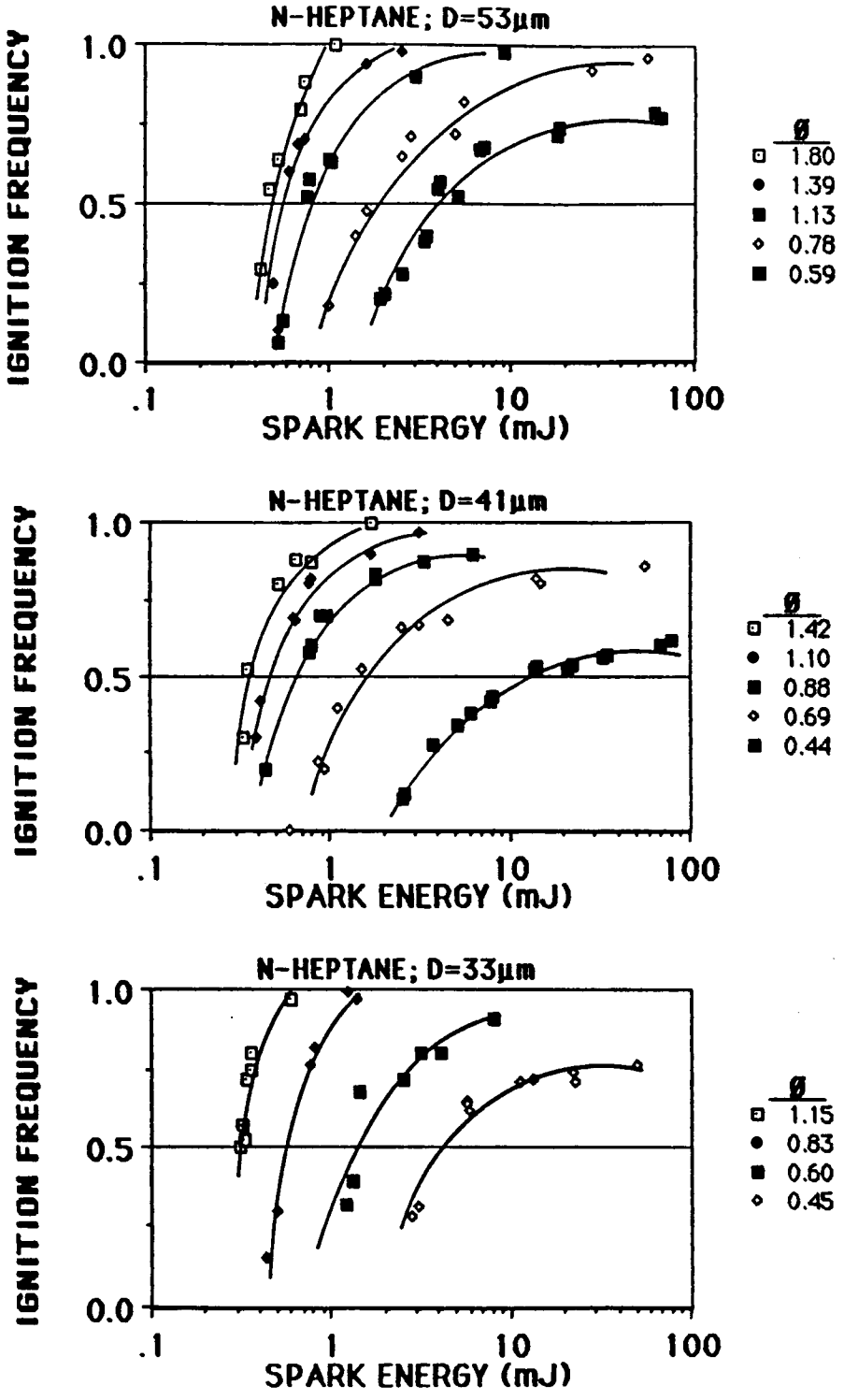

Figure A.4 Effect of Spark Energy and Equivalence Ratio on the Ignition Frequency of N-Heptane Sprays (D = 53, 41 and 33 µm)

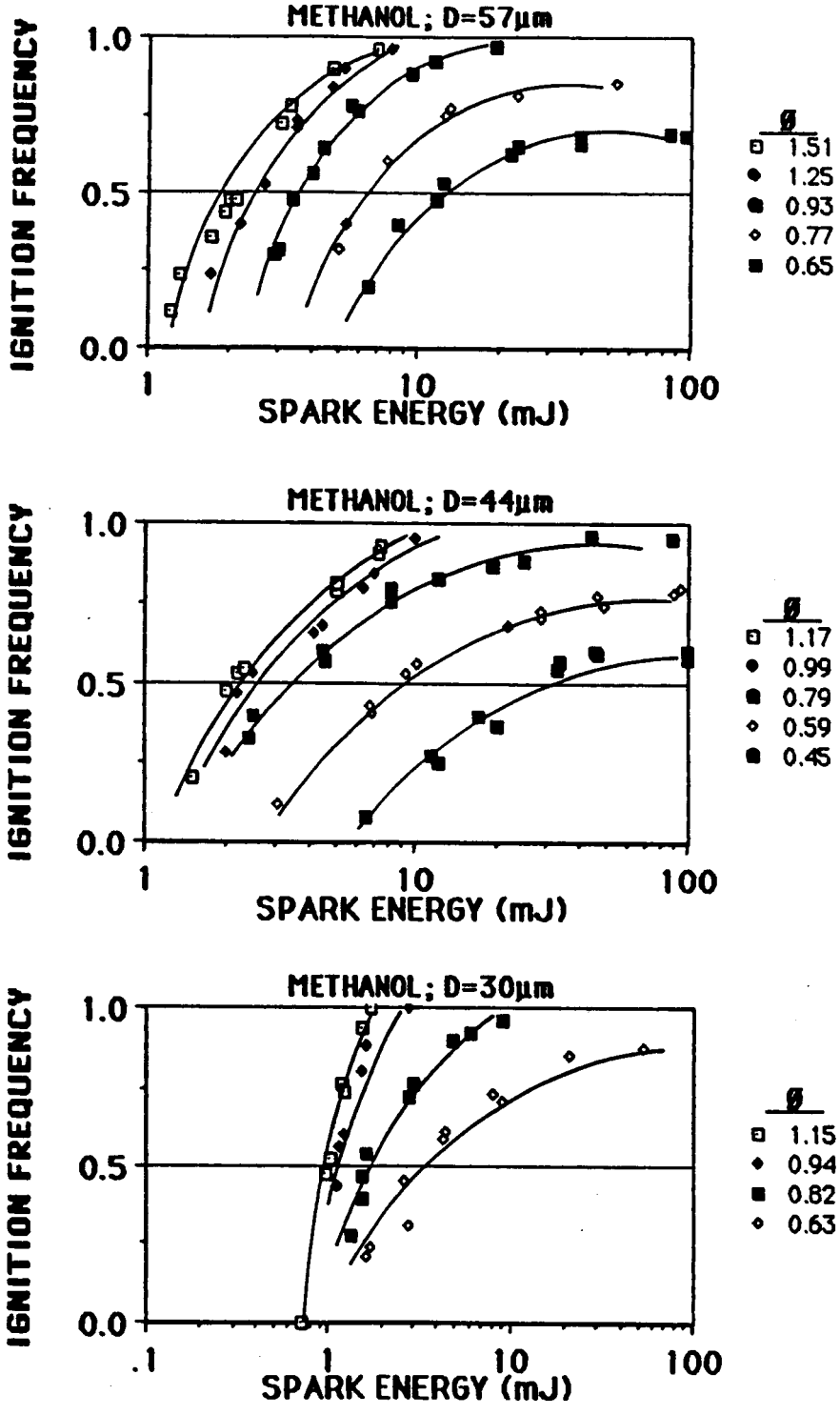

Figure A.5 Effect of Spark Energy and Equivalence Ratio on the Ignition Frequency of Methanol Sprays (D = 57, 44 and 30 µm)

APPENDIX B

COMPUTER PROGRAM FOR LDV DATA COLLECTION AND ANALYSIS

```
      PROGRAM LDA4
C*************************************************************
C     EXPONENT = 8; NCYCLES = 2^4
C     THIS PROGRAM ACQUIRES AND ANALYZES DATA FROM A
C     TSI MDL 1990 LDV SYSTEM; THE LDV DATA READY PULSE
C     IS USED TO TRIGGER CH.0 A/D VELOCITY DATA CONVERSION
C     THROUGH THE A/D EXTERNAL TRIGGER; THE CLOCK COUNTS
C     THE TIME FOR NSAMP DATA, GIVING THE DROPLET RATE;
C     THE LDV SETTINGS ARE: CYCLES/BURST=2^4; EXP=8;
C     COMP%=7; FREQ=100:1; GAIN=1; AMP LIM OFF;
C     FILTERS: HI=3MHZ; LO=30KHZ;
C*************************************************************
      INTEGER*2 IBELL
      DATA IBELL/"07/
      DIMENSION  IDAT(100),DAT(100),VOLT(100),VEL(100)
      DIMENSION  DFREQ(100),VELMN(100),VELRMS(100),RMSP(100)
C*************************************************************
C     MACRO DATA TRANSFER ROUTINE (ADCLS.MAC) ARGUMENTS:
C     IDAT: ARRAY FOR VELOCITY DATA
C     ICNT: VARIABLE FOR FREQUENCY DATA
C     NSAMP: NUMBER OF DATA TAKEN (UP TO 1000)
C*************************************************************
      WRITE(5,96)
 96   FORMAT('0ENTER THRESHOLD VELOCITY (M/S):')
      READ(5,*)VTH
 97   CONTINUE
      NSAMP=100
      WRITE(5,98)
 98   FORMAT(' ENTER NAVG (1-100):')
      READ(5,*)NMN
 99   CONTINUE
      VBUF=0.
      FBUF=0.
      RBUF=0.
      DO 103 J=1,NMN
      CALL ADCLS(IDAT,ICNT,NSAMP)
C*************************************************************
C     CALCULATE MEAN VELOCITY (M/S)
C     NOTE: VEL=FREQ*FRINGE SPACING
C     FREQ=VOLT*(16*10^10/2^(n+10))
C     n=8; FREQ=VOLT*610352
C     FRINGE SPACING=3.3 MICRONS
C*************************************************************
```

```
      SUM=0.
      DO 100 I=1,NSAMP
      VOLT(I)=5.*FLOAT(IDAT(I))/4095.
      VEL(I)=VOLT(I)*2.0142
      IF (VEL(I).GT.VTH) GO TO 100
      SUM=SUM+VEL(I)
  100 CONTINUE
      VELMN(J)=SUM/NSAMP
C*****************************************************
C     CALCULATE RMS VELOCITY (M/S)
C*****************************************************
      SUMM=0.
      DO 101 I=1,NSAMP
      SUMM=SUMM+((VEL(I)-VELMN(J))**2)
  101 CONTINUE
      SUMMM=SUMM/FLOAT(NSAMP)
      VELRMS(J)=SQRT(SUMMM)
      RMSP(J)=VELRMS(J)/VELMN(J)
C*****************************************************
C     CALCULATE DROPLET RATE (KHZ): (CLOCK RATE=0.1 KHZ)
C*****************************************************
      RATE=0.1
      DFREQ(J)=FLOAT(NSAMP)/(FLOAT(ICNT)/RATE)
C*****************************************************
C     STORE VALUES FOR MEAN
C*****************************************************
      VBUF=VBUF+VELMN(J)
      FBUF=FBUF+DFREQ(J)
      RBUF=RBUF+DFREQ(J)
  103 CONTINUE
C*****************************************************
C     CALCULATE MEAN VALUES
C*****************************************************
      VELMNM=VBUF/FLOAT(NMN)
      DFREQM=FBUF/FLOAT(NMN)
      TINTM=RBUF/FLOAT(NMN)
      WRITE(5,104)DFREQM,VELMNM,TINTM
  104 FORMAT(' MEAN VALUES (N,V,T): ',3F7.3)
      WRITE(5,1000)IBELL
 1000 FORMAT('+',A1)
      GO TO 97
      STOP
      END
```

SUBROUTINE ADCLS.MAC:

```
                .TITLE ADCLS                ;ADCLS.MAC MAKES 1000 A/D
                .GLOBL ADCLS                ;CONVERSIONS ON CH.0
                ADCSR=170400                ;OF VELOCITY DATA FROM
                ADBUF=170402                ;THE ANALOG OUTPUT OF
                CCSR=170420                 ;THE LDV TIMER.  IT ALSO
                CBUF=170422                 ;RECORDS THE # OF COUNTER
ADCLS:          CLR ADCSR                   ;TICS DURING ACQUISITION
                CLR ADBUF                   ;TO GIVE DROPLET FREQUENCY
                CLR CCSR
                CLR CBUF
                MOV 2(R5),R1                ;IVOLT ARRAY LOCATION
                MOV 4(R5),R2                ;ICNT VARIABLE LOCATION
                MOV @6(R5),R3               ;SET NSAMP
                BIS #55,CCSR                ;SET RATE=0.1KHZ, MODE=2, GO
                BIS #20,ADCSR               ;SET A/D CH=0, EXT. TRIG. ENABLE
LOOP:           TSTB ADCSR                  ;CHECK IF CONV. DONE
                BGE LOOP                    ;LOOP TILL DONE (NEGATIVE)
                MOV ADBUF,(R1)+             ;PUT IVOLT(I) INTO ARRAY
                SOB R3,LOOP                 ;COUNT# OF CONVERSIONS
                BIS #1000,CCSR              :SIMULATE ST2 INPUT
                MOV CBUF,(R2)               ;READ COUNTER # INTO ICNT
                CLR ADCSR
                CLR ADBUF
                CLR CCSR
                CLR CBUF
                RTS PC
                .END
```

APPENDIX C

APL IGNITION FREQUENCY MODEL PROGRAM

```
     ∇IGNITION;N;PHIBAR;PHISTD;PHI;EMIN;DROP;OMEGA;CPA;RHOA;LNB;DTST;PROB;COMB;M
[1]   'INPUT THE SPARK GAP DROPLET DIAMETER:'
[2]   DROP ← □
[3]   'INPUT OMEGA:'
[4]   OMEGA ← □
[5]   'INPUT THE MEAN SPARK GAP EQUIVALENCE RATIO:'
[6]   PHIBAR ← □
[7]   'INPUT THE STANDARD DEVIATION OF THE SPARK EQUIVALENCE RATIO (PERCENT):'
[8]   PHISTD ← □
[9]   N ← 50
[10]  M ← N×28
[11]  'INPUT THE STANDARD DEVIATION OF THE SPARK ENERGY (PERCENT):'
[12]  ESTD ← □
[13]  PHI ← SIMNORM M
[14]  PHI ← PHIBAR + (((PHISTD×.01)×PHIBAR)×PHI)
[15]  PHIT ← PHI×(PHI>0)
[16]  PHI ← PHIT + ((PHIT=0)×.01)
[17]  PHI ← (28 50)⍴PHI
[18]  ESPARK←SPARKY ESTD
[19]  CPA ← 1200
[20]  RHOA ← .271
[21]  DTST ← 1983
[22]  RHOF ← 688
[23]  LNB ← 1.92
[24]  EMIN ← .676×CPA×DTST×(RHOA*¯0.5)
[25]  EMIN ← EMIN×((RHOF÷LNB)*1.5)×(DROP*3)×(((1-OMEGA)÷PHI)*1.5)
[26]  EMIN ← EMIN×1E¯15
[27]  PROB ← (+/(EMIN≤ESPARK))÷N
[28]  PROB ← (28 1)⍴PROB
[29]  ''
[30]  ''
[31]  'THE SPARK ENERGIES AND IGNITION PROBABILITIES ARE:'
[32]  ESPMN,PROB
[33]  COMB ← ESPMN,PROB
[34]  NUMPUT COMB

     ∇Z ← SPARKY ESTD;ESPEXP;ONE;M;ESPARK
[1]   ONE ← (1 50)⍴ONE←1
[2]   ESPEXP ← ESPMN +.× ONE
[3]   M ← 50×28
[4]   ESPARK ← SIMNORM M
[5]   ESPARK ← (28 50)⍴ESPARK
[6]   Z ← ESPEXP + (((ESTD×.01)×ESPEXP)×ESPARK)

     ∇Z←SIMNORM N;A;B;THETA;R
[1]   N←N÷2
[2]   A←UNIFORM N
[3]   B←UNIFORM N
[4]   THETA←(○2)×A
[5]   R←(¯2×(⍟B))*0.5
[6]   Z←(R×(1○THETA)),(R×(2○THETA))
```

VITA

Allen M. Danis was born [redacted] in [redacted]. He attended Denison University, from which he graduated in 1977 with a Bachelor of Science degree in Physics. After working at Owens Corning Fiberglas Research Center for several years, he enrolled at Drexel University in the Fall of 1980 to pursue graduate studies. He recieved a Master of Science degree in Mechanical Engineering in June of 1982 and a Doctor of Philosophy degree in Mechanical Engineering in September of 1987. During this period, he served as a Hess Fellow, a graduate research assistant and a teaching assistant in the Mechanical Engineering and Mechanics Department.

Mr. Danis has co-authored six technical papers in the areas of spray ignition and diesel emissions while studying at Drexel. He was also awarded the Frederic O. Hess Fellowship in Combustion in 1982 and 1984.

Mr. Danis was elected to associate member of Sigma Xi in 1986 and promoted to full member in 1987. He is also a member of the American Society of Mechanical Engineers, the Society of Automotive Engineers and the Combustion Institute.